



Entergy Operations, Inc.
1340 Echelon Parkway
Jackson, MS 39213-8298
Tel 601 368 5758

Michael A. Krupa
Director
Nuclear Safety & Licensing

CNRO-2003-00020

June 11, 2003

U. S. Nuclear Regulatory Commission
Attn: Document Control Desk
Washington, DC 20555

SUBJECT: Entergy Operations, Inc.
Relaxation Requests to NRC Order EA-03-009

Arkansas Nuclear One, Unit 2
Docket No. 50-368
License No. NPF-6

Waterford Steam Electric Station, Unit 3
Docket No. 50-382
License No. NPF-38

REFERENCE: NRC Order EA-03-009, "Issuance of Order Establishing Interim Inspection Requirements for Reactor Pressure Vessel Heads at Pressurized Water Reactors," dated February 11, 2003

Dear Sir or Madam:

Pursuant to Section IV.F of NRC Order EA-03-009, Entergy Operations, Inc. (Entergy) requests relaxation from Section IV.C(1)(b) of the Order for Arkansas Nuclear One, Unit 2 (ANO-2) and Waterford Steam Electric Station, Unit 3 (Waterford 3). Specifically, the bottom of the ANO-2 and Waterford 3 control element assembly (CEA) drive nozzles contain threads that cannot be effectively examined in accordance with Section IV.C(1)(b).

Enclosures 1 and 2 contain the relaxation requests for ANO-2 and Waterford 3, respectively. Enclosure 3 contains a copy of the fracture mechanics analyses report (Engineering Report M-EP-2003-002) that supports the relaxation requests. Enclosure 4 contains Appendix I while Enclosure 5 contains Appendices II and III of this report.

Entergy considers the information contained in Enclosure 5 to be proprietary and confidential in accordance with 10 CFR 2.790(a)(4) and 10 CFR 9.17(a)(4). As such, Entergy requests this information be withheld from public disclosure. The affidavit supporting this request is provided in Enclosure 6. Because the vast majority of the information contained in these appendices is considered proprietary, Entergy considers it impractical to provide non-proprietary versions.

A101

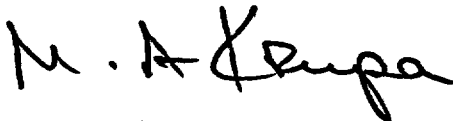
The NRC has approved similar requests for other nuclear plants.

Entergy requests approval of the proposed relaxation requests by August 1, 2003 in order to support activities scheduled during the upcoming fall 2003 refueling outages at ANO-2 and Waterford 3.

This letter contains no new commitments.

If you have any questions or require additional information, please contact Guy Davant at (601) 368-5756.

Sincerely,



MAK/GHD/bal

Enclosures:

1. Relaxation Request for Arkansas Nuclear One, Unit 2
2. Relaxation Request for Waterford Steam Electric Station, Unit 3
3. Engineering Report M-EP-2003-02
4. Appendix I of Engineering Report M-EP-2003-002the Fracture Mechanics Analyses Report
5. Proprietary Information – Appendices II and III of the Fracture Mechanics Analyses Report
6. Affidavit for Withholding Information from Public Disclosure

cc: Mr. C. G. Anderson (ANO)
Mr. W. A. Eaton (ECH)
Mr. G. D. Pierce (ECH)
Mr. J. E. Venable (W3)

Mr. T. W. Alexion, NRR Project Manager (ANO-2)
Mr. R. L. Bywater, NRC Senior Resident Inspector (ANO)
Mr. T. P. Gwynn, NRC Region IV Regional Administrator
Mr. M. C. Hay, NRC Senior Resident Inspector (W3)
Mr. N. Kalyanam, NRR Project Manager (W3)

ENCLOSURE 1

CNRO-2003-00020

**RELAXATION REQUEST FOR
ARKANSAS NUCLEAR ONE, UNIT 2**

**ENTERGY OPERATIONS, INC.
ARKANSAS NUCLEAR ONE, UNIT 2**

I. COMPONENT/EXAMINATION

Component/Number: 2R-1

Description: Reactor Pressure Vessel (RPV) head penetration nozzles

Code Class: 1

- References:
1. NRC Order EA-03-009, Issuance of Order Establishing Interim Inspection Requirements for Reactor Pressure Vessel Heads at Pressurized Water Reactors
 2. Letter 2CAN020304 from Entergy Operations, Inc. to the NRC, "Entergy Operations, Inc. – Answer to Issuance of Order Establishing Interim Inspection Requirements for Reactor Pressure Vessel Heads at pressurized Water Reactors", dated February 28, 2003
 3. Engineering Report M-EP-2003-002, *Fracture Mechanics Analysis for Primary Water Stress Corrosion Crack (PWSCC) Growth in the Un-Inspected Regions of the Control Element Drive Mechanism (CEDM) Nozzles at Arkansas Nuclear One Unit 2 & Waterford Steam Electric Station Unit 3*
 4. EPRI Material Reliability Program Crack Growth Rates for Evaluating Primary Water Stress Corrosion Cracking (PWSCC) of Thick-Wall Alloy 600 Materials (MRP-55) Revision 1

Unit: Arkansas Nuclear One Unit 2 (ANO-2)

Inspection Interval: Third (3rd) 10-Year Interval

II. REQUIREMENTS

The NRC issued Order EA-03-009 (the Order) that modified the current licenses at nuclear facilities utilizing pressurized water reactors (PWRs), which includes Arkansas Nuclear One, Unit 2 (ANO-2). The NRC Order establishes inspection requirements for RPV head penetration nozzles. ANO-2 is categorized as a "High" PWSCC susceptibility plant based on an effective degradation year (EDY) greater than 12. According to Section IV.C.1(b) of the Order, RPV head penetration nozzles in the "High" PWSCC susceptibility category shall be inspected using either of the following methods each refueling outage:

- (i) Ultrasonic testing of each RPV head penetration nozzle (i.e., nozzle base material) from two (2) inches above the J-groove weld to the bottom of the nozzle and an assessment to determine if leakage has occurred into the interference fit zone.

- (ii) Eddy current testing or dye penetrant testing of the wetted surface of each J-groove weld and RPV head penetration nozzle base material to at least two (2) inches above the J-groove weld.

III. PROPOSED ALTERNATIVE

A. Background

The ANO-2 RPV head has ninety (90) penetration nozzles that include eighty-one (81) Control Element Drive Mechanism (CEDM) nozzles, eight (8) Incore Instrument (ICI) nozzles, and one (1) vent line nozzle. Nozzle dimensions are identified below.

RPV Penetration Nozzle	Nozzle Dimensions		
	Outside Dia.	Inside Dia.	Thickness
CEDM	4.050 inches	2.718 inches	0.6660 inches
ICI	5.563 inches	4.750 inches	0.4065 inches
Vent Line	1.050 inches	0.742 inches	0.1540 inches

Entergy Operations, Inc. (Entergy) plans to inspect RPV head penetration nozzles at ANO-2 using the ultrasonic testing (UT) method in accordance with Section IV.C.1(b)(i) of the Order. However, due to nozzle configuration at the guide cone connection and UT coverage limitations, CEDM nozzles cannot be inspected to the bottom as required by the Order. Therefore, Entergy requests relaxation from the UT coverage requirements of Section IV.C.1(b)(i) of the Order and proposes an alternative in Section III.B, below.

This relaxation request does not apply to ICI nozzles or the vent line nozzle due to different configurations.

B. Proposed Alternative

Paragraph IV.C.1(b)(i) of the Order requires that the UT inspection of each RPV head penetration nozzle extend “from two (2) inches above the J-groove weld to the bottom of the nozzle.” Entergy requests relaxation from this provision for CEDM nozzles and proposes the following alternative:

- CEDM nozzles (i.e., nozzle base material) shall be ultrasonically examined from two (2) inches above the J-groove weld to 1.544 inches above the bottom of the nozzle. A fracture mechanics evaluation has been performed and demonstrates that residual stresses in the bottom portion of the nozzle are insufficient to cause an axial flaw to propagate into the pressure boundary region of the nozzle along the J-groove weld (nozzle J-groove weld region) prior to re-inspection during the next refueling outage.

IV. BASIS FOR PROPOSED ALTERNATIVE

A. Background

UT inspection of CEDM nozzles will be performed using a combination of time-of-flight diffraction (TOFD) and standard 0° pulse-echo techniques. The TOFD approach utilizes two pairs of 0.250-inch diameter, 55° refracted-longitudinal wave transducers aimed at each other. One of the transducers sends sound into the inspection volume while the other receives the reflected and diffracted signals as they interact with the material. There will be one TOFD pair looking in the axial direction of the penetration nozzle tube and one TOFD pair looking in the circumferential direction of the tube. The TOFD technique is primarily used to detect and characterize planer-type defects within the full volume of the tube.

The standard 0° pulse-echo ultrasonic approach utilizes two 0.250-inch diameter straight beam transducers. One transducer uses a center frequency of 2.25 MHz while the other uses a frequency of 5.0 MHz. The 0° technique is primarily used to plot the penetration tube outside diameter location and the J-groove attachment weld location, which are used to characterize the orientation and size of the defect. Additionally, the 0° technique is capable of locating and sizing any laminar-type defects that may be encountered.

The UT inspection procedures and techniques to be utilized at ANO-2 have been satisfactorily demonstrated under the EPRI Materials Reliability Program (MRP) Inspection Demonstration Program.

B. Hardship and Unusual Difficulty

Section VI.C.1(b)(i) of the Order requires UT inspection of RPV head penetration nozzles (i.e., nozzle base material) from two (2) inches above the J-groove weld to the bottom of the nozzle. However, a UT inspection of CEDM nozzles at ANO-2 can only be performed from 2 inches above the J-groove weld down to a point approximately 1.544 inches above the bottom of the nozzle. The reduced coverage is due to CEDM nozzle configuration (1.344 inches) and inspection probe design limitations (0.200 inch) as described below.

- Nozzle Configuration Limitation

Guide cones (funnels) are attached to the bottoms of the ANO-2 CEDM nozzles. The funnels are connected to the CEDM nozzles by threaded connections - the CEDM nozzles have internal threads while the funnels have external threads. The length of the threaded connection region is 1.25 inches. Additionally, a 45° chamfer exists immediately above the threaded connection region. The length of the chamfer region is 0.094 inch. (See Figure 1 for additional details.)

Due to the threaded connection and chamfer region at the bottom of each CEDM nozzle, a meaningful UT examination in that area cannot be performed. The UT scans of the region are obscured by multiple signals reflected back by the threaded surfaces and chamfer. Therefore, UT of the bottom 1.344 inches of the CEDM nozzles is impractical. To resolve UT limitations due to nozzle configuration, the existing CEDM nozzle-to-funnel threaded connections would

have to be eliminated, redesigned, and physically modified to provide for an acceptable UT examination.

- **Inspection Probe Blind Zone**

The inspection probe to be used in the inspection of ANO-2 CEDM nozzles consists of seven (7) individual transducers, as shown in Figure 2. Transducers 1 and 2 perform circumferential scans using TOFD; transducers 3 and 4 perform axial scans using TOFD; transducers 5 and 6 perform a standard 0° scan; and transducer 7 performs eddy current testing (ECT). (Note that the TOFD circumferential scans have demonstrated the capability to detect axial flaws in addition to circumferential flaws.) In order to achieve the maximum ultrasonic inspection coverage, the inspection probe is operated in such a way as to allow transducers 1 and 2 (UT TOFD for circumferential scans) to scan down to the top of the chamfer at the completion of the downward scan.

The inspection probe is designed so that the ultrasonic transducers are slightly recessed into the probe holder. This recess must be filled with water to provide coupling between the transducer and the component (i.e., nozzle wall). Because of this design, the complete diameter of the transducer must fully contact the inspection surface before ultrasonic information can be collected. Because UT probes 1 and 2 have a diameter of 0.250 inch, these transducers should, in theory, be able to collect meaningful UT data down to a point approximately 0.125 inch (1/2 diameter) above the chamfer. However, based on prior UT inspection experience and a review of UT data from previous inspections, the circumferential-shooting TOFD transducer pair only collects meaningful data down to a point 0.200 inch above the chamfer. Below this point, UT data cannot be collected with transducers 1 and 2. To resolve the probe's blind zone limitation, new UT equipment would have to be developed and appropriately qualified.

In conclusion, CEDM nozzles can be inspected in accordance with the Order from 2 inches above the J-groove weld to a point approximately 1.544 inches above the bottom of the nozzle. Below this point, compliance to the Order would result in hardship or unusual difficulty without a compensating increase in the level of quality and safety.

C. Suitability of Proposed Alternative

The suitability of the proposed alternative was established by an engineering evaluation that includes a finite element stress analysis (FEA) and fracture mechanics evaluations. The intent of the engineering evaluation was to determine whether residual stresses in the bottom 1.544 inches of the ANO-2 CEDM nozzles were sufficient to cause an axial flaw to propagate to the nozzle J-groove weld region. As explained in Section IV.A above, the 1.544-inch dimension defines the *UT examination lower limit* with respect to the bottom of the CEDM nozzle. The axial flaw geometry was selected for evaluation because of its potential to propagate to the nozzle J-groove weld region.

Four (4) CEDM nozzle locations were selected for analysis in the engineering evaluation. Selected locations were 0°, 8.8°, 28.8°, and 49.6° with the 0° location at the vertical centerline of the RPV head, the 49.6° location being the outermost nozzles, and the other two being intermediate locations between the center and outermost locations. The selected nozzle locations provide an adequate representation of residual stress profiles and a proper basis for analysis to bound all nozzle locations.

Postulated flaw locations along the nozzle circumference were identified by an azimuth angle, zero degrees being the furthest point from the center of the RPV head (downhill side of nozzle). Hoop stress distributions for each of the selected nozzles were determined for flaws located at 0° and 90° because these locations represent the shortest distance that a flaw would have to propagate to reach the nozzle J-groove weld region.

The stress distributions in the selected CEDM nozzles were evaluated in the "free-span length" from the bottom of the nozzle to the face of the J-groove weld (at the projected cladding interface), exclusive of the fillet weld reinforcement. See Figure 3 for additional details. The free-span length used in the FEA was 2.70 inches. However, based on ANO-2 design drawings, the minimum free-span length for the selected nozzles was determined to be 2.48 inches, which is 0.22 inch shorter than that used in the FEA. To compensate for the longer free-span nozzle length of the FEA model, the location for determining the through-wall hoop stress distribution in the FEA was also adjusted to align the FEA location from which the residual stresses were determined with the design location of the *UT examination lower limit*.

To determine whether residual stresses at the *UT examination lower limit* were sufficient to cause an axial flaw to propagate to the nozzle J-groove weld region, partial-depth surface flaws on the inside and outside diameter surfaces and through-wall flaws were analyzed at the 0° and 90° azimuthal locations for each of the selected nozzles. Crack growth rates from EPRI Report MRP-55 were utilized. Twenty-one (21) different flaw cases were analyzed with the following results:

Nozzle Location on RPV Head	Flaw Location on Nozzle (Azimuth)	Axial Flaw Evaluated	Flaw Evaluation Results *
0°	N/A	ID Surface	13.12 years to reach J-weld
		OD Surface	20.90 years to reach J-weld
		Through-wall	3.52 years to reach J-weld
8.8°	Downhill	ID Surface	17.56 years to reach J-weld
		OD Surface	19.02 years to reach J-weld
		Through-wall	3.80 years to reach J-weld
	90°	ID Surface	No potential for flaw growth
		OD Surface	No potential for flaw growth
		Through-wall	9.72 years to reach J-weld
28.8°	Downhill	ID Surface	No potential for flaw growth
		OD Surface	4.58 years to reach J-weld
		Through-wall	4.16 years to reach J-weld
	90°	ID Surface	No potential for flaw growth
		OD Surface	No potential for flaw growth
		Through-wall	No potential for flaw growth
49.6°	Downhill	ID Surface	No potential for flaw growth
		OD Surface	2.01 years to reach J-weld
		Through-wall	4.88 years to reach J-weld
	90°	ID Surface	No potential for flaw growth
		OD Surface	No potential for flaw growth
		Through-wall	No potential for flaw growth

* - Indicating operating years

In conclusion, the fracture mechanics evaluation demonstrated that residual stresses in the bottom 1.544 inches of the CEDM nozzle are insufficient to cause an axial flaw to propagate into the nozzle J-groove weld region prior to re-inspection during the next refueling outage. Based on the flaw evaluation, the shortest time for a flaw to grow from the *UT examination lower limit* to the nozzle J-groove weld region would be 2.01 years. Conservatism in the analysis (i.e., pressure applied to the flaw faces and high aspect ratio) provides additional assurance that an undetected flaw at the *UT examination lower limit* would not reach the nozzle J-groove weld region within one (1) operating cycle. Because stresses in CEDM nozzles below the *UT examination lower limit* are either lower than those at the limit or compressive, the potential for crack growth in this region is also significantly lower. For details regarding the engineering evaluation and its conclusions, see Engineering Report M-EP-2003-002, which is contained in Enclosure 3 of this submittal letter.

Impracticality of Supplemental Liquid Penetrant (PT) or ECT

Entergy also evaluated the feasibility of inspecting the bottom 1.544 inches of each CEDM nozzle using either the PT or ECT examination method. However, to perform a PT inspection, the guide cones would have to be removed from and reinstalled on all eighty-one (81) CEDM nozzles before and after performing the PT examinations. Entergy does not have the tooling to perform these operations remotely; therefore, the removal/reinstallation of the guide cones and the PT examinations would have to be performed manually. Manual performance of these operations would result in a significant increase in personnel radiation exposure. Entergy estimates that the dose associated with performing this PT inspection to be approximately 3 REM per nozzle.

The feasibility of using ECT was also evaluated. However, as with the UT inspection, the bottom 1.344 inches could not be inspected due to the design of CEDM nozzle in the guide cone connection and chamfer region. Additionally, a small ECT blind zone would exist above this region, which would further reduce the effectiveness of ECT.

V. CONCLUSION

Section IV.F of the Order states:

“Licensees proposing to deviate from the requirements of this Order shall seek relaxation of this Order pursuant to the procedure specified below. The Director, Office of Nuclear Reactor Regulation, may, in writing, relax or rescind any of the above conditions upon demonstration by the Licensee of good cause. A request for relaxation regarding inspection of specific nozzles shall also address the following criteria:

- (1) The proposed alternative(s) for inspection of specific nozzles will provide an acceptable level of quality and safety, or
- (2) Compliance with this Order for specific nozzles would result in hardship or unusual difficulty without a compensating increase in the level of quality and safety.”

Entergy believes that compliance with the UT inspection provisions of Section IV.C.1.b(i) of the Order as described in Section II, above, would result in hardship or unusual difficulty without a compensating increase in the level of quality and safety. The proposed alternative, described in Section III.B, would provide an acceptable level of quality and safety. The technical basis for the proposed alternative is documented in Engineering Report M-EP-2003-002, which is contained in Enclosure 3 of this submittal letter. Therefore, Entergy requests that the proposed alternative be authorized pursuant to Section IV.F of the Order.

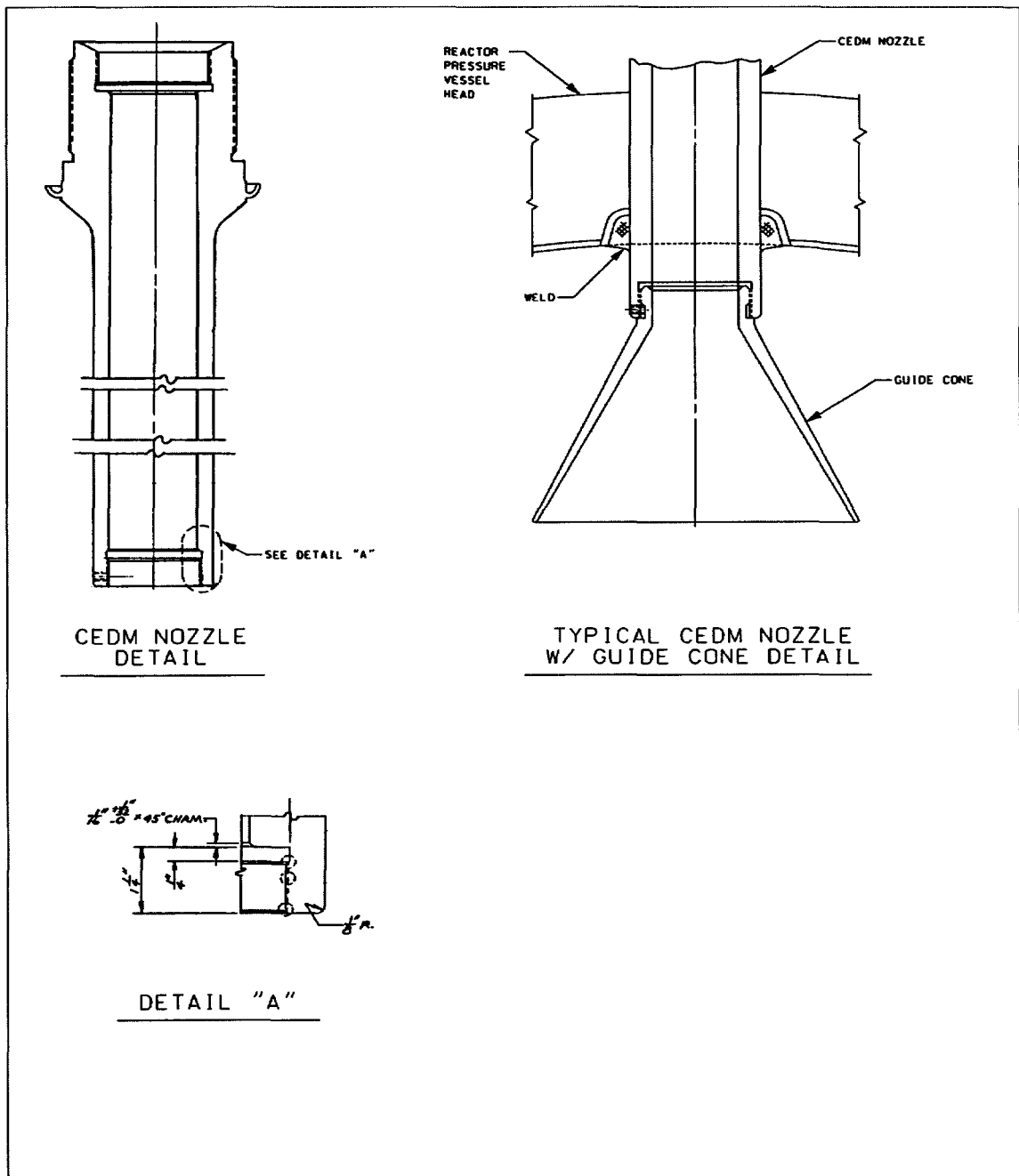
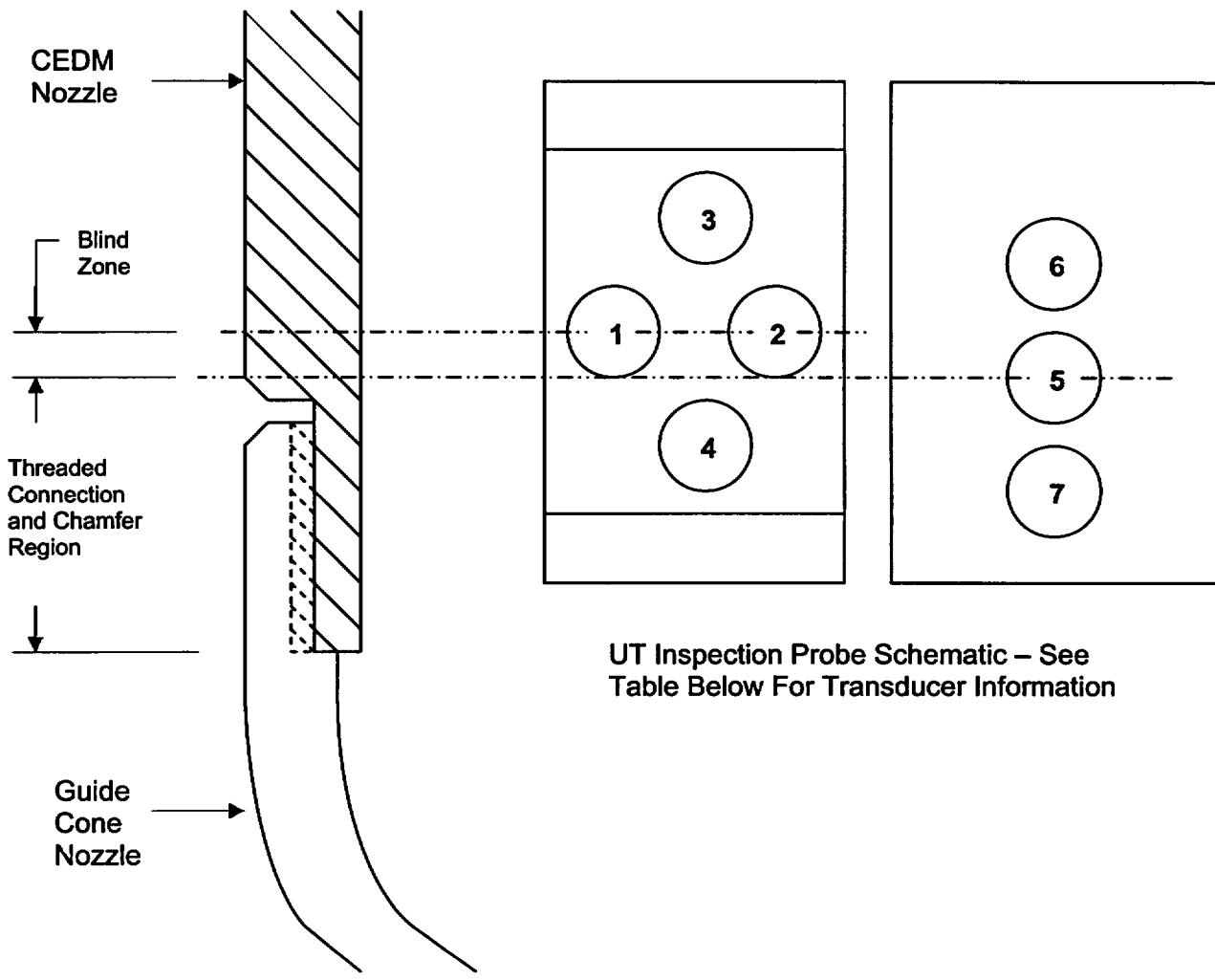


FIGURE 1
TYPICAL CEDM NOZZLE DETAILS



UT Inspection Probe Schematic – See Table Below For Transducer Information

Position	Mode	Diameter	Description
1	Transmit	0.25 inch	Circumferential Scan Using TOFD
2	Receive	0.25 inch	Circumferential Scan Using TOFD
3	Transmit	0.25 inch	Axial Scan Using TOFD
4	Receive	0.25 inch	Axial Scan Using TOFD
5	Transmit Receive	0.25 inch	Standard Zero Degree Scan
6	Transmit Receive	0.25 inch	Standard Zero Degree Scan
7	N/A	0.25 inch	Eddy Current

FIGURE 2
TYPICAL CEDM NOZZLE DETAILS

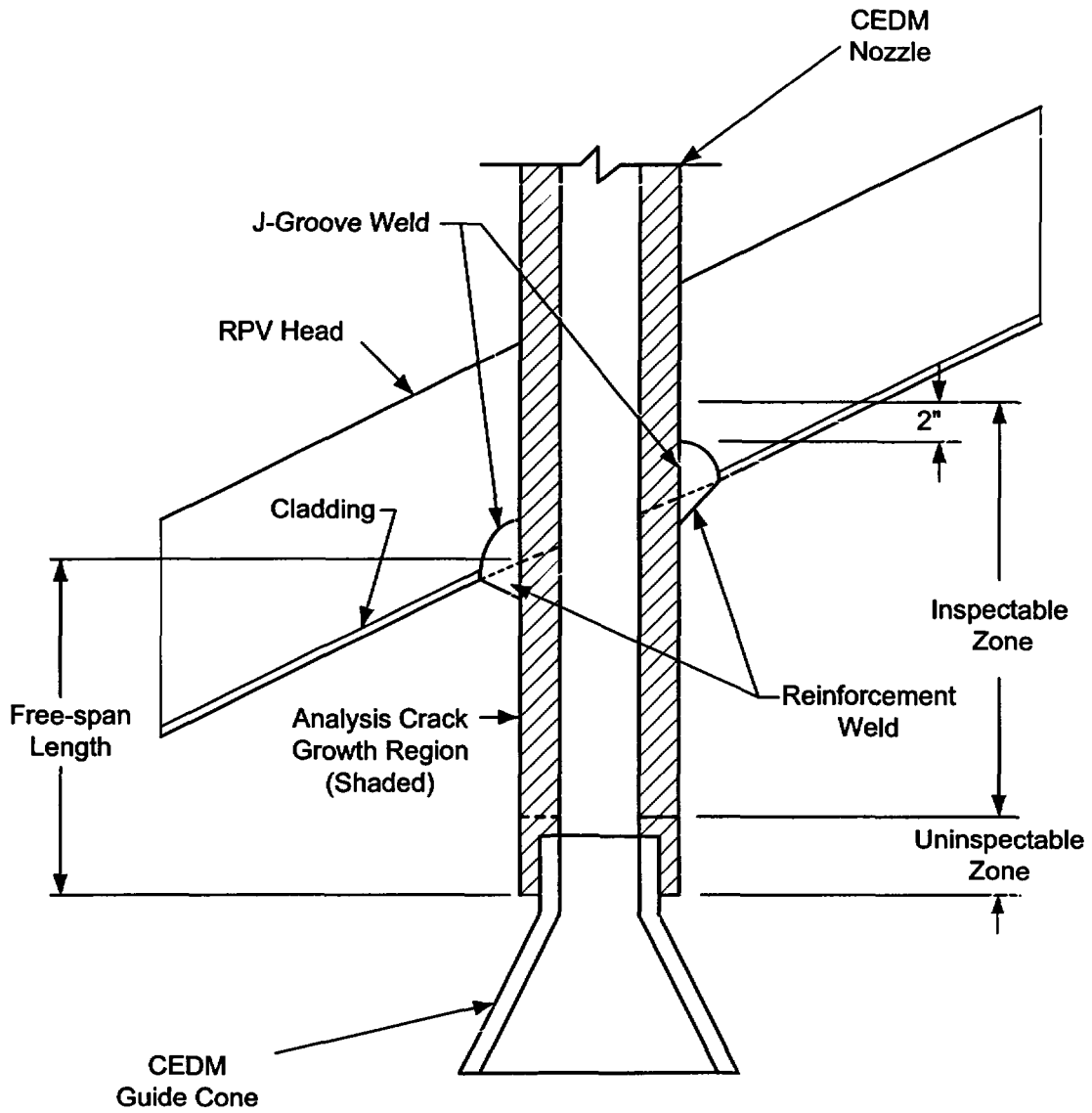


FIGURE 3
 DETAIL OF ANALYSIS CRACK GROWTH REGION

ENCLOSURE 2

CNRO-2003-00020

**RELAXATION REQUEST FOR
WATERFORD STEAM ELECTRIC STATION, UNIT 3**

**ENTERGY OPERATIONS, INC.
WATERFORD STEAM ELECTRIC STATION, UNIT 3**

I. COMPONENT/EXAMINATION

Component/Number: RC MRCT001

Description: Reactor Pressure Vessel (RPV) Head Penetration Nozzles

Code Class: 1

References:

1. NRC Order EA-03-009, Issuance of Order Establishing Interim Inspection Requirements for Reactor Pressure Vessel Heads at Pressurized Water Reactors
2. Letter W3F1-2003-0014 from Entergy Operations, Inc. to the NRC: "Entergy Operations, Inc. – Answer to Issuance of Order Establishing Interim Inspection Requirements for Reactor Pressure Vessel Heads at Pressurized Water Reactors", dated February 28, 2003
3. Engineering Report M-EP-2003-002, *Fracture Mechanics Analysis for Primary Water Stress Corrosion Crack (PWSCC) Growth in the Un-Inspected Regions of the Control Element Drive Mechanism (CEDM) Nozzles at Arkansas Nuclear One Unit 2 & Waterford Steam Electric Station Unit 3*
4. EPRI Material Reliability Program Crack Growth Rates for Evaluating Primary Water Stress Corrosion Cracking (PWSCC) of Thick-Wall Alloy 600 Materials (MRP-55) Revision 1

Unit: Waterford Steam Electric Station, Unit 3 (Waterford 3)

Inspection Interval: Second (2nd) 10-Year Interval

II. REQUIREMENTS

The NRC issued Order EA-03-009 (the Order) that modified the current licenses at nuclear facilities utilizing pressurized water reactors (PWRs), which includes Waterford Steam Electric Station, Unit 3 (Waterford 3). The NRC Order establishes inspection requirements for RPV head penetration nozzles. Waterford 3 is categorized as a "High" PWSCC susceptibility plant based on an effective degradation year (EDY) greater than 12. According to Section IV.C.1(b) of the Order, RPV head penetration nozzles in the "High" PWSCC susceptibility category shall be inspected using either of the following methods each refueling outage:

- (i) Ultrasonic testing of each RPV head penetration nozzle (i.e. nozzle base material) from two (2) inches above the J-groove weld to the bottom of the nozzle and an assessment to determine if leakage has occurred into the interference fit zone.

- (ii) Eddy current testing or dye penetrant testing of the wetted surface of each J-groove weld and RPV head penetration nozzle base material to at least two (2) inches above the J-groove weld.

III. PROPOSED ALTERNATIVE

A. Background

The Waterford 3 RPV head has one hundred-two (102) penetration nozzles that include ninety-one (91) Control Element Drive Mechanism (CEDM) nozzles, ten (10) Incore Instrument (ICI) nozzles, and one (1) vent line nozzle. Nozzle dimensions are identified below.

RPV Penetration Nozzle	Nozzle Dimensions		
	Outside Dia.	Inside Dia.	Thickness
CEDM	4.050 inches	2.728 inches	0.6610 inches
ICI	5.563 inches	4.750 inches	0.4065 inches
Vent Line	1.050 inches	0.742 inches	0.1540 inches

Entergy Operations, Inc. (Entergy) plans to inspect RPV head penetration nozzles at Waterford 3 using the ultrasonic testing (UT) method in accordance with Section IV.C.1(b)(i) of the Order. However, due to nozzle configuration at the guide cone connection and UT coverage limitations, CEDM nozzles cannot be inspected to the bottom as required by the Order. Therefore, Entergy requests relaxation from the UT coverage requirements of Section IV.C.1(b)(i) of the Order and proposes an alternative in Section III.B, below.

This relaxation request does not apply to ICI nozzles or the vent line nozzle.

B. Proposed Alternative

Paragraph IV.C.1(b)(i) of the Order requires that the UT inspection of each RPV head penetration nozzle extend "from two (2) inches above the J-groove weld to the bottom of the nozzle." Entergy requests relaxation from this provision for CEDM nozzles and proposes the following alternative:

- CEDM nozzles (i.e., nozzle base material) shall be ultrasonically examined from two (2) inches above the J-groove weld to 1.544 inches above the bottom of the nozzle. A fracture mechanics evaluation has been performed and demonstrates that residual stresses in the bottom portion of the nozzle are insufficient to cause an axial flaw to propagate into the pressure boundary region of the nozzle along the J-groove weld (nozzle J-groove weld region) prior to re-inspection during the next refueling outage.

IV. BASIS FOR PROPOSED ALTERNATIVE

A. Background

UT inspection of CEDM nozzles will be performed using a combination of time-of-flight diffraction (TOFD) and standard 0° pulse-echo techniques. The TOFD approach utilizes two pairs of 0.250-inch diameter, 55° refracted-longitudinal wave transducers aimed at each other. One of the transducers sends sound into the inspection volume while the other receives the reflected and diffracted signals as they interact with the material. There will be one TOFD pair looking in the axial direction of the penetration nozzle tube and one TOFD pair looking in the circumferential direction of the tube. The TOFD technique is primarily used to detect and characterize planer-type defects within the full volume of the penetration tube.

The standard 0° pulse-echo ultrasonic approach utilizes two 0.250-inch diameter straight beam transducers. One transducer uses a center frequency of 2.25 MHz while the other uses a frequency of 5.0 MHz. The 0° technique is primarily used to plot the penetration tube outside diameter location and the J-groove attachment weld location, which are used to characterize orientation and size of the defect. Additionally, the 0° technique is capable of locating and sizing any laminar-type defects that may be encountered.

The UT inspection procedures and techniques to be utilized at Waterford 3 have been satisfactorily demonstrated under the EPRI Materials Reliability Program (MRP) Inspection Demonstration Program.

B. Hardship and Unusual Difficulty

Section VI.C.1(b)(i) of the Order requires UT inspection of RPV head penetration nozzles (i.e., nozzle base material) from two (2) inches above the J-groove weld to the bottom of the nozzle. However, a UT inspection of CEDM nozzles at Waterford 3 can only be performed from 2 inches above the J-groove weld down to a point approximately 1.544 inches above the bottom of the nozzle. The reduced coverage is due to CEDM nozzle configuration (1.344 inches) and inspection probe design limitations (0.200 inch) as described below.

- Nozzle Configuration Limitation

Guide cones (funnels) are attached to the bottoms of the Waterford 3 CEDM nozzles. The funnels are connected to the CEDM nozzles by threaded connections – the CEDM nozzles have internal threads while the funnels have external threads. The length of the threaded connection region is 1.25 inches. Additionally, a 45° chamfer exists immediately above the threaded connection region. The length of the chamfer region is 0.094 inch. (See Figure 1 for additional details.)

Due to the threaded connection and chamfer region at the bottom of each CEDM nozzle, a meaningful UT examination in that area cannot be performed. The UT scans of the region are obscured by multiple signals reflected back by the threaded surfaces and chamfer. Therefore, UT of the bottom 1.344 inches of the CEDM nozzles is impractical. To resolve UT limitations due to nozzle

configuration, the existing CEDM nozzle-to-funnel threaded connections would have to be eliminated, redesigned, and physically modified to provide for an acceptable UT examination.

- Inspection Probe Blind Zone

The inspection probe to be used in the inspection of Waterford 3 CEDM nozzles consists of seven (7) individual transducers, as shown in Figure 2. Transducers 1 and 2 perform circumferential scans using TOFD; transducers 3 and 4 perform axial scans using TOFD; transducers 5 and 6 perform a standard 0° scan; and transducer 7 performs eddy current testing (ECT). (Note that the TOFD circumferential scans have demonstrated the capability to detect axial flaws in addition to circumferential flaws.) In order to achieve the maximum ultrasonic inspection coverage, the inspection probe is operated in such a way as to allow transducers 1 and 2 (UT TOFD for circumferential scans) to scan down to the top of the chamfer at the completion of the downward scan.

The inspection probe is designed so that the ultrasonic transducers are slightly recessed into the probe holder. This recess must be filled with water to provide coupling between the transducer and the component (i.e., nozzle wall). Because of this design, the complete diameter of the transducer must fully contact the inspection surface before ultrasonic information can be collected. Because UT probes 1 and 2 have a diameter of 0.250 inch, these transducers should, in theory, be able to collect meaningful UT data down to a point approximately 0.125 inch (1/2 diameter) above the chamfer. However, based on prior UT inspection experience and a review of UT data from previous inspections, the circumferential-shooting TOFD transducer pair only collects meaningful data down to a point 0.200 inch above the chamfer. Below this point, UT data cannot be collected with transducers 1 and 2. To resolve the probe's blind zone limitation, new UT equipment would have to be developed and appropriately qualified.

In conclusion, CEDM nozzles can be inspected in accordance with the Order from 2 inches above the J-groove weld to a point approximately 1.544 inches above the bottom of the nozzle. Below this point, compliance to the Order would result in hardship or unusual difficulty without a compensating increase in the level of quality and safety.

C. Suitability of Proposed Alternative

The suitability of the proposed alternative was established by an engineering evaluation that includes a finite element stress analysis (FEA) and fracture mechanics evaluations. The intent of the engineering evaluation was to determine whether residual stresses in the bottom 1.544 inches of the Waterford 3 CEDM nozzles were sufficient to cause an axial flaw to propagate to the nozzle J-groove weld region. As explained in Section IV.A above, the 1.544-inch dimension defines the *UT examination lower limit* with respect to the bottom of the CEDM nozzle. The axial flaw geometry was selected for evaluation because of its potential to propagate to the nozzle J-groove weld region.

Four (4) CEDM nozzle locations were selected for analysis in the engineering evaluation. Selected locations were 0°, 7.8°, 29.1°, and 49.7° with the 0° location at the vertical centerline of the RPV head, the 49.7° location being the outermost nozzles, and the other two being intermediate locations between the center and outermost locations. The selected nozzle locations provide an adequate representation of residual stress profiles and a proper basis for analysis to bound all nozzle locations.

Postulated flaw locations along the nozzle circumference were identified by an azimuth angle, zero degrees being the furthest point from the center of the RPV head (downhill side of nozzle). Hoop stress distributions for each of the selected nozzles were determined for flaws located at 0° and 90° because these locations represent the shortest distance that a flaw would have to propagate to reach the nozzle J-groove weld region.

The stress distributions in the selected CEDM nozzles were evaluated in the “free-span length” from the bottom of the nozzle to the face of the J-groove weld (at the projected cladding interface), exclusive of the fillet weld reinforcement. See Figure 3 for additional details. The free-span length used in the FEA was 2.70 inches. However, based on Waterford 3 design drawings, the minimum free-span length for the selected nozzles was determined to be 2.86 inches, which is 0.16 inch longer than that used in the FEA. As a result, the location of the *UT examination lower limit* in the FEA model is higher than the design location by 0.16 inch. Although the FEA location provides a higher through-wall hoop stress distribution, this location was used in the analysis for conservatism.

To determine whether residual stresses at the *UT examination lower limit* are sufficient to cause an axial flaw to propagate to the nozzle J-groove weld region, partial-depth surface flaws on the inside and outside diameter surfaces and through-wall flaws were analyzed at the 0° and 90° azimuthal locations for each of the selected nozzles. Crack growth rates from EPRI Report MRP-55 were utilized. Twenty-one (21) different flaw cases were analyzed with the following results:

Nozzle Location on RPV Head	Flaw Location on Nozzle (Azimuth)	Axial Flaw Evaluated	Flaw Evaluation Results *
0°	N/A	ID Surface	23.44 years to reach J-weld
		OD Surface	No potential for flaw growth
		Through-wall	8.56 years to reach J-weld
7.8°	Downhill	ID Surface	> 40 years to reach J-weld
		OD Surface	No potential for flaw growth
		Through-wall	8.92 years to reach J-weld
	90°	ID Surface	No potential for flaw growth
		OD Surface	No potential for flaw growth
		Through-wall	35.52 years to reach J-weld
29.1°	Downhill	ID Surface	No potential for flaw growth
		OD Surface	No potential for flaw growth
		Through-wall	28.08 years to reach J-weld
	90°	ID Surface	No potential for flaw growth
		OD Surface	No potential for flaw growth
		Through-wall	No potential for flaw growth
49.7°	Downhill	ID Surface	No potential for flaw growth
		OD Surface	No potential for flaw growth
		Through-wall	No potential for flaw growth
	90°	ID Surface	No potential for flaw growth
		OD Surface	No potential for flaw growth
		Through-wall	No potential for flaw growth

* - Indicating operating years

In conclusion, the fracture mechanics evaluation demonstrated that residual stresses in the bottom 1.544 inches of the CEDM nozzle are insufficient to cause an axial flaw to propagate into the nozzle J-groove weld region prior to re-inspection during the next refueling outage. Based on the flaw evaluation, the shortest time for a flaw to grow from the *UT examination lower limit* to the nozzle J-groove weld region would be 8.56 years. Conservatism in the analysis (i.e., pressure applied to the flaw faces and high aspect ratio) provides additional assurance that an undetected flaw at the *UT examination lower limit* would not reach the J-groove weld interface within one (1) operating cycle. Because stresses in CEDM nozzles below the *UT examination lower limit* are either lower than those at the limit or compressive, the potential for crack growth in this region is also significantly lower. For details regarding the engineering evaluation and its conclusions, see Engineering Report M-EP-2003-002, which is contained in Enclosure 3 of this submittal letter.

Impracticality of Supplemental Liquid Penetrant (PT) or ECT

Entergy also evaluated the feasibility of inspecting the bottom 1.544 inches of each CEDM nozzle using either the PT or ECT examination method. However, to perform a PT inspection, the guide cones would have to be removed from and reinstalled on all ninety-one (91) CEDM nozzles before and after performing the PT examinations. Entergy does not have the tooling to perform these operations remotely; therefore, the removal/reinstallation of the guide cones and the PT examinations would have to be performed manually. Manual performance of these operations would result in a significant increase in personnel radiation exposure. Entergy estimates that the dose associated with performing this PT inspection to be approximately 3 REM per nozzle.

The feasibility of using ECT was also evaluated. However, as with the UT inspection, the bottom 1.344 inches could not be inspected due to the design of CEDM nozzle in the guide cone connection and chamfer region. Additionally, a small ECT blind zone would exist above this region, which would further reduce the effectiveness of ECT.

V. CONCLUSION

Section IV.F of the Order states:

“Licensees proposing to deviate from the requirements of this Order shall seek relaxation of this Order pursuant to the procedure specified below. The Director, Office of Nuclear Reactor Regulation, may, in writing, relax or rescind any of the above conditions upon demonstration by the Licensee of good cause. A request for relaxation regarding inspection of specific nozzles shall also address the following criteria:

- (1) The proposed alternative(s) for inspection of specific nozzles will provide an acceptable level of quality and safety, or
- (2) Compliance with this Order for specific nozzles would result in hardship or unusual difficulty without a compensating increase in the level of quality and safety.”

Entergy believes that compliance with the UT inspection provisions of Section IV.C.1(b)(i) of the Order as described in Section II, above, would result in hardship or unusual difficulty without a compensating increase in the level of quality and safety. The proposed alternative described in Section III.B of the request would provide an acceptable level of quality and safety. The technical basis for the proposed alternative is documented in Engineering Report M-EP-2003-002, which is contained in Enclosure 3 of this submittal letter. Therefore, Entergy requests that the proposed alternative be authorized pursuant to Section IV.F of the Order.

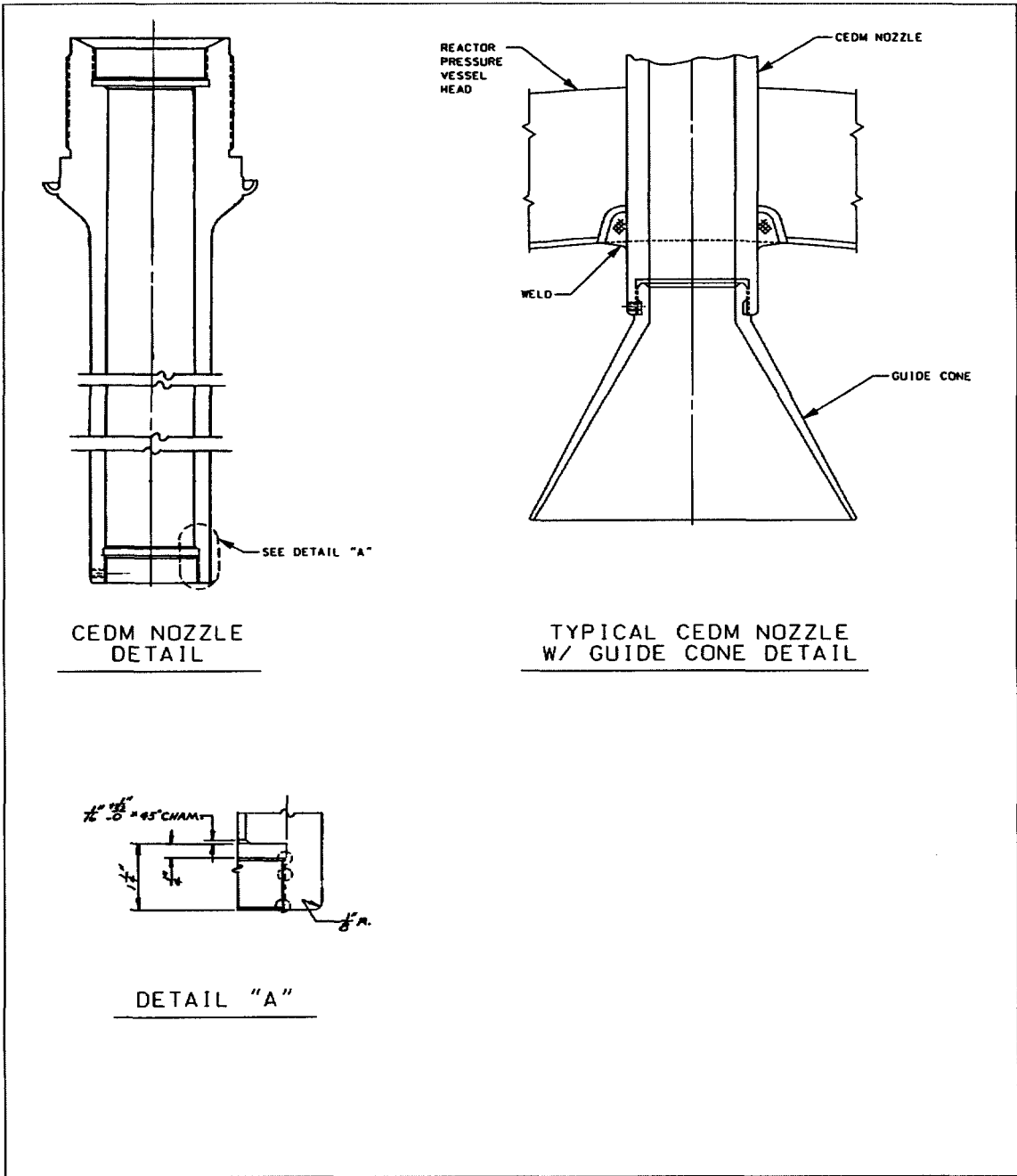
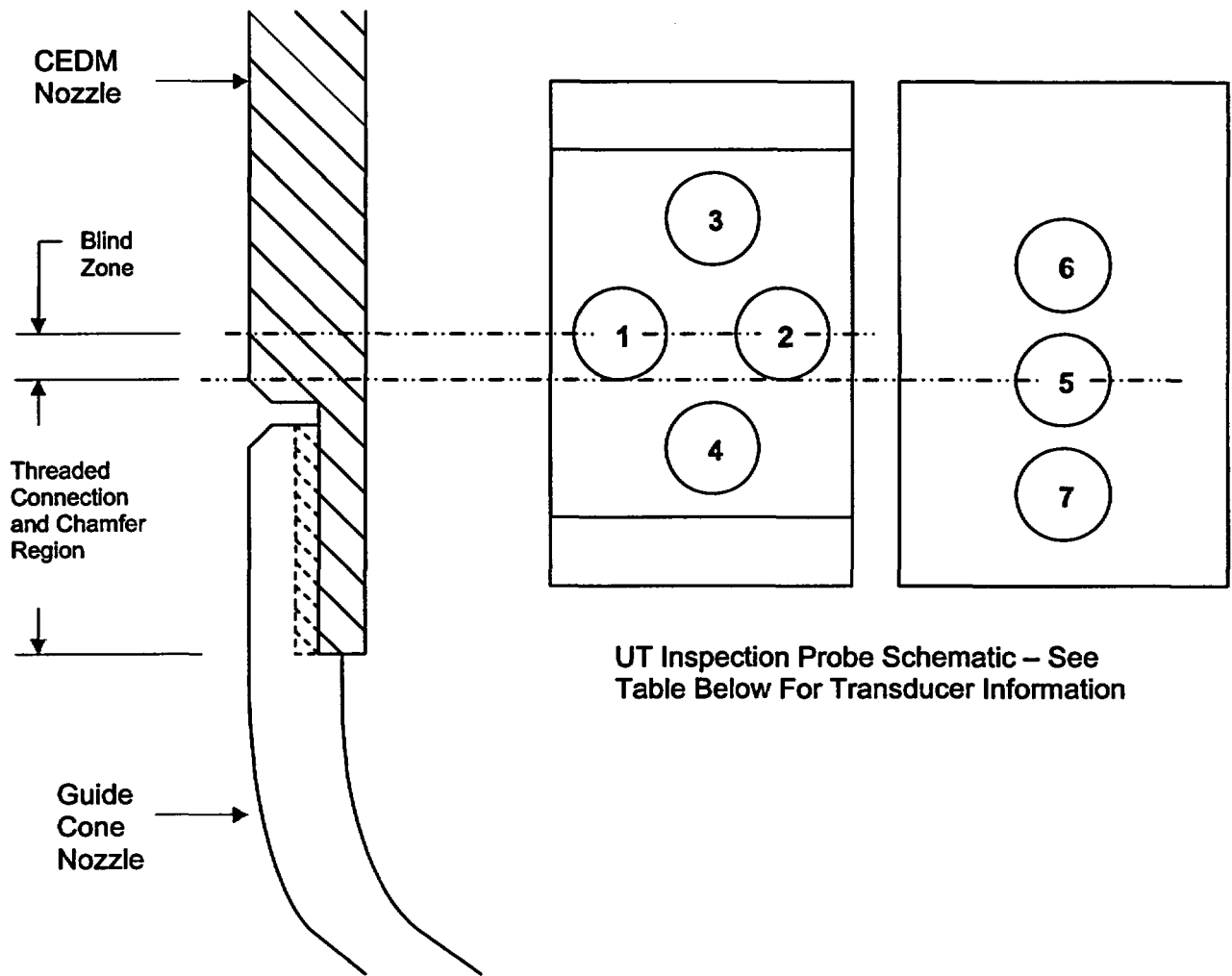


FIGURE 1
TYPICAL CEDM NOZZLE DETAILS



UT Inspection Probe Schematic – See Table Below For Transducer Information

Position	Mode	Diameter	Description
1	Transmit	0.25 inch	Circumferential Scan Using TOFD
2	Receive	0.25 inch	Circumferential Scan Using TOFD
3	Transmit	0.25 inch	Axial Scan Using TOFD
4	Receive	0.25 inch	Axial Scan Using TOFD
5	Transmit Receive	0.25 inch	Standard Zero Degree Scan
6	Transmit Receive	0.25 inch	Standard Zero Degree Scan
7	N/A	0.25 inch	Eddy Current

FIGURE 2
Inspection Probe Module Detail

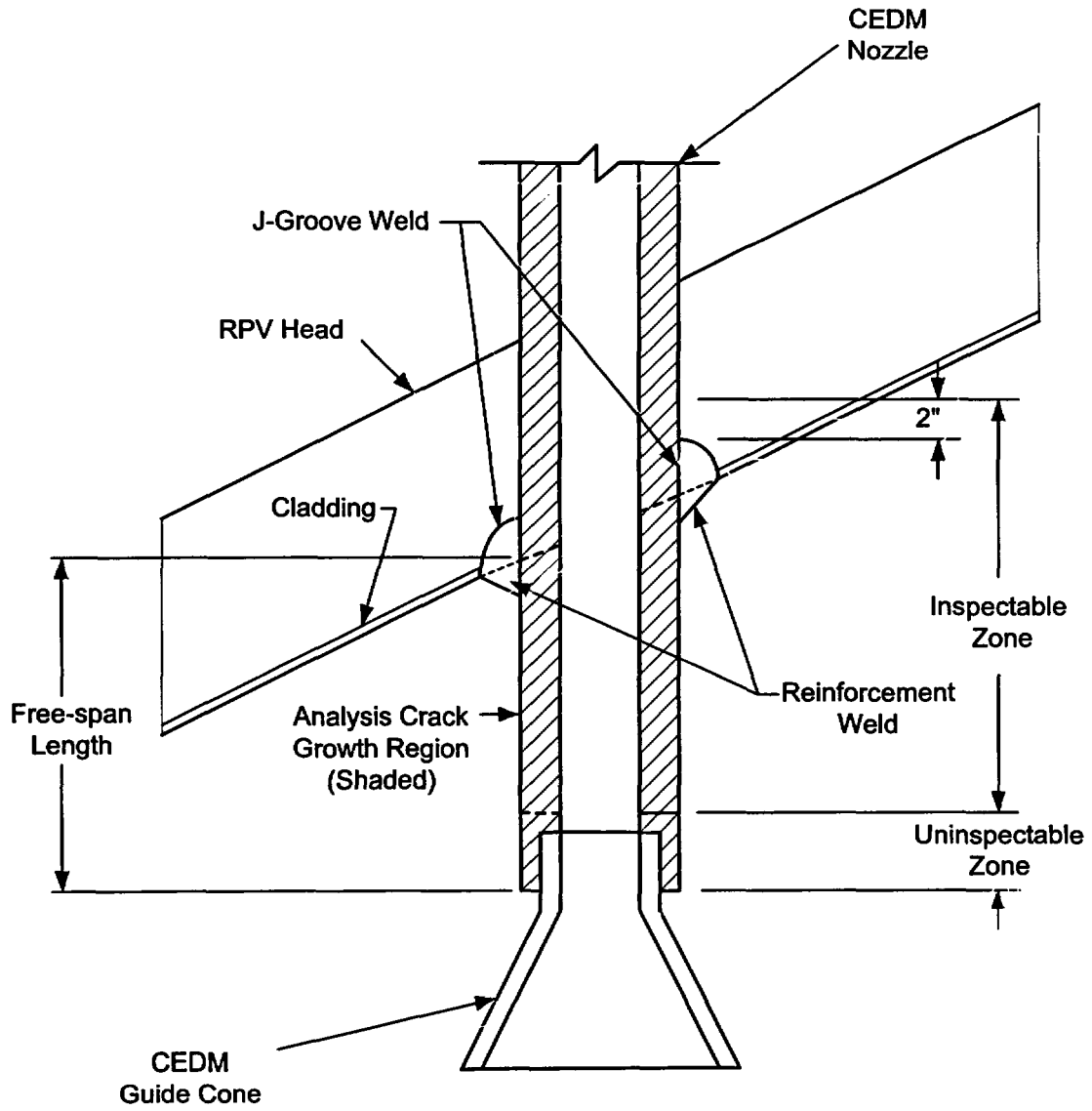


FIGURE 3
 DETAIL OF ANALYSIS CRACK GROWTH REGION

ENCLOSURE 3

ENGINEERING REPORT M-EP-2003-002

**FRACTURE MECHANICS ANALYSIS FOR THE ASSESSMENT OF THE
POTENTIAL FOR PRIMARY WATER STRESS CORROSION CRACK (PWSCC)
GROWTH IN THE UNINSPECTED REGIONS OF THE
CONTROL ELEMENT DRIVE MECHANISM (CEDM) NOZZLES AT
ARKANSAS NUCLEAR ONE UNIT 2 &
WATERFORD STEAM ELECTRIC STATION UNIT 3**



**ENTERGY NUCLEAR SOUTH
 Engineering Report Coversheet**

**Fracture Mechanics Analysis for the Assessment
 of the
 Potential for Primary Water Stress Corrosion Crack (PWSCC) Growth
 in the
 Un-Inspected Regions of the Control Element Drive Mechanism (CEDM) Nozzles
 at
 Arkansas Nuclear One Unit 2 & Waterford Steam Electric Station Unit 3**

Engineering Report Type:

New Revision Deleted Superseded

Applicable Site(s)

ANO Echelon GGNS RBS WF3

Report Origin: ENS Vendor Safety-Related: Yes No

Vendor Document No. _____

Prepared by:	<u>2. S. Baharadaram</u>	Date:	<u>6/6/2003</u>	Comments:	Attached:
	Responsible Engineer			<input type="checkbox"/> Yes	<input type="checkbox"/> Yes
Verified/ Reviewed by:	<u>Brian C. Gray</u>	Date:	<u>6/6/03</u>	<input checked="" type="checkbox"/> No	<input checked="" type="checkbox"/> No
	Design Verifier/Reviewer			<input checked="" type="checkbox"/> Yes	<input type="checkbox"/> Yes
				<input type="checkbox"/> No	<input checked="" type="checkbox"/> No
Approved by:	<u>Charles J. [Signature]</u>	Date:	<u>6/9/03</u>	<input type="checkbox"/> Yes	<input type="checkbox"/> Yes
	Responsible Supervisor or Responsible Central Engineering Manager (for multiple site reports only)			<input checked="" type="checkbox"/> No	<input checked="" type="checkbox"/> No

Engineering Report No. _____ Rev. _____
Page _____ of _____

RECOMMENDATION FOR APPROVAL FORM

		Date:	Comments:	Attached:
			<input type="checkbox"/> Yes	<input type="checkbox"/> Yes
Prepared by:	<u>William Ding 6/6/03</u>		<input type="checkbox"/> No	<input type="checkbox"/> No
	Responsible Engineer	<u>4/6/03</u>		
Concurrence:	<u>Keith Lichol</u>	Date: <u>6/6/3</u>	<input type="checkbox"/> Yes	<input type="checkbox"/> Yes
	Responsible Engineering Manager, ANO		<input checked="" type="checkbox"/> No	<input checked="" type="checkbox"/> No
Concurrence:	Not Applicable	Date: _____	<input type="checkbox"/> Yes	<input type="checkbox"/> Yes
	Responsible Engineering Manager, GGNS		<input type="checkbox"/> No	<input type="checkbox"/> No
Concurrence:	Not Applicable	Date: _____	<input type="checkbox"/> Yes	<input type="checkbox"/> Yes
	Responsible Engineering Manager, RBS		<input type="checkbox"/> No	<input type="checkbox"/> No
Concurrence:	See Page 2b for WF3 signature(s)	Date: _____	<input type="checkbox"/> Yes	<input type="checkbox"/> Yes
	Responsible Engineering Manager, WF3		<input type="checkbox"/> No	<input type="checkbox"/> No

Engineering Report No. _____ Rev. _____
Page _____ of _____

RECOMMENDATION FOR APPROVAL FORM

		Date:	Comments:	Attached:
Prepared by:	See Page 2a for ANO signature(s)	_____	<input type="checkbox"/> Yes	<input type="checkbox"/> Yes
	Responsible Engineer	_____	<input type="checkbox"/> No	<input type="checkbox"/> No
Concurrence:	_____	Date: _____	<input type="checkbox"/> Yes	<input type="checkbox"/> Yes
	Responsible Engineering Manager, ANO	_____	<input type="checkbox"/> No	<input type="checkbox"/> No
	Not Applicable			
Concurrence:	_____	Date: _____	<input type="checkbox"/> Yes	<input type="checkbox"/> Yes
	Responsible Engineering Manager, GGNS	_____	<input type="checkbox"/> No	<input type="checkbox"/> No
	Not Applicable			
Concurrence:	_____	Date: _____	<input type="checkbox"/> Yes	<input type="checkbox"/> Yes
	Responsible Engineering Manager, RBS	_____	<input type="checkbox"/> No	<input type="checkbox"/> No
Concurrence:	<i>Joseph S. Reese</i>	Date: <i>6/9/03</i>	<input type="checkbox"/> Yes	<input type="checkbox"/> Yes
	Responsible Engineering Manager, WF3		<input checked="" type="checkbox"/> No	<input checked="" type="checkbox"/> No

NRay

Table of Contents

Section	Title	Page Number
	List of Tables	3
	List of Figures	4
	List of Appendices	7
1.0	Introduction	8
2.0	Stress Analysis	11
3.0	Fracture Mechanics Analysis	32
4.0	Discussion and Results	38
5.0	Conclusions	50
6.0	References	51

List of Tables

Table Number	Title	Page Number
IA	ANO-2 CEDM Downhill Location Nodal Stresses	22
IB	ANO-2 CEDM Ninety Degree Location Nodal Stresses	23
IIA	WSES-3 CEDM Downhill Location Nodal Stresses	24
IIB	WSES-3 CEDM Ninety Degree Location Nodal Stresses	25
III	Hoop Stress Distribution Used for Analysis {1.644" above Nozzle Bottom}	26
IV	ANO-2 Evaluation Results	40
V	WSES-3 Evaluation Results	41
VI	Available Nozzle Length for (PWSCC) Flaw Growth	42
VII	ANO-2 Results for PWSCC Growth Cases	47
VIII	WSES-3 Results for PWSCC Growth Cases	50

List of Figures

Figure Number	Title	Page Number
1	Details of funnel connection to CEDM [2]. Detail extracted from Drawing M-2001-C2-107 [2]. The threaded region in the CEDM is 1.125 inch. Both ANO-2 and WSES-3 have similar connection geometry	9
2	Sketch of the inspection probe [3a]. Both probes (EC and UT) have a diameter 0.25 inch. The UT probes to detect axial flaws are numbered 1 and 2 and the EC probe is numbered 7.	10
3	ANO-2 CEDM Nozzles at four locations on the head. The region of interest is located at the bottom. The cyan contour ranges fro 10ksi (tensile) to zero; the light blue contour from zero to -10 ksi 9compressive and the dark blue contour is compressive stresses in excess of -10 ksi.	12
4	WSES-3 CEDM Nozzles at four locations on the head. The region of interest is located at the bottom. The cyan contour ranges fro 10ksi (tensile) to zero; the light blue contour from zero to -10 ksi 9compressive and the dark blue contour is compressive stresses in excess of -10 ksi.	13
5	ANO-2 Hoop stress profile (ID & OD) for the zero degree nozzle.	14
6	ANO-2 Hoop stress profile (ID & OD) for the "8.8" degree nozzle at the downhill location.	15
7	ANO-2 Hoop stress profile (ID & OD) for the "28.8" degree nozzle at the downhill location.	15
8	ANO-2 Hoop stress profile (ID & OD) for the "49.6" degree nozzle at the downhill location.	16
9	ANO-2 Hoop stress profile (ID & OD) for the "8.8" degree nozzle at the ninety degree location.	16
10	ANO-2 Hoop stress profile (ID & OD) for the "28.8" degree nozzle at the ninety degree location.	17
11	ANO-2 Hoop stress profile (ID & OD) for the "49.6" degree nozzle at the ninety degree location.	17
12	WSES-3 Hoop stress profile (ID & OD) for the "zero" degree nozzle.	18
13	WSES-3 Hoop stress profile (ID & OD) for the "7.8" degree nozzle at the downhill location.	19
14	WSES-3 Hoop stress profile (ID & OD) for the "29.1" degree nozzle at the downhill location.	19
15	WSES-3 Hoop stress profile (ID & OD) for the "49.7" degree nozzle at the downhill location.	20
16	WSES-3 Hoop stress profile (ID & OD) for the "7.8" degree nozzle at the ninety degree location.	20
17	WSES-3 Hoop stress profile (ID & OD) for the "29.1" degree nozzle at the ninety degree location.	21
18	WSES-3 Hoop stress profile (ID & OD) for the "49.7" degree nozzle at the ninety degree location.	21

List of Figures (Continued)

Figure Number	Title	Page Number
19	ANO-2 downhill location for all nozzles evaluated. The stress distribution is from the ID to OD. The coefficients in the respective equations will be used in the fracture mechanics analysis.	27
20	ANO-2 90° azimuth location for all nozzles evaluated. The stress distribution is from the ID to OD. The coefficients in the respective equations will be used in the fracture mechanics analysis.	28
21	ANO-2 downhill location for all nozzles evaluated. The stress distribution is from the OD to ID. The coefficients in the respective equations will be used in the fracture mechanics analysis.	28
22	ANO-2 90° azimuth location for all nozzles evaluated. The stress distribution is from the OD to ID. The coefficients in the respective equations will be used in the fracture mechanics analysis.	29
23	WSES-3 downhill location for all nozzles evaluated. The stress distribution is from the ID to OD. The coefficients in the respective equations will be used in the fracture mechanics analysis.	30
24	WSES-3 90° azimuth location for all nozzles evaluated. The stress distribution is from the ID to OD. The coefficients in the respective equations will be used in the fracture mechanics analysis.	30
25	WSES-3 downhill location for all nozzles evaluated. The stress distribution is from the OD to ID. The coefficients in the respective equations will be used in the fracture mechanics analysis.	31
26	WSES-3 90° azimuth location for all nozzles evaluated. The stress distribution is from the OD to ID. The coefficients in the respective equations will be used in the fracture mechanics analysis.	31
27	Comparison of SIF from reference 8 and 9 utilizing the same stress distribution (WSES-3, 7.8° nozzle at the 0° azimuth at an axial elevation of 1.644" above bottom of nozzle).	34
28	Curve fit equations for the "extension and "bending" components in reference 10. Table 1c and 1d for membrane loading and tables 1g and 1h for bending loading.	36
29	ANO-2; Plots for an ID surface crack growth and SIF versus operating time for the 0° nozzle at the 0° azimuth (downhill position).	43
30	ANO-2; Plots for an ID surface crack growth and SIF versus operating time for the 8.8° nozzle at the 0° azimuth (downhill position).	43
31	ANO-2; Plots for an OD surface crack growth and SIF versus operating time for the 0° nozzle at the 0° azimuth (downhill position).	43
32	ANO-2; Plots for an OD surface crack growth and SIF versus operating time for the 8.8° nozzle at the 0° azimuth (downhill position).	44
33	ANO-2; Plots for an OD surface crack growth and SIF versus operating time for the 28.8° nozzle at the 0° azimuth (downhill position).	44

List of Figures (Continued)

Figure Number	Title	Page Number
34	ANO-2; Plots for an OD surface crack growth and SIF versus operating time for the 49.6° nozzle at the 0° azimuth (downhill position).	44
35	ANO-2; Plots for a through-wall axial crack growth and SIF versus operating time for the 0° nozzle at the 0° azimuth (downhill position).	45
36	ANO-2; Plots for a through-wall axial crack growth and SIF versus operating time for the 8.8° nozzle at the 0° azimuth (downhill position).	45
37	ANO-2; Plots for a through-wall axial crack growth and SIF versus operating time for the 28.8° nozzle at the 0° azimuth (downhill position).	45
38	ANO-2; Plots for a through-wall axial crack growth and SIF versus operating time for the 49.6° nozzle at the 0° azimuth (downhill position).	46
39	ANO-2; Plots for a through-wall axial crack growth and SIF versus operating time for the 8.8° nozzle at the 90° azimuth	46
40	WSES-3; Plots for an ID surface axial crack growth and SIF versus operating time for the 0° nozzle at the 0° azimuth (downhill position).	47
41	WSES-3; Plots for an ID surface axial crack growth and SIF versus operating time for the 7.8° nozzle at the 0° azimuth (downhill position).	48
42	WSES-3; Plots for a through-wall axial crack growth and SIF versus operating time for the 0° nozzle at the 0° azimuth (downhill position).	48
43	WSES-3; Plots for a through-wall axial crack growth and SIF versus operating time for the 7.8° nozzle at the 0° azimuth (downhill position).	48
44	WSES-3; Plots for a through-wall axial crack growth and SIF versus operating time for the 29.1° nozzle at the 0° azimuth (downhill position).	49
45	WSES-3; Plots for a through-wall axial crack growth and SIF versus operating time for the 7.8° nozzle at the 90° azimuth.	49

List of Appendices

Appendix Number	Content of Appendix	Number of Attachments In Appendix
I	Design Input Information- Concurrence from Site	4
II	Mathcad worksheets for ANO-2 Analyses	21
III	Mathcad worksheets for WSES-3 Analyses	21

1.0 Introduction

The US Nuclear Regulatory Commission (NRC) issued Order EA-03-009 [1], which modified licenses, requiring inspection of all Control Element Drive Mechanism (CEDM), In-Core Instrumentation (ICI), and vent penetration nozzles in the reactor vessel head. The region for inspection, specified in the Order paragraph IV.C.1.b, requires the inspection to cover a region from the bottom of the nozzle to two (2.0) inches above the J-groove weld. In the Combustion Engineering (CE) design the CEDM nozzles have a funnel attached to the bottom of each CEDM. Figure 1 [2] provides a drawing showing the attachment detail and a sketch showing the typical CEDM arrangement in the reactor vessel head. The attachment is a threaded connection with a securing set-screw between the funnel and the CEDM nozzle. The CEDM nozzle is internally threaded and the funnel has external threads. Thus, the CEDM nozzles in the region of attachment, including the chamfered region, become in-accessible for both Eddy Current (EC) and Ultrasonic Testing (UT) to interrogate the nozzle base metal in this region. The design of the EC probe would have a small dead zone above the chamfer region whereas the design of the UT probes would have a larger region above the chamfer (0.200 inch [reference 3a & 3b]) that cannot be inspected. Therefore, the region of the CEDM base metal that can be inspected extends from about 1.544 inches (UT) above the bottom of the CEDM nozzle to two (2.0) inches above the J-groove weld. The unexamined length constitutes the threaded region, the chamfer region, and the UT dead zone ($1.250 + 0.094 + 0.200$). Therefore, the examination region would be the difference between the freespan length of the nozzle below the J-weld and the un-examinable region. The freespan length for both Arkansas Nuclear One, Unit 2 (ANO-2) and Waterford Steam Electric Station, Unit 3 (WSES-3) were determined by a detailed review of applicable design drawings and are provided as an attachment in Appendix I. The freespan lengths were compared to the freespan length used in the finite element based residual stress analysis to ascertain the location for the determination of throughwall stress distribution. This aspect is discussed in more detail in Section 2.

In order to exclude the inaccessible region from the inspection campaign, a relaxation of the Order is required pursuant to the requirements prescribed in Section IV.F and footnote 2 of the order [1]. This relaxation request must demonstrate that not examining the full extent of the nozzle tube below the J-weld will not negatively impact the level of quality and safety.

The purpose of this engineering report is to document the analyses performed for ANO-2 and WSES-3 to assess the propensity for primary water stress corrosion cracking (PWSCC) based on postulated flaws existing in the un-inspectable region. The results of the various analyses performed demonstrate that not inspecting the inaccessible region will not negatively impact the level of quality and safety.

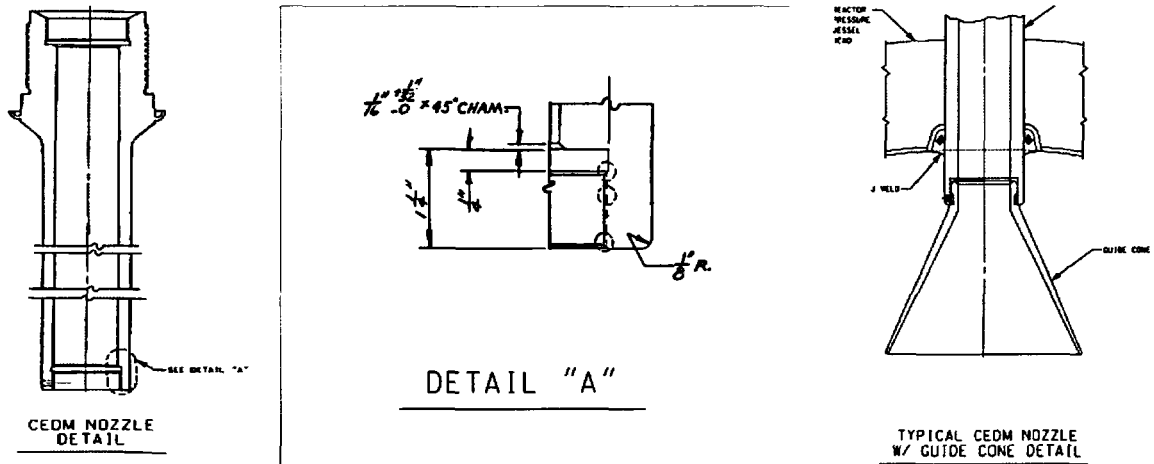
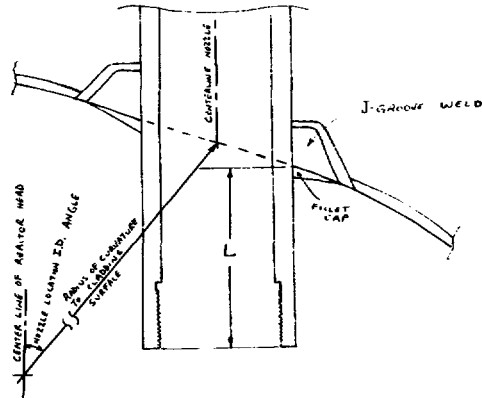


Figure 1: a) CEDM Nozzle tube.

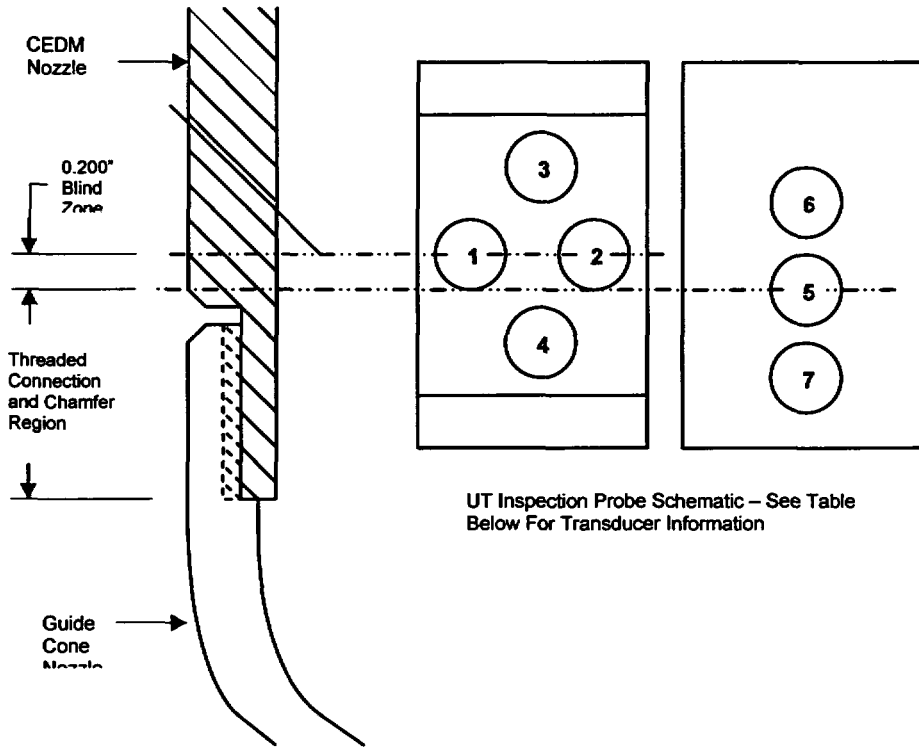
- b) Details of the chamfer in the machined recess of the threaded region. Provides dimensions for the threaded and chamfer regions.
- c) Details of funnel connection to CEDM [2].
- d) Sketch of a typical CEDM penetration showing the region of interest. The freespan of the CEDM labeled "L" is the nozzle extension below the J-weld and is the freespan length.

Detail extracted from Drawing M-2001-C2-23 (ANO-2) & 1564-506 (WSES-3) [2]. The threaded region in the CEDM is 1.344 inches (Threads plus Recess plus chamfer). Both ANO-2 and WSES-3 have similar connection geometry.



d

The detail of the funnel-to-CEDM connection shows that the threaded + chamfer region is 1.344 inches in height. The UT dead zone, determined to be 0.200 inch above the top of the threaded region in the CEDM, is based on the inspection probe design [3b], (shown in Figure 2).



UT Inspection Probe Schematic – See Table Below For Transducer Information

Position	Mode	Diameter	Description
1	Transmit	0.25"	Circumferential Scan Using TOFD
2	Receive	0.25"	Circumferential Scan Using TOFD
3	Transmit	0.25"	Axial Scan Using TOFD
4	Receive	0.25"	Axial Scan Using TOFD
5	Transmit Receive	0.25"	Standard Zero Degree Scan
6	Transmit Receive	0.25"	Standard Zero Degree Scan

Figure 2: Sketch of the inspection probe [3a]. Probe 7 is a Eddy Current (EC) probe.

Based on the probe design and the geometry of the nozzle at the threaded connection, the explanation provided in Reference 3b shows the dead zone to extend 0.200 inch above the chamfer region immediately above the threads. Therefore, to account for the thread region, chamfer and the NDE dead zone, the un-inspected height is determined to be 1.544 inch (1.250" + 0.094"+0.2") above the bottom of the nozzle. Thus, the stresses in the region of interest are 1.544 inches above the bottom of the nozzle tube. The hoop stress at this location will be utilized to evaluate the PWSCC growth potential given an assumed axial part through-wall surface flaw equal

to the smallest flaw successfully detected by UT. The details of the geometrical input, stress analysis, and crack growth rate utilized for the analyses presented in this report are provided in Appendix I. The initial flaw size is obtained from Reference 4 (ID axial flaw is 0.035 inch deep; OD axial flaw is 0.0665 inch deep). The flaw length is estimated based on an aspect ratio of ten (10) such that the stress intensity factors (SIF) are conservatively maximized for the given depth. In addition, a through-wall axial flaw having a length of 0.5 inch is evaluated to ensure completeness of the assessment. The axially oriented flaws at this location have the potential for propagation towards the attachment weld. Therefore, axial flaws are postulated for the fracture mechanics based analysis.

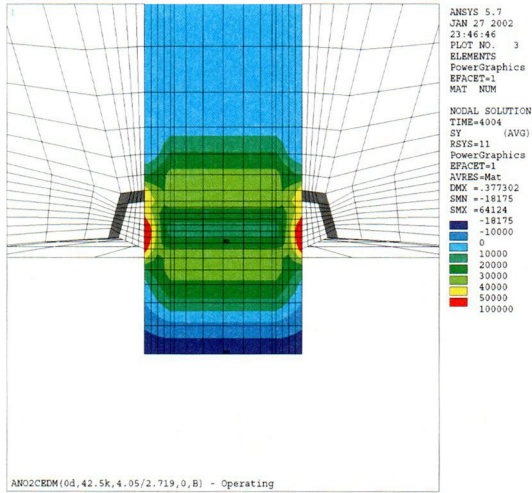
The analyses performed include a finite element stress analysis of the CEDM nozzles and fracture mechanics based crack growth analysis for PWSCC. These analyses were performed for four nozzles in each reactor vessel head (ANO-2 and WSES-3) to account for the varied geometry of the nozzle penetration. The sections that follow contain a description of the analyses, the results, and conclusions supported by the analyses.

2.0 Stress Analysis

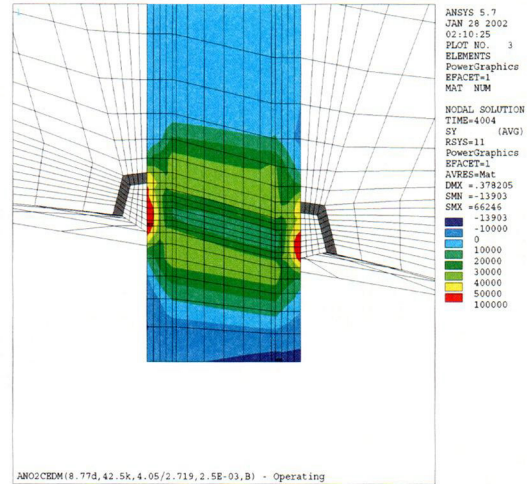
Finite element based stress analysis for the ANO-2 and WSES-3 CEDM and ICI nozzle penetrations, using the highest tensile yield strength for each group of nozzles in each plant, were performed in February 2002 to ensure that sufficient information existed to perform fracture mechanics analyses in the event flaws were discovered during the inspection campaign of 2002. Four nozzle locations that spanned the CEDM penetrations were selected for analyses. The locations were selected to provide an adequate representation of residual stress distribution and, hence, facilitate proper analyses. The yield strength values used are presented in tables IA, IB, IIA, and IIB with the hoop stress values. These analyses were performed to assess the stress profiles using both the welding induced residual and the operating stresses in the nozzle and the J-groove welds. The analysis for ANO-2 is documented in Reference 5a and for WSES 3 in Reference 5b.

Four CEDM nozzles representing the various hillside angle were selected for analyses described in this report. The stress contours for ANO-2 [5a] CEDM nozzles are presented in Figure 3 and for WSES-3 [5b] in Figure 4. The hoop stress plots for the ANO-2 CEDMs show that the stresses in the region of interest, the bottom part of the nozzle, range from a very low tensile value to predominantly compressive stress.

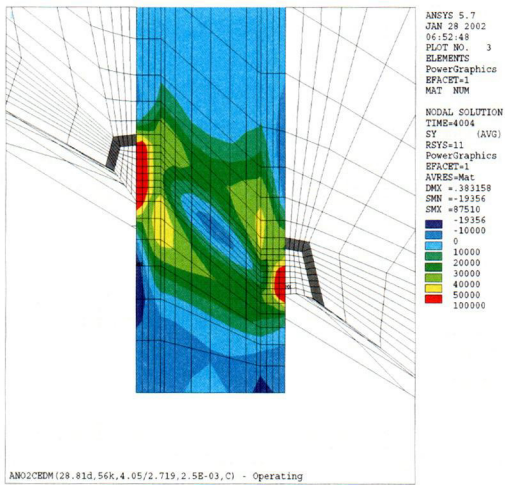
The nozzle extension below the J-groove weld on the downhill side is shorter than on the uphill side, indicating that a flaw in the uphill region would have to propagate a longer distance. Therefore, the region of interest for analysis is the downhill and an azimuthal plane ninety degree rotated from the downhill location.



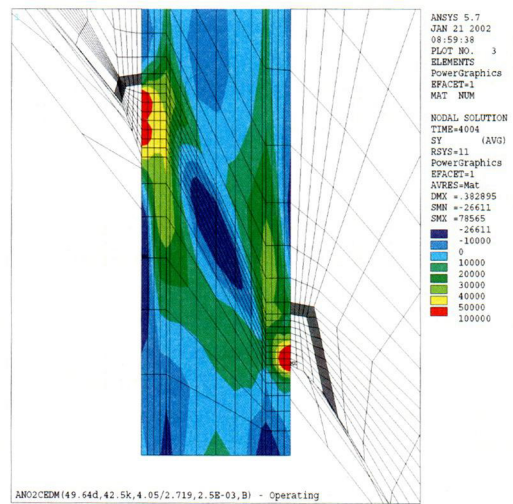
“0” Degree CEDM



“8.8” Degree CEDM



“28.8” Degree CEDM



“49.6” Degree CEDM

Figure 3: ANO-2 CEDM Nozzle at four locations on the head. The region of interest is located at the bottom. The cyan contour ranges from 10 ksi (tensile) to 0 ksi; the light blue contour from 0 ksi to -10 ksi (compressive) and the dark blue contour indicate compressive stresses in excess of -10 ksi.

The CEDM at zero degree (0°) is axi-symmetric and the contours show the symmetric behavior. The other CEDM nozzles at higher penetration angles begin to show asymmetry. The CEDM at 8.8° shows the compressive stress and the low stress regions in the bottom of the nozzle in the region of interest. The distribution is skewed towards the downhill side of the nozzle. The distance from the bottom of the CEDM to the attachment J-weld on the downhill side is shorter than on the uphill side. In addition, the stress distribution change on the downhill side occurs over a shorter nozzle length. At ninety degrees from the downhill side the distribution appears to be between the downhill and uphill side distributions. At these higher hillside angles the stress profiles at both the downhill and at the ninety degree locations were evaluated.

C-01

The nozzles at higher penetration angles show the asymmetric distribution to a higher degree. Therefore, for these nozzles both locations were evaluated.

The stress contours for the WSES-3 CEDMs are presented in Figure 4 below.

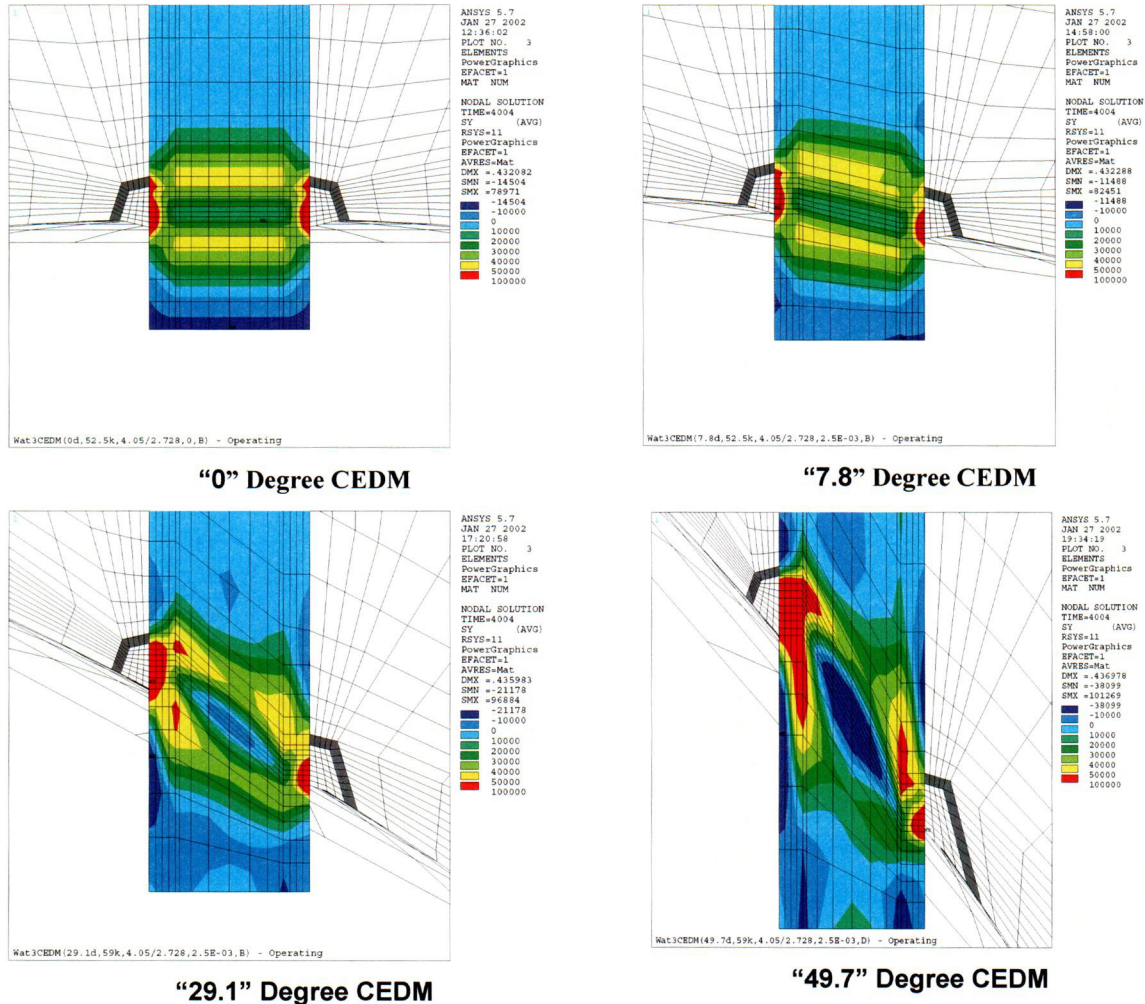


Figure 4: WSES-3 CEDM Nozzle at four locations on the head. The region of interest is located at the bottom. The cyan contour ranges from 10ksi (tensile) to 0 ksi; the light blue contour from 0 ksi to -10 ksi (compressive) and the dark blue contour indicates compressive stresses in excess of -10 ksi.

The stress contours for WSES-3 are similar to those for ANO-2, presented in Figure 3. Therefore, the locations for the evaluations are also similar. The hoop stress distribution along the nozzle height from the bottom of the nozzle to the bottom of the J-weld was plotted for both units at the two regions of interest (downhill and the ninety degree plane). Figures 5 through 11 present the information for ANO-2 and Figures 12 through 18 present the information for WSES-3. In these figures, the hoop stress for both the ID and OD surfaces are plotted and the lower inspection limit is shown for reference.

The CEDM nozzle lengths for the ANO-2 nozzles were determined (Appendix I, Attachment 4) and the minimum freespan length was found to be 2.48 inches. However, the freespan length used in the finite element residual stress analysis was 2.70 inches. Therefore, the actual nozzle is 0.22 inch shorter than that used in the residual stress analysis. The stresses at the end of the nozzle are compressive and hence the use of a shorter length in the finite element analysis is inconsequential. To account for the shorter design length of the nozzle, the location where the through-wall residual stress would be estimated was determined as the sum of the un-inspectable length (1.544 inch) plus the difference in the nozzle length (0.22 inch). Thus, the location for determining the through-wall hoop stress distribution was established to be 1.764 inches. This location is shown on Figures 5 through 11 as a red line labeled "Analysis Elevation". The nozzle bottom is shown in blue.

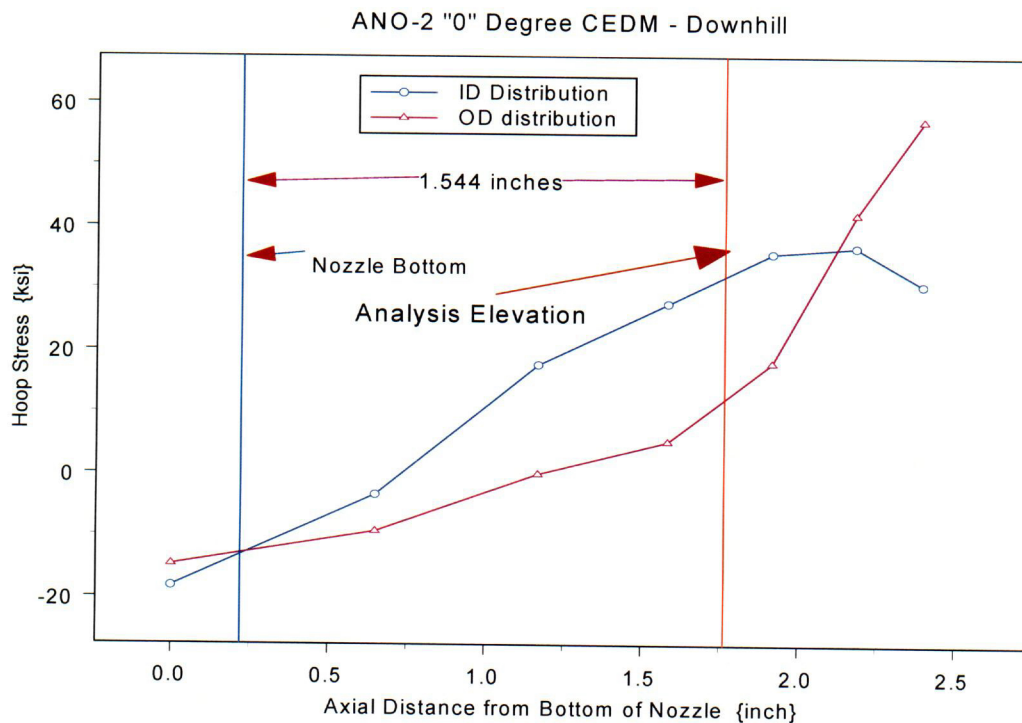


Figure 5: ANO-2 hoop stress profile (ID & OD) for the zero degree nozzle. This nozzle is symmetric about its central axis, hence this distribution would exist at all azimuthal locations.

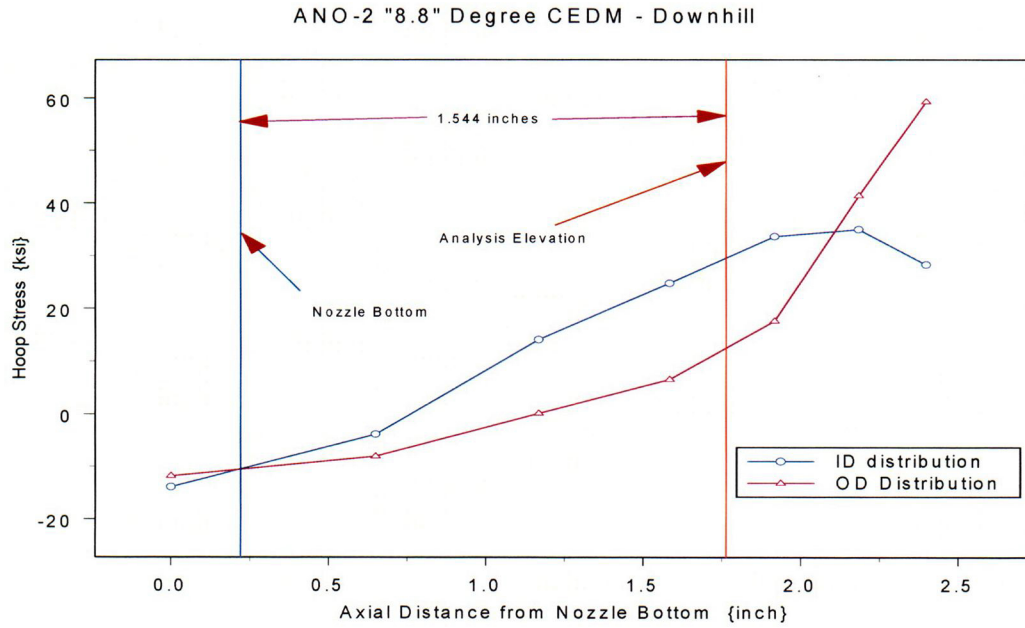


Figure 6: ANO-2 hoop stress profile (ID & OD) for the "8.8" degree nozzle at the downhill location.

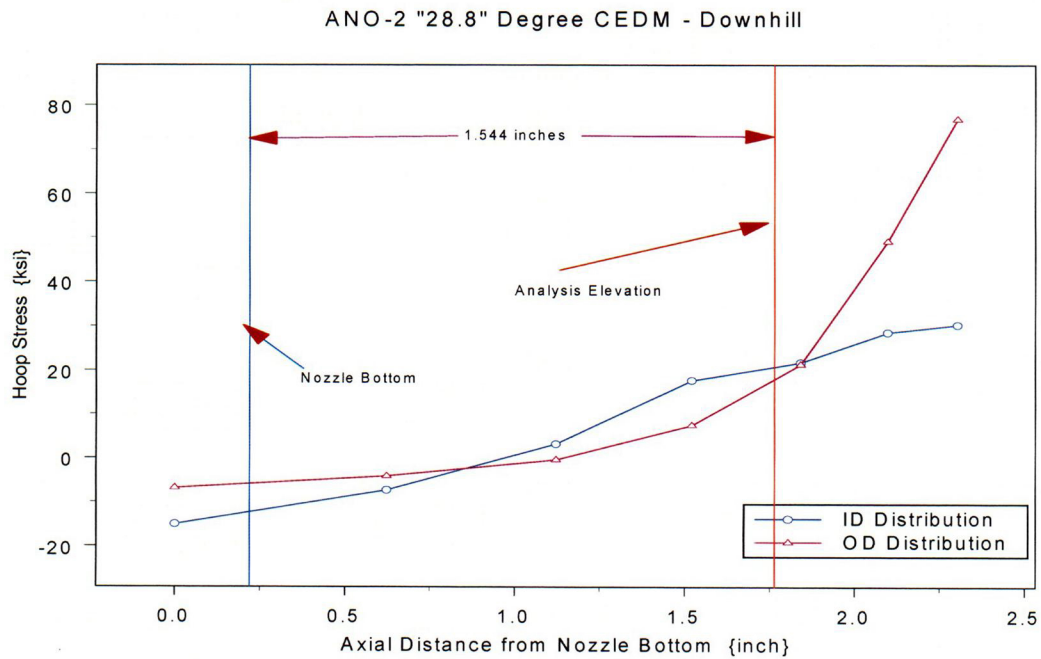


Figure 7: ANO-2 hoop stress profile (ID & OD) for the "28.8" degree nozzle at the downhill location.

C-04

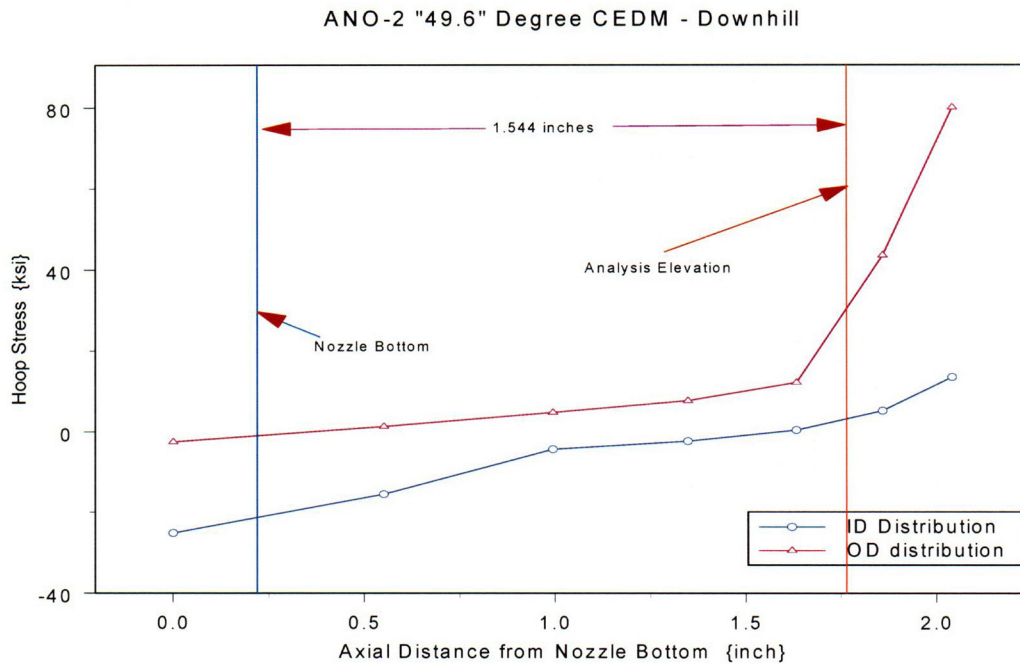


Figure 8: ANO-2 hoop stress profile (ID & OD) for the "49.6" degree nozzle at the downhill location.

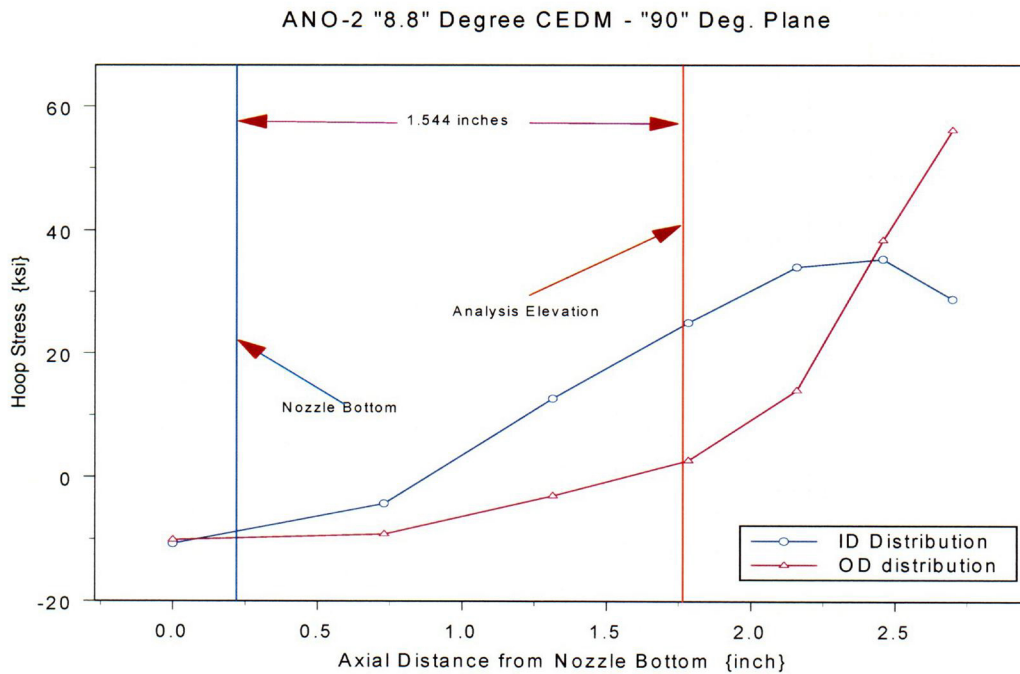


Figure 9: ANO-2 hoop stress profile (ID & OD) for the "8.8" degree nozzle at the ninety degree location.

C-05

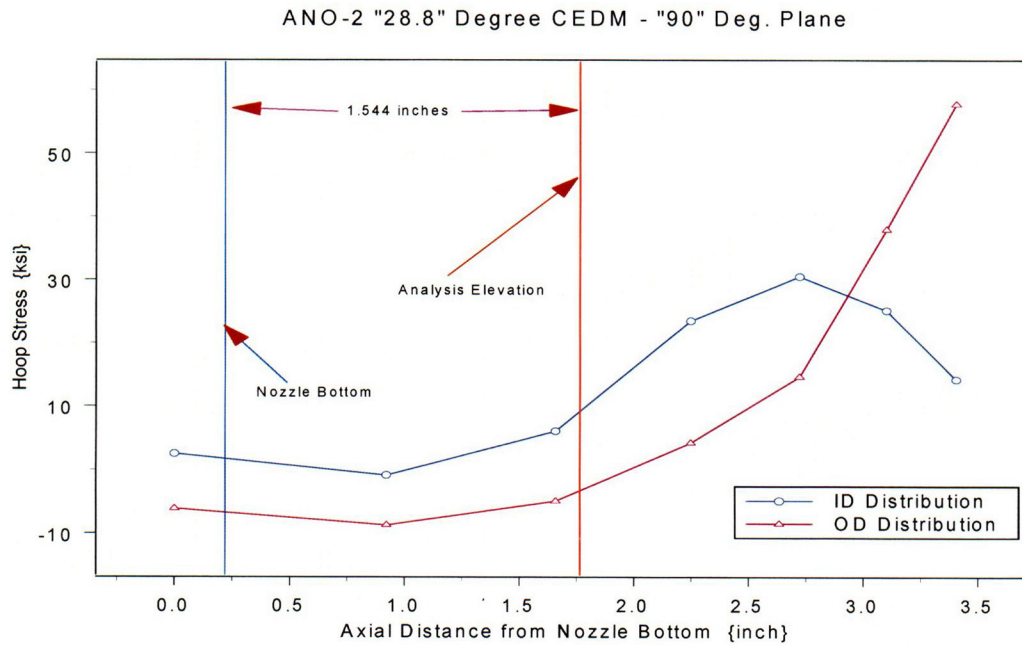


Figure 10: ANO-2 hoop stress profile (ID & OD) for the "28.8" degree nozzle at the ninety degree location.

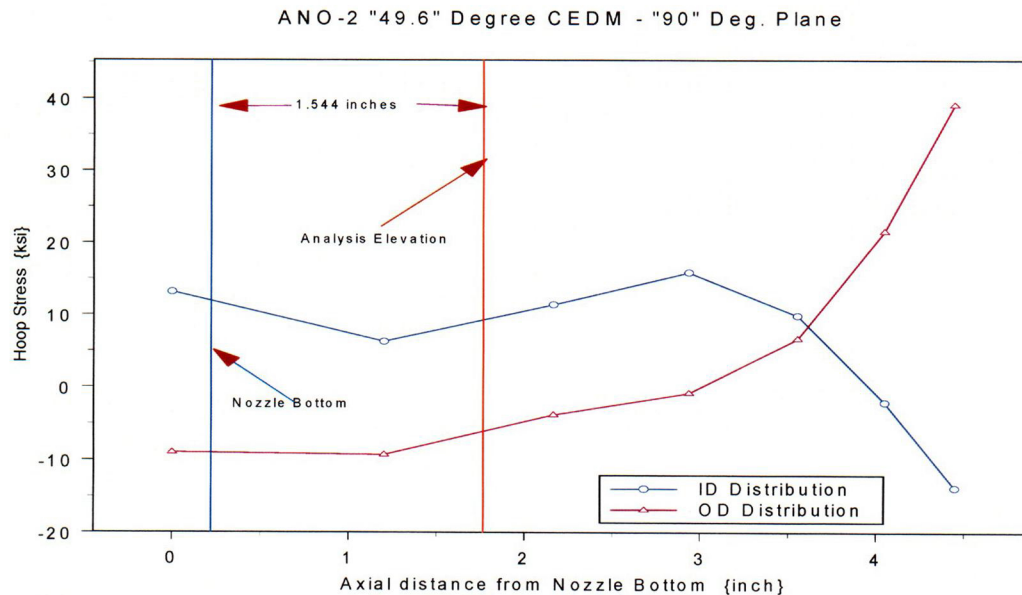


Figure 11: ANO-2 hoop stress profile (ID & OD) for the "49.6" degree nozzle at the ninety degree location.

The CEDM nozzle lengths for the WSES-3 nozzles were determined (Appendix I, Attachment 4) and the minimum freespan length was found to be 2.86 inches. However, the freespan length used in the finite element residual stress analysis was

2.70 inches; therefore, the actual nozzle is 0.16 inch longer than that used in the residual stress analysis. The analysis location was measured at 1.544 inches from the finite element analysis model nozzle bottom. As a result the analysis location is actually higher than the lower limit of the inspection zone. This provides a conservatively higher hoop stress distribution at the analysis location. Thus, the location for determining the through-wall hoop stress distribution was established at 1.544 inches. This location is shown on Figures 12 through 18 as a red line labeled "Analysis Elevation". The nozzle bottom is shown in blue and the measurement for the analysis location is from the green line (finite element model nozzle bottom).

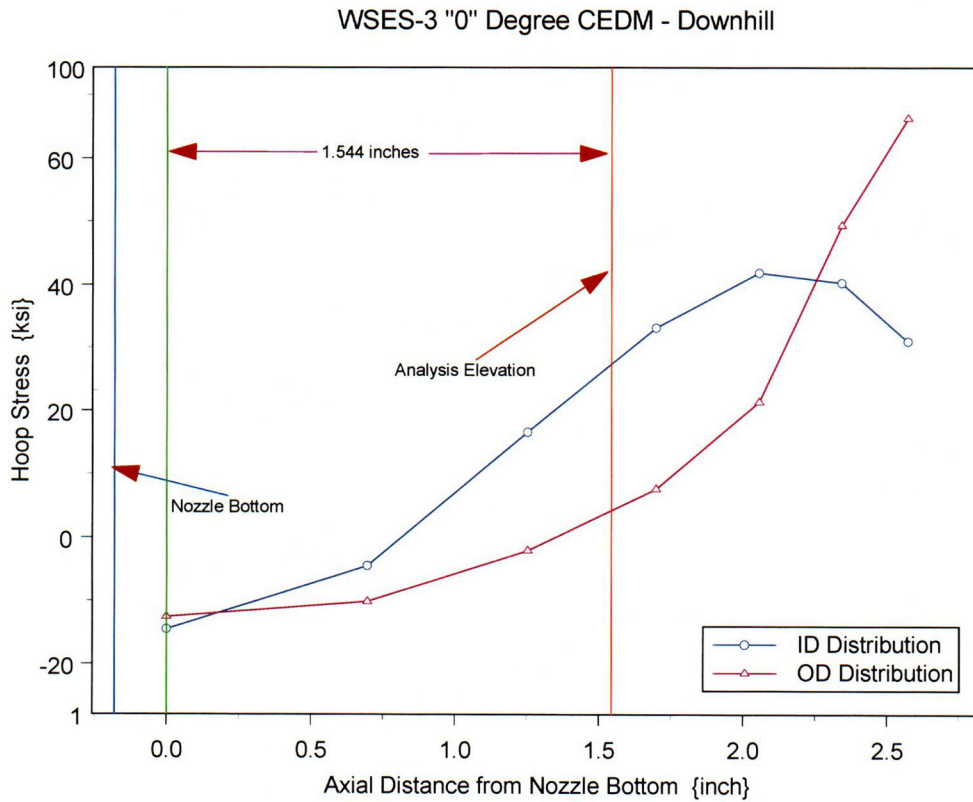


Figure 12: WSES-3 hoop stress profile (ID & OD) for the "zero" degree nozzle. This nozzle is symmetric about its central axis, hence this distribution would exist at all azimuthal locations.

WSES-3 "7.8" Degree CEDM - Downhill

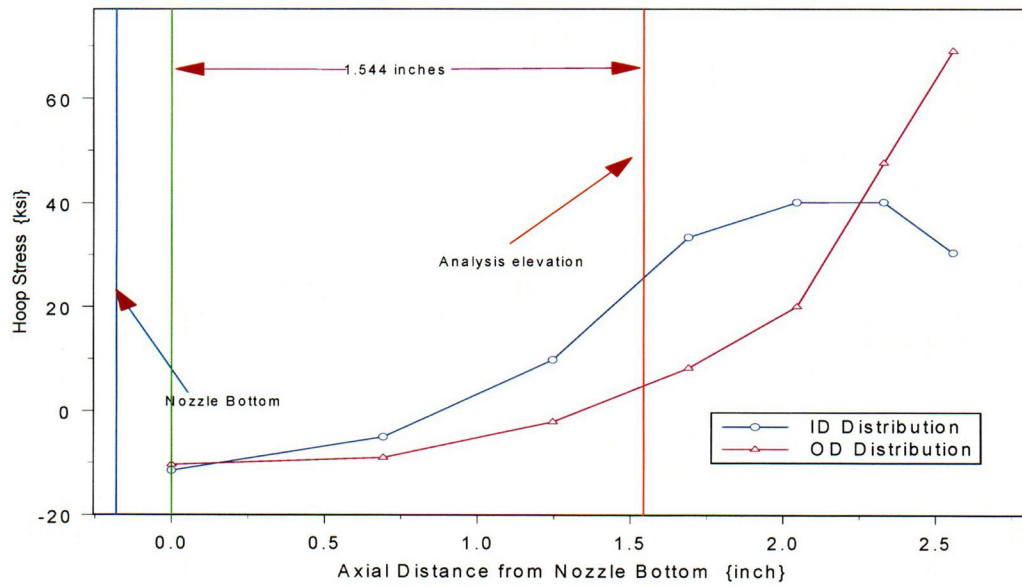


Figure 13: WSES-3 hoop stress profile (ID & OD) for the "7.8" degree nozzle at the downhill location.

WSES-3 "29.1" Degree CEDM - Downhill

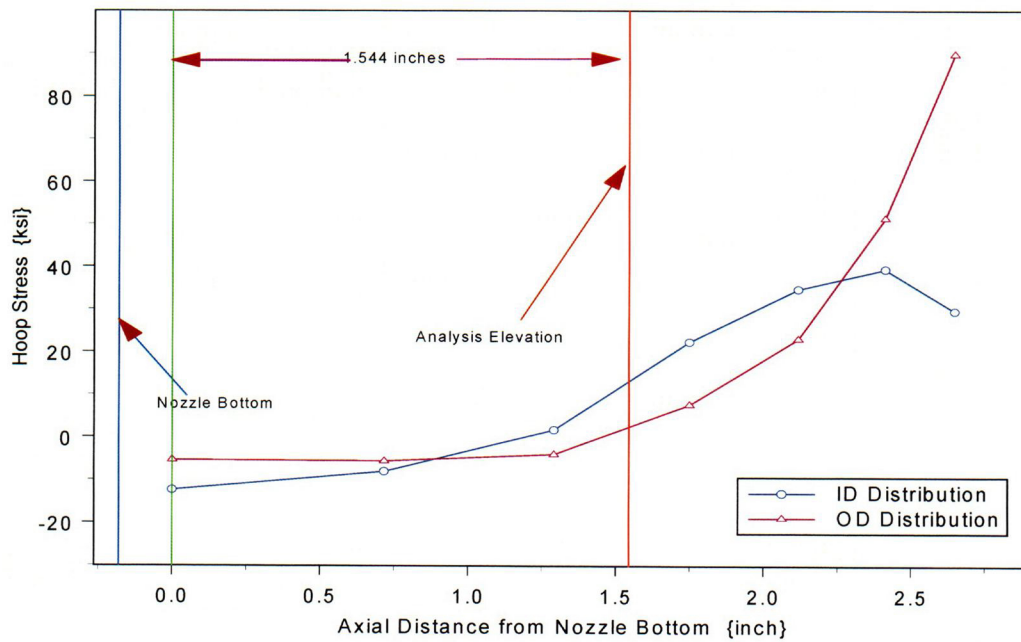


Figure 14: WSES-3 hoop stress profile (ID & OD) for the "29.1" degree nozzle at the downhill location.

C-08

WSES-3 "49.7" Degree CEDM - Downhill

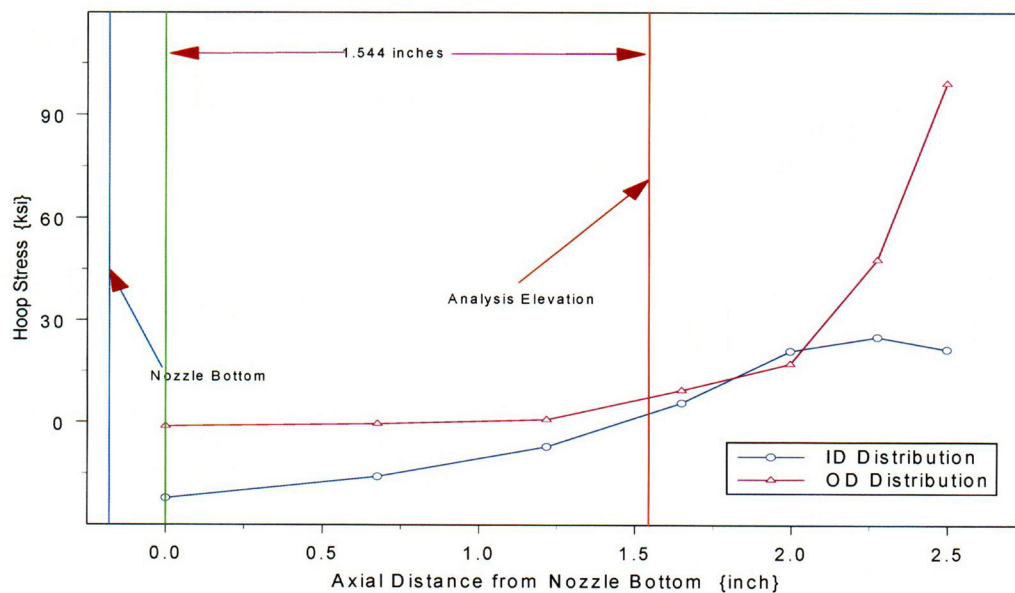


Figure 15: WSES-3 hoop stress profile (ID & OD) for the "49.7" degree nozzle at the downhill location.

WSES-3 "7.8" Degree CEDM - "90" Degree Plane

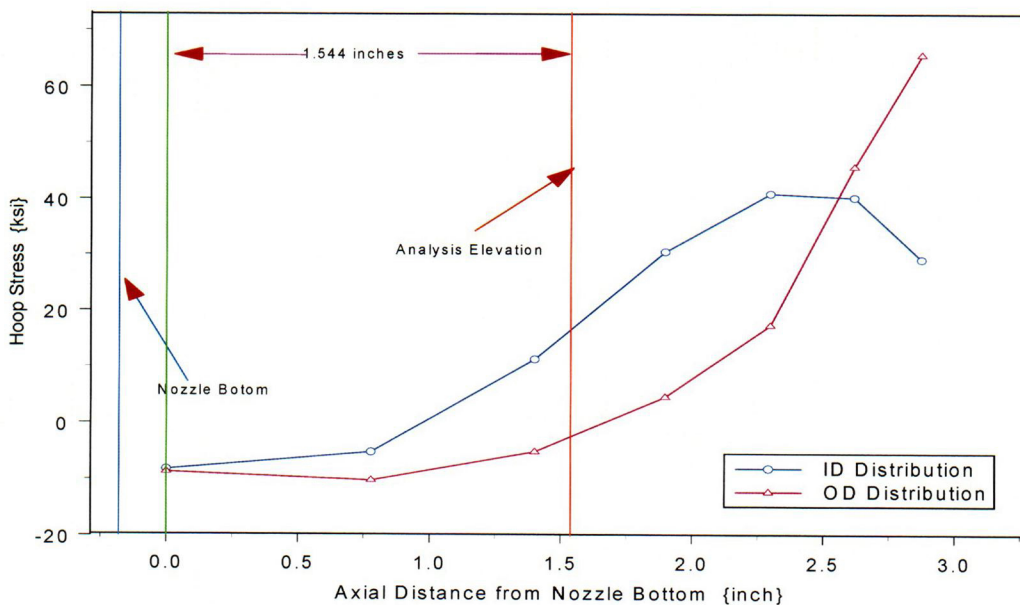


Figure 16: WSES-3 hoop stress profile (ID & OD) for the "7.8" degree nozzle at the ninety degree location.

C-09

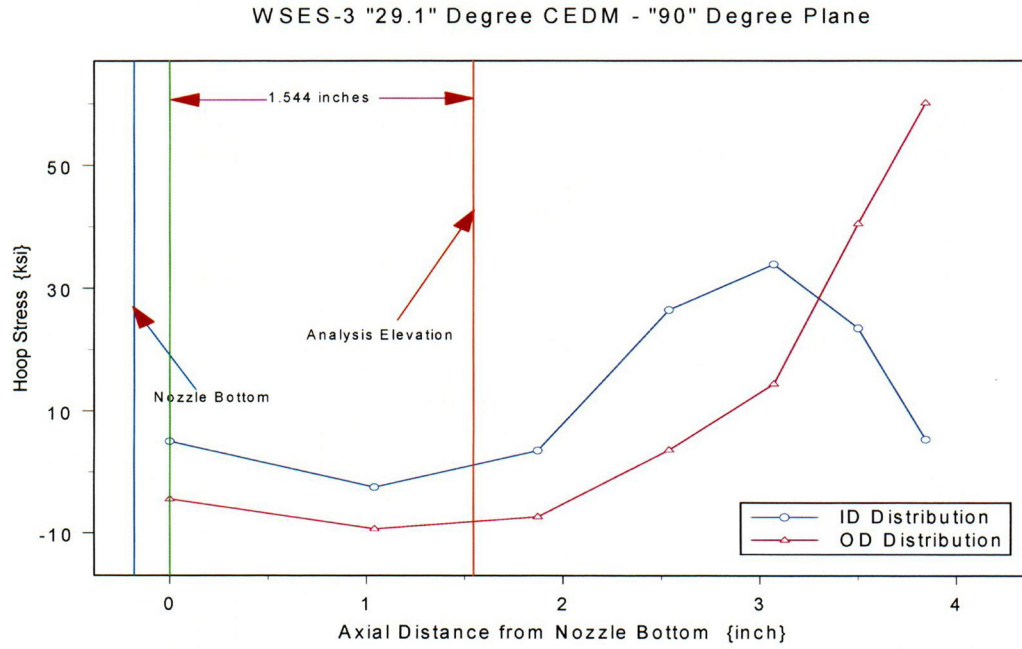


Figure 17: WSES-3 hoop stress profile (ID & OD) for the "29.1" degree nozzle at the ninety degree location.

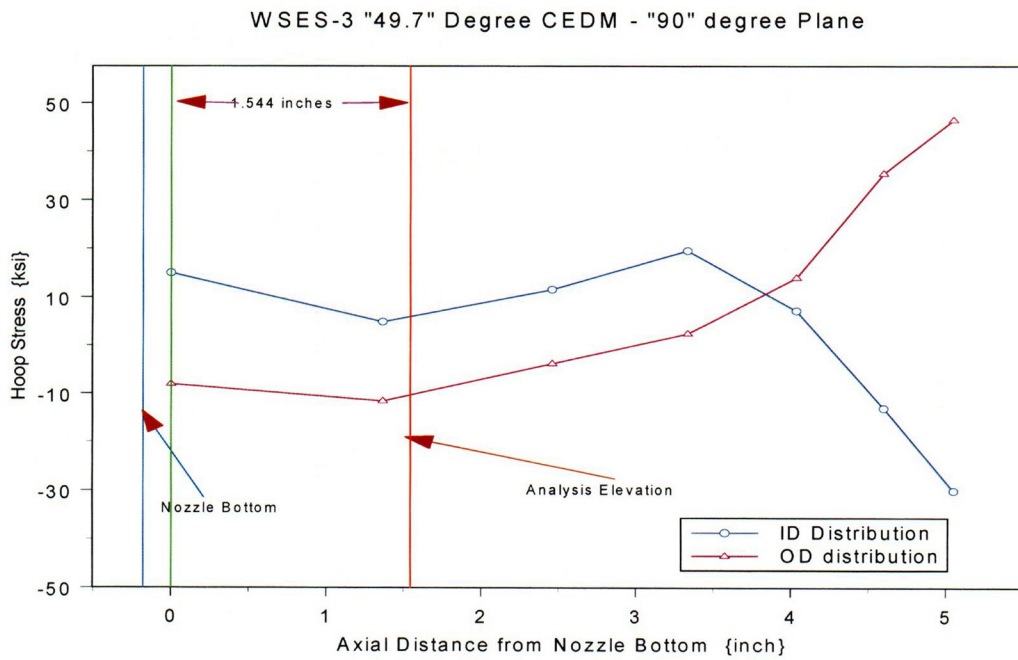


Figure 18: WSES-3 hoop stress profile (ID & OD) for the "49.7" degree nozzle at the ninety degree location.

C-10

The nodal stresses at each location within the region of interest, including the CEDM nozzle through-wall distribution, were obtained. The data for ANO-2 [5a] are presented in Table IA (downhill) and IB (ninety degree).

Table IA: ANO-2 CEDM Downhill Location Nodal Stresses

0 Degree CEDM: Nozzle Yield Strength 42.5 ksi						
Through-wall (%)	Hoop Stress (ksi) at Axial Elevation above Nozzle Bottom (Inch)					
	0.000"	0.648"	1.167"	1.582"	1.915"	2.182"
ID	-18.174	-3.378	17.707	27.601	35.706	36.728
25	-16.566	-4.971	13.472	24.308	30.013	30.156
50	-15.827	-6.589	8.529	18.751	24.861	27.991
75	-15.241	-8.046	4.002	13.672	21.360	33.445
OD	-14.746	-9.230	-0.022	5.239	18.031	41.952
8.8 Degree CEDM: Nozzle Yield Strength 42.5 ksi						
Through-wall (%)	Hoop Stress (ksi) at Axial Elevation above Nozzle Bottom (Inch)					
	0.000"	0.649"	1.168"	1.584"	1.918"	2.185"
ID	-13.903	-3.845	14.107	24.745	33.654	34.984
25	-12.842	-4.967	9.739	19.809	27.773	29.025
50	-12.437	-6.115	5.959	15.965	23.761	27.507
75	-12.104	-7.186	2.702	12.974	20.928	32.595
OD	-11.845	-8.071	0.107	6.544	17.580	41.361
28.8 Degree CEDM: Nozzle Yield Strength 56.0 ksi						
Through-wall (%)	Hoop Stress (ksi) at Axial Elevation above Nozzle Bottom (Inch)					
	0.000"	0.623"	1.121"	1.521"	1.841"	2.097"
ID	-15.079	-7.353	3.146	17.682	21.792	28.594
25	-12.024	-6.067	1.976	15.261	23.215	31.061
50	-10.260	-5.324	1.019	14.009	23.236	32.744
75	-8.553	-4.750	0.316	11.128	24.993	38.493
OD	-6.900	-4.182	-0.486	7.402	21.289	49.119
49.6 Degree CEDM: Nozzle Yield Strength 42.5 ksi						
Through-wall (%)	Hoop Stress (ksi) at Axial Elevation above Nozzle Bottom (Inch)					
	0.000"	0.551"	0.994"	1.348"	1.632"	1.859"
ID	-25.184	-15.541	-4.320	-2.348	0.394	5.222
25	-17.168	-9.772	-1.460	1.854	6.302	15.202
50	-11.981	-5.649	0.195	6.109	11.947	27.448
75	-7.221	-2.000	2.671	8.699	16.295	37.283
OD	-2.522	1.254	4.723	7.663	12.200	43.599

Table IB: ANO-2 CEDM Ninety Degree Location Nodal Stresses

8.8 Degree CEDM: Nozzle Yield Strength 42.5 ksi					
Through-wall (%)	Hoop Stress (ksi) at Axial Elevation above Nozzle Bottom (Inch)				
	0.000	0.730"	1.314"	1.783"	2.158"
ID	-10.731	-4.281	12.692	24.989	34.068
25	-10.112	-5.586	8.192	20.902	28.570
50	-10.106	-6.943	3.707	15.434	23.531
75	-10.114	-8.196	-0.094	10.477	19.021
OD	-10.115	-9.191	-3.033	2.675	14.013
28.8 Degree CEDM: Nozzle Yield Strength 56.0 ksi					
Through-wall (%)	Hoop Stress (ksi) at Axial Elevation above Nozzle Bottom (Inch)				
	0.000"	0.921"	1.658"	2.248"	2.722"
ID	2.507	-0.870	6.063	23.514	30.524
25	-0.271	-3.316	1.576	17.081	24.882
50	-2.420	-5.308	-1.711	12.746	21.125
75	-4.253	-7.142	-3.799	8.482	18.233
OD	-6.128	-8.711	-4.940	4.216	14.638
49.6 Degree CEDM: Nozzle Yield strength 42.5 ksi					
Through-wall (%)	Hoop Stress (ksi) at Axial Elevation above Nozzle Bottom (Inch)				
	0.000"	1.202"	2.165"	2.937"	3.555"
ID	13.205	6.283	11.399	15.862	9.889
25	5.620	0.693	4.622	10.927	7.302
50	0.451	-3.364	2.033	7.467	7.076
75	-4.177	-6.778	-0.817	3.172	7.085
OD	-8.970	-9.281	-3.788	-0.814	6.674

The nodal stresses at each location within the region of interest, including the CEDM nozzle through-wall distribution, were obtained. The data for WSES-3 [5b] are presented in Table IIA (downhill) and IIB (ninety degree).

Table IIA: WSES-3 CEDM Downhill Location Nodal Stresses

0 Degree CEDM: Nozzle Yield Strength 52.5 ksi					
Through-wall (%)	Hoop Stress (ksi) at Axial Elevation above Nozzle Bottom (inch)				
	0.000"	0.696"	1.253"	1.699"	2.057"
ID	-14.500	-4.490	16.567	33.118	41.880
25	-13.368	-5.979	10.041	30.631	35.593
50	-13.089	-7.512	3.380	24.076	29.972
75	-12.849	-8.946	-0.004	16.650	26.244
OD	-12.575	-10.116	-2.125	7.590	21.339
7.8 Degree CEDM: Nozzle Yield Strength 52.5 ksi					
Through-wall (%)	Hoop Stress (ksi) at Axial Elevation above Nozzle Bottom (inch)				
	0.000"	0.692"	1.246"	1.69"	2.045"
ID	-11.488	-4.984	9.838	33.456	40.203
25	-10.750	-5.963	5.152	26.212	33.889
50	-10.612	-7.074	1.606	20.615	29.000
75	-10.497	-8.133	-0.676	15.121	25.574
OD	-10.364	-8.997	-2.072	8.298	20.134
29.1 Degree CEDM: Nozzle Yield Strength 59.0 ksi					
Through-wall (%)	Hoop Stress (ksi) at Axial Elevation above Nozzle Bottom (inch)				
	0.000"	0.716"	1.29"	1.749"	2.117"
ID	-12.397	-8.061	1.677	22.321	34.745
25	-9.637	-7.005	-0.108	17.800	32.422
50	-8.301	-6.463	-1.732	13.249	30.144
75	-6.813	-6.130	-2.813	9.424	27.897
OD	-5.430	-5.664	-4.077	7.569	23.028
49.7 Degree CEDM: Nozzle Yield Strength 59.0 ksi					
Through-wall (%)	Hoop Stress (ksi) at Axial Elevation above Nozzle Bottom (inch)				
	0.000"	0.675"	1.216"	1.649"	1.997"
ID	-22.205	-15.824	-7.096	5.740	21.020
25	-14.637	-10.492	-4.329	6.370	22.571
50	-10.002	-6.695	-2.708	7.491	22.166
75	-5.449	-3.499	-0.646	8.396	22.359
OD	-1.196	-0.489	0.843	9.419	17.193

Table IIB: WSES-3 CEDM Ninety Degree Location Nodal Stresses

7.8 Degree CEDM: Nozzle Yield Strength 52.5 ksi				
Through-wall (%)	Hoop Stress (ksi) at Axial Elevation above Nozzle Bottom (inch)			
	0.000"	0.777"	1.4"	1.898"
ID	-8.232	-5.188	11.329	30.559
25	-7.953	-6.473	5.581	27.114
50	-8.301	-7.828	-0.398	20.483
75	-8.554	-9.125	-3.343	13.027
OD	-8.717	-10.159	-5.068	4.659
29.1 Degree CEDM: Nozzle yield strength 59.0 ksi				
Through-wall (%)	Hoop Stress (ksi) at Axial Elevation above Nozzle Bottom (inch)			
	0.000"	1.039"	1.871"	2.538"
ID	5.028	-2.506	3.494	26.467
25	2.012	-4.591	-0.645	19.804
50	-0.454	-6.325	-4.005	14.930
75	-2.381	-8.016	-5.897	9.303
OD	-4.504	-9.380	-7.383	3.556
49.7 Degree CEDM: Nozzle Yield Strength 59.0 ksi				
Through-wall (%)	Hoop Stress (ksi) at Axial Elevation above Nozzle Bottom (inch)			
	0.000"	1.365"	2.459"	3.335"
ID	15.024	4.876	11.553	19.564
25	7.228	-0.670	4.623	15.107
50	1.713	-4.692	0.302	11.645
75	-3.023	-8.447	-1.890	6.550
OD	-8.086	-11.634	-3.866	2.396

The hoop stress at the location selected for evaluation of the potential for PWSCC crack growth was obtained by linear interpolation between two axial nodal positions at each through-wall location. The axial heights above the nozzle bottom based on the earlier discussions were 1.764 inches above the nozzle bottom for ANO-2 and 1.544 inches above the nozzle bottom for WSES-3.

Table III provides the hoop stress data at the location for the two nozzle orientations (downhill and ninety degree). The zero degree CEDM penetration has a hoop stress distribution that is axi-symmetric; hence, no separate ninety degree location data is needed for this orientation.

**Table III: Hoop Stress Distribution Used for Analysis
{ANO-2 : 1.764"; WSES-3: 1.544" above Nozzle Bottom}**

Through-wall (%)	ANO-2 "0" Degree Nozzle		WSES-3 "0" Degree Nozzle	
	Downhill	90° Azimuth	Down Hill	90° Azimuth
	Hoop Stress (ksi)	Hoop Stress (ksi)	Hoop Stress (ksi)	Hoop Stress (ksi)
ID	32.0308	Values are the same as for the downhill location because the nozzle has a symmetric geometry.	27.366.	Values are the same as for the downhill location because the nozzle has a symmetric geometry.
25	27.426		23.475	
50	21.992		16.883	
75	17.8738		10.862	
OD	12.2304		4.214	
Through-wall (%)	ANO-2 "8.8" Degree Nozzle		WSES-3 "7.8" Degree Nozzle	
	Downhill	90° Azimuth	Downhill	90° Azimuth
	Hoop Stress (ksi)	Hoop Stress (ksi)	Hoop Stress (ksi)	Hoop Stress (ksi)
ID	29.5463	24.491	25.69	16.889
25	24.101	20.387	19.287	11.807
50	20.1664	14.959	14.364	5.639
75	17.2606	10.049	9.926	1.39
OD	12.4915	2.444	4.888	-2.255
Through-wall (%)	ANO-2 "28.8" Degree Nozzle		WSES-3 "29.1" Degree Nozzle	
	Downhill	90° Azimuth	Downhill	90° Azimuth
	Hoop Stress (ksi)	Hoop Stress (ksi)	Hoop Stress (ksi)	Hoop Stress (ksi)
ID	20.803	9.198	13.101	1.136
25	21.3011	4.362	9.802	-2.196
50	21.0158	0.886	6.558	-4.917
75	21.6567	-1.593	3.959	-6.73
OD	17.9474	-3.295	2.368	-8.168
Through-wall (%)	ANO-2 "49.6" Degree Nozzle		WSES-3 "49.7" Degree Nozzle	
	Downhill	90° Azimuth	Downhill	90° Azimuth
	Hoop Stress (ksi)	Hoop Stress (ksi)	Hoop Stress (ksi)	Hoop Stress (ksi)
ID	3.2015	9.269	2.627	5.968
25	11.4773	2.986	3.776	0.137
50	20.9608	-0.214	5.018	-3.875
75	28.4995	-3.299	6.203	-7.374
OD	30.4584	-6.075	7.135	-10.363

The hoop stress data tabulated in Table III were curve fit with a third order polynomial to obtain the stress coefficients that would be used in the fracture

mechanics evaluation for the ID and OD part through-wall surface flaws. The curve fit and the curve fit equation were obtained using Axxum software [6]. The stress coefficients are multiplied by the shape coefficients to obtain the influence coefficients for determining the SIF. The method for determining the SIF using influence coefficients is provided in the following section.

Figures 19 through 22 present the through-wall hoop stress distributions for the ANO-2 nozzles at the locations shown in Table III. The equations, with coefficients, provided in the table are annotated to show the nozzle location. The nozzle location is in front of the equation and an arrow indicates the respective curve. For the zero degree nozzle, at the ninety degree azimuth location, no curve is provided since the nozzle at this location is symmetric about its axis.

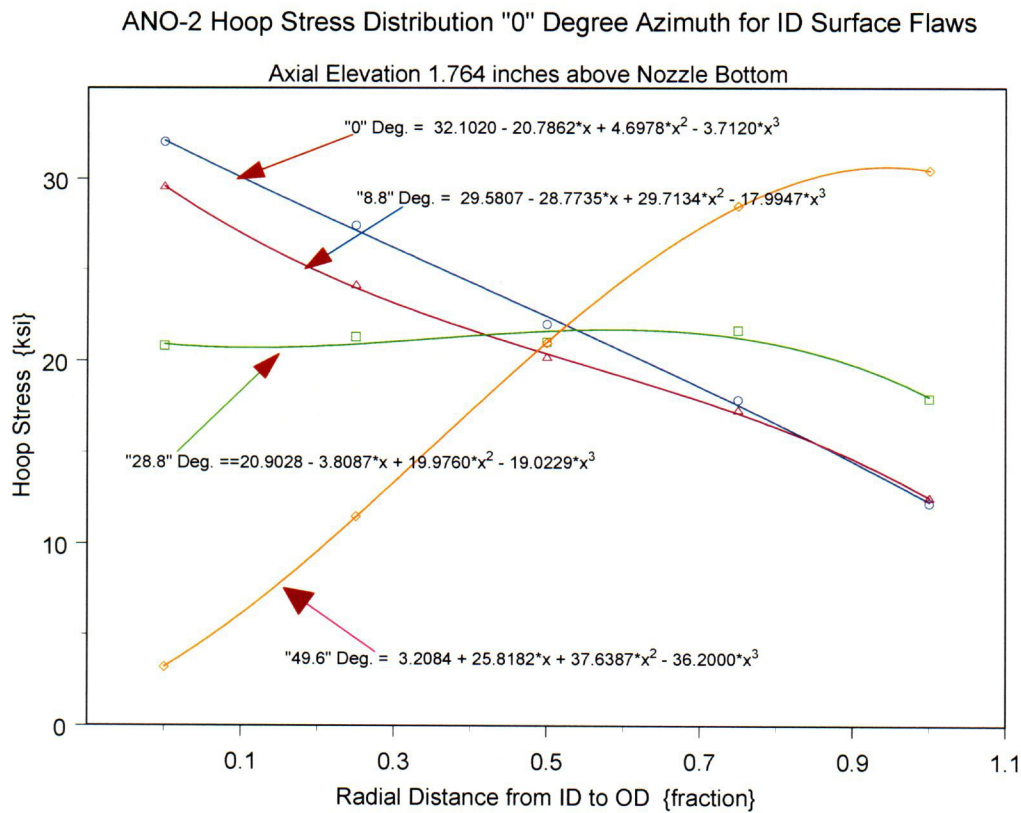


Figure 19: ANO-2 downhill location for all nozzles evaluated. The stress distribution is from the ID to OD. The coefficients in the respective equations will be used in the fracture mechanics analysis.

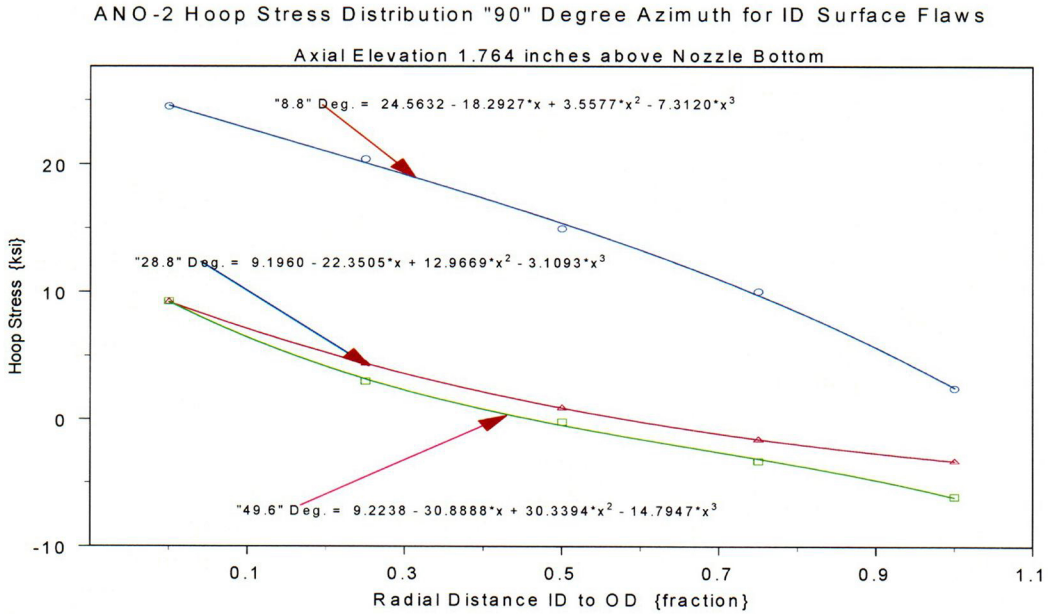


Figure 20: ANO-2 90° azimuth location for all nozzles evaluated. The stress distribution is from the ID to OD. The coefficients in the respective equations will be used in the fracture mechanics analysis.

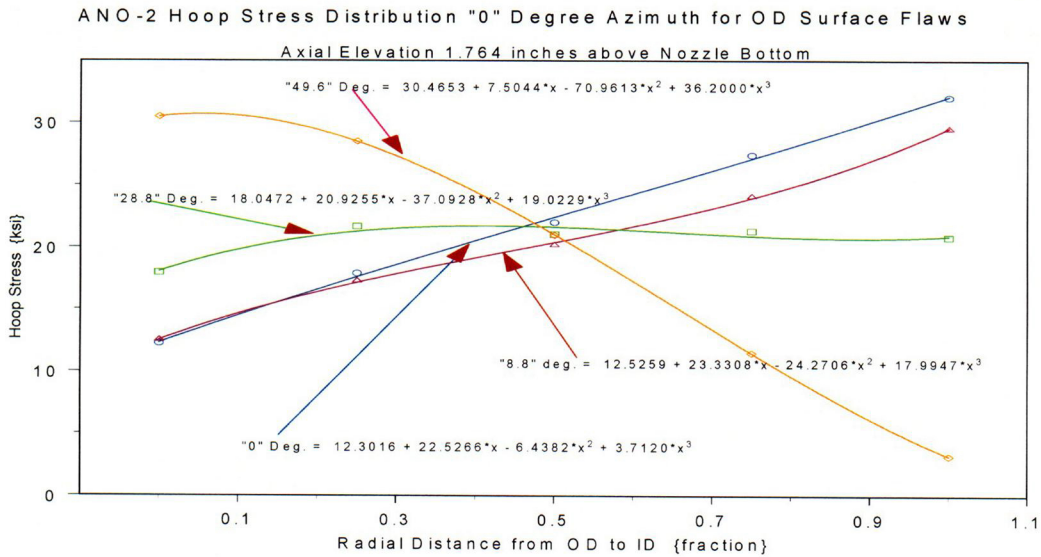


Figure 21: ANO-2 downhill location for all nozzles evaluated. The stress distribution is from the OD to ID. The coefficients in the respective equations will be used in the fracture mechanics analysis.

ANO-2 Hoop Stress Distribution "90" Degree Azimuth for OD Surface Flaws

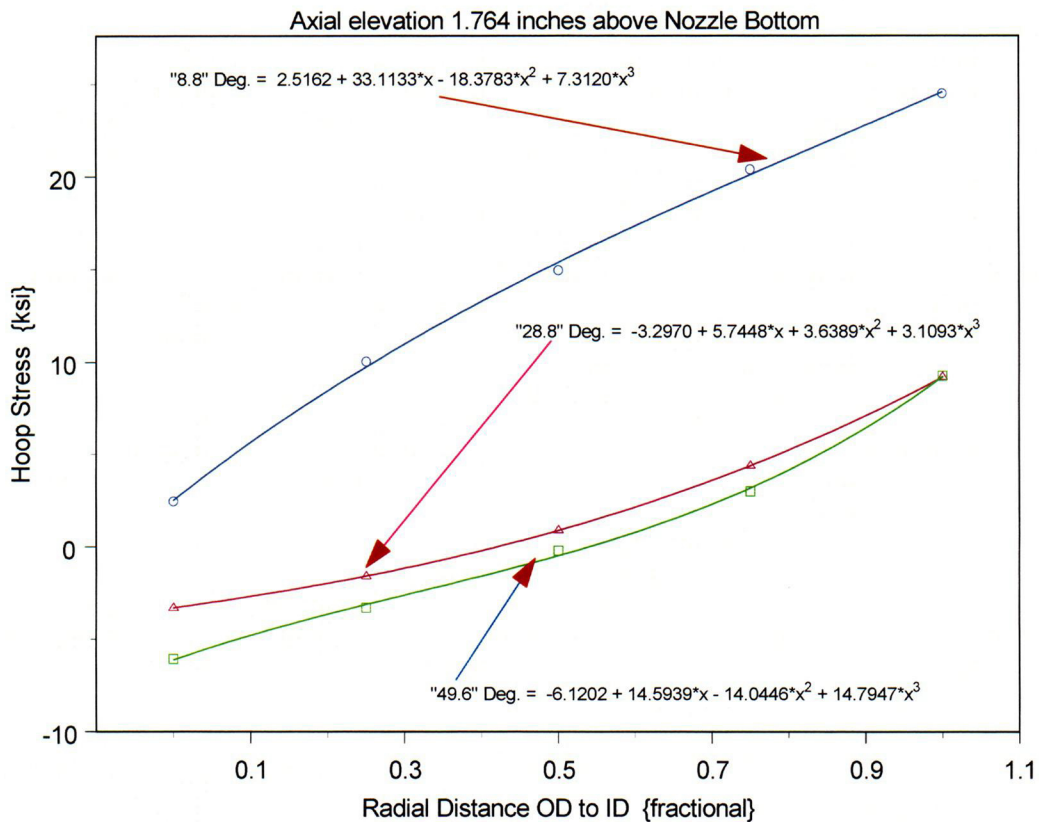


Figure 22: ANO-2 90° azimuth location for all nozzles evaluated. The stress distribution is from the OD to ID. The coefficients in the respective equations will be used in the fracture mechanics analysis.

The data for WSES-3 nozzles, presented in Table III, were fit to a third order polynomial in a similar manner. The results of the fitting and the polynomial coefficients are presented in Figures 23 through 26. The equations and coefficients for each of the nozzle location provided in Table III are shown in the respective figure. The nozzle location is appended to each equation and an arrow points to the respective curve. For the zero degree nozzle, at the ninety degree azimuth location, no curve is provided since the nozzle at this location is symmetric about its axis.

WSES-3 Hoop Stress Distribution "0" Degree Azimuth for ID Surface Flaws

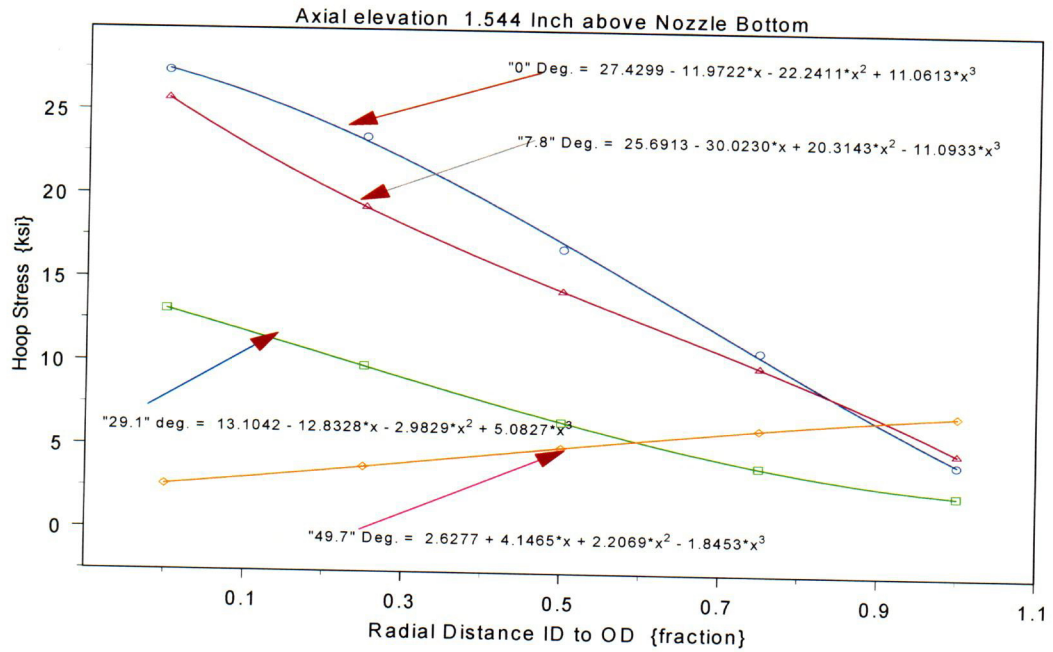


Figure 23: WSES-3 downhill location for all nozzles evaluated. The stress distribution is from the ID to OD. The coefficients in the respective equations will be used in the fracture mechanics analysis.

WSES-3 Hoop Stress distribution "90" Degree Azimuth for ID Surface Flaws

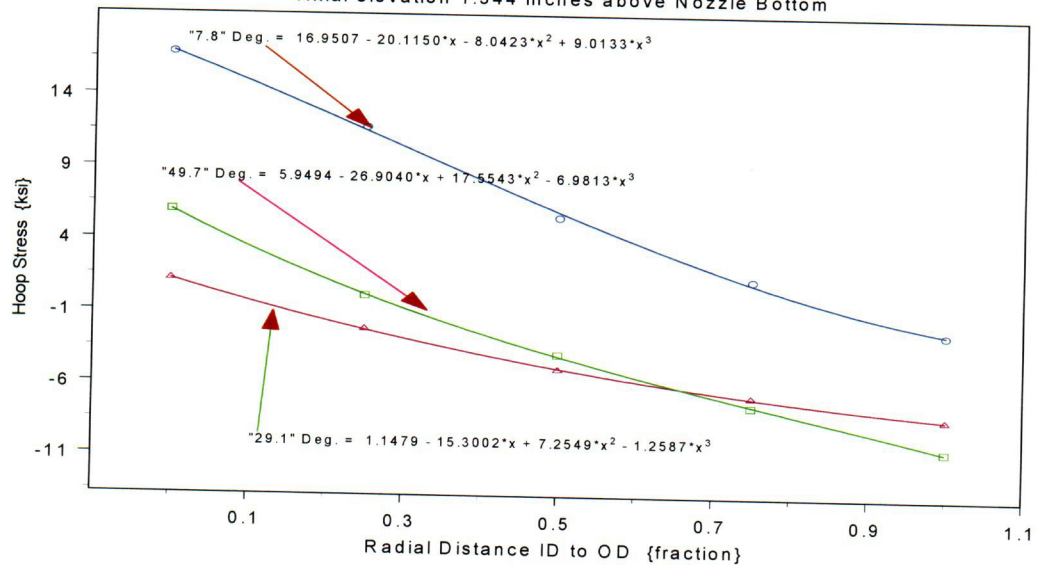


Figure 24: WSES-3 90° azimuth location for all nozzles evaluated. The stress distribution is from the ID to OD. The coefficients in the respective equations will be used in the fracture mechanics analysis.

WSES-3 Hoop Stress Distribution "0" Degree Azimuth for OD surface Flaws
Axial elevation 1.544 inches above Nozzle Bottom

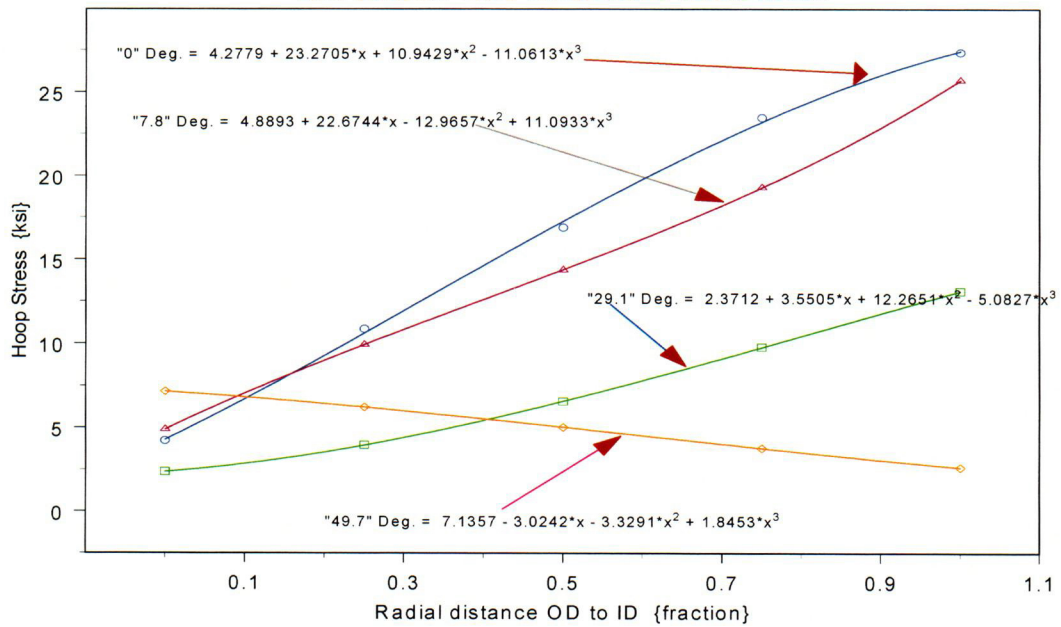


Figure 25: WSES-3 downhill location for all nozzles evaluated. The stress distribution is from the OD to ID. The coefficients in the respective equations will be used in the fracture mechanics analysis.

WSES-3 Hoop Stress Distribution "90" Degree Azimuth for OD Surface Flaws
Axial Elevation 1.544 inches above Nozzle Bottom

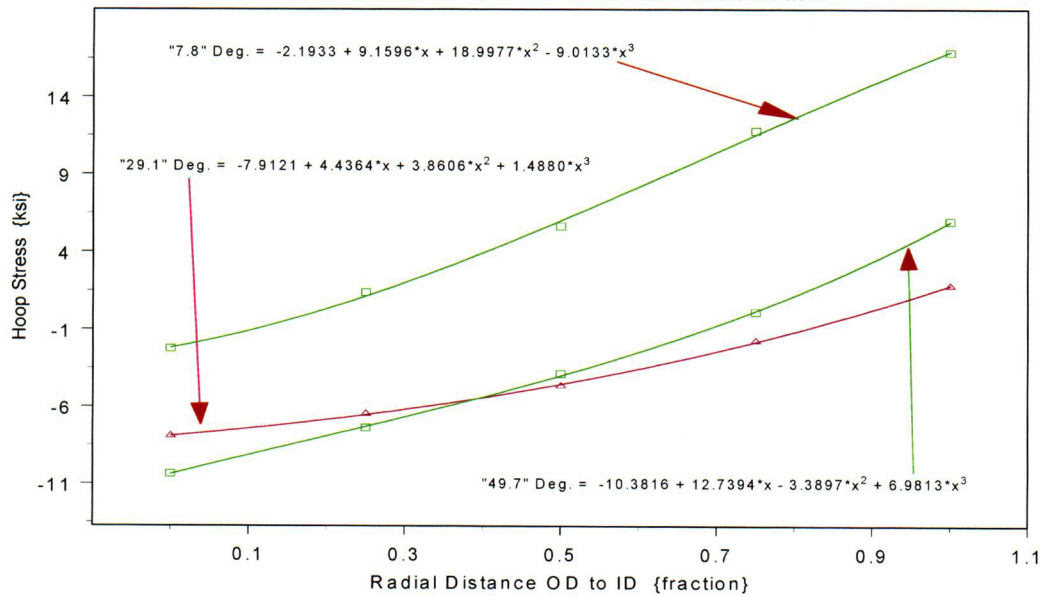


Figure 26: WSES-3 90° azimuth location for all nozzles evaluated. The stress distribution is from the OD to ID. The coefficients in the respective equations will be used in the fracture mechanics analysis.

C-15

3.0 Fracture Mechanics Analysis

Surface Flaw

The outside radius-to-thickness ratio (R_o/t) for the CEDM nozzle was about 3.0. The fracture mechanics equation used in the proposed revision to the ASME Code Section XI is based on the solution from Reference 7. This solution is valid for " R_o/t " ratio from 4.0 to 10.0. Since the CEDM nozzle " R_o/t " ratio is lower indicating that the CEDM nozzle is a thicker wall cylinder than those considered in Reference 7. Therefore the fracture mechanics formulations presented in Reference 8 were chosen (the applicable " R_o/t " ratio is from 1.0 to 10.0).

The SIF for the postulated flaw under the stress distribution presented in the section above was determined using the formulation from the Ductile Fracture Handbook [8a and 8b]. The model chosen was for an internal part-through-wall flaw subjected to an arbitrary stress distribution. This model is valid for a ratio of the inside radius (R_{inner})-to-thickness (t) between 1.0 and 10.0. Since the ratio for the CEDM nozzle is about 2.0, hence this model is considered applicable.

The equation for the stress intensity factor for the deepest point of the crack is given as [8a]:

$$K_I = (\pi)^{0.5} * \left[\sum_{i=0}^3 \sigma_i G_i \right]$$

Where:

K_I = The SIF {ksi√in.}

t = The CEDM wall thickness {inch}

σ_i = Coefficients of the stress polynomial describing the hoop stress variation through the wall thickness {obtained from the previous section}.

G_i = Shape factors associated with the stress coefficients defined as:

$$G_i = A_0 + (A_1\alpha_i + A_2\alpha_i^2 + A_3\alpha_i^3 + A_4\alpha_i^4 + A_5\alpha_i^5) / [0.102(R_i / t) - 0.02]^{0.05}$$

Where:

$$\alpha_i = (a/t) / (a/c)^m$$

R_i = Inside radius {inch}

a = Flaw depth {inch}

c = One half of flaw length {inch}

A and m are the coefficients provided in Reference 8a.

The SIF for the surface point of the crack is given as [8a]:

$$K_I = (\pi)^{0.5} * \left[\sum_{i=0}^3 \sigma_i G_{si} \right]$$

Where:

$$G_{si} = G_i [A_6 + A_7(a/t)^2]/(a/c)^r$$

The coefficients "A" and the exponent "r" were obtained from Reference 8a.

The SIF equations for the deepest point and for the surface point are decoupled in this model. This separation enables independent evaluation of the potential for growth at the deepest point and at the surface independently.

The SIF for an external flaw originating on the OD surface was also obtained from Reference 8b and the SIF is given as:

$$K_I = (\pi)^{0.5} * \left[\sum_{i=0}^3 \sigma_i G_i \right]$$

The above equation is similar to the SIF equation for the deepest point, presented earlier. However, the shape function coefficients are different and are defined [8b] as:

$$G_i = A_0 + (A_1\alpha_i + A_2\alpha_i^2 + A_3\alpha_i^3)/(A_4\{R_{inside}/t\} - A_5)^n$$

and :

$$\alpha_i = [a/t]/[a/c]^m$$

The values for the coefficients "A_x" and the constants "n and m" were obtained from Reference 8b. In Reference 8b there was no separate formulation provided for the SIF for the surface point. Therefore, the surface length of the flaw is derived using the aspect ratio (a/c).

To ensure the formulations used in the current report provide a reasonable value for the SIF, a comparison was made with NASGRO-3 [9]. The NASGRO-3 model for the geometry considered was SC04. The stress distribution for the WSES-3 CEDM nozzle at 7.8 degrees at the downhill location ("0" degree azimuth) was used. The flaw aspect ratio (a/c) and flaw depth were obtained from the output from the analyses performed for the current evaluation (Appendix III). The analysis method used in both References 8 and 9 is based on influence function method for an arbitrary stress distribution. The stress coefficients used in Reference 8 use the stress fit to the full thickness of the nozzle, whereas in Reference 9 the stress coefficients are obtained from a fit over the flaw depth. The SIF obtained from the two analyses are presented in Figure 27 for ID (internal) surface flaws. The comparison shows that the SIF calculated in the current analysis is always greater than those obtained from the analysis performed using Reference 9. The significance of this comparison shows that the SIF obtained in this analysis is conservative and will result in higher PWSCC crack growth rates. A similar comparison for OD (external) flaw

was performed and showed that the SIF in the current evaluation was higher than that obtained from Reference 9 (5.93 ksi $\sqrt{\text{in}}$ vs. 4.34 ksi $\sqrt{\text{in}}$).

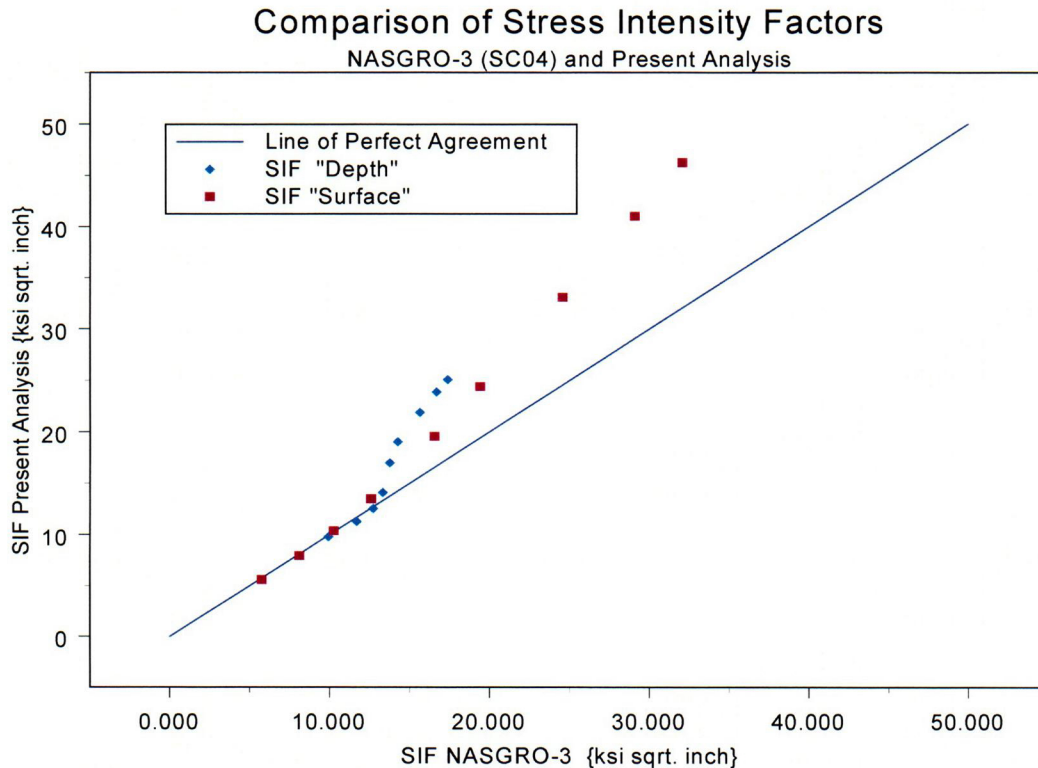


Figure 27: Comparison of SIF from References 8 and 9 utilizing the same stress distribution (WSES-3, 7.8° nozzle at the 0° azimuth at an axial elevation of 1.544" above bottom of nozzle).

Through-Wall Axial Flaw

The analysis for a through-wall axial flaw was evaluated using the formulation of Reference 10. This formulation was chosen since the underlying analysis, presented in Reference 10, was performed considering thick wall cylinders that had "R_o/t" ratio in the range of the application herein. The analysis used the outside surface (OD) as the reference surface and, hence, the same notation is used here.

It was noted in Reference 10 that the formulations based on thin shell theory do not consider the complete three-dimensional nature of the highly localized stress distribution. This would be the case for the residual stress distribution from welding. The nonlinear three-dimensional stress distribution coupled with shell curvature must be properly addressed to account for the material behavior at the crack tip, which controls the SIF, such that the SIF is not underestimated. The information presented in Reference 10 compared the results from formulations derived using thin shell theory

and that derived using thick shell formulation which, highlighted the need to use thick shell based formulation for situations such as the current application.

The formulation provides the correction factors, which account for the “ R_o/t ” ratio and flaw geometry (λ), that are used to correct the SIF for a flat plate solution subjected to similar loadings. The correction factors were given for both “extension” and “bending” components. The flat plate solutions for both membrane and bending loads were to be used to obtain the applied SIF. The formulations for SIF were given as [10];

$$K_{outer} = \{A_e + A_b\} * K_p \text{ For the OD surface;}$$

and,

$$K_{inner} = \{A_e - A_b\} * K_p \text{ For the ID surface;}$$

where:

*A_e and A_b are the “extension” and “bending” components; and,
 K_p is the SIF for a cracked Flat Plate subject to the same boundary condition and loading as the cracked cylinder.*

The flat plate SIF solutions are written as:

$$K_{p-Membrane} = \sigma_h * \sqrt{\pi * l} \text{ for membrane loading, and}$$

$$K_{p-Bending} = \sigma_b * \sqrt{\pi * l} \text{ for bending loading.}$$

Where:

σ_h and σ_b are the membrane and bending stresses and “ l ” is one-half the crack length.

The reference surface used in the evaluation was the OD surface. The stresses at the ID and OD at the axial elevation of interest (1.764 ANO-2 and 1.544 WSES-3 inches above nozzle bottom) were decomposed into membrane and bending components as follows:

$$\sigma_h = \frac{\sigma_{res-OD} + \sigma_{res-ID}}{2} \text{ for membrane loading; and}$$

$$\sigma_b = \frac{\sigma_{res-OD} - \sigma_{res-ID}}{2} \text{ for bending loading.}$$

where:

σ_{res-OD} is the residual stress on the OD surface; and,

σ_{res-ID} is the residual stress on the ID surface.

The data presented in the tables in Reference 10 for determining the A_e and A_b components were curve fit using a fifth order polynomial such that they could be calculated knowing the parameter λ , which is defined as [10]:

$$\lambda = \{[12 * (1 - \nu^2)]\}^{0.25} * \frac{l}{(R * t)^{0.5}}$$

where ν is Poisson's ratio and R is the mean radius.

The curve fit results for the components are presented in figure 28 below.

Extension and Bending Constants for Throughwall Axial Flaws R/t = 3.0
(ASME PVP 350, 1997; pp 143)

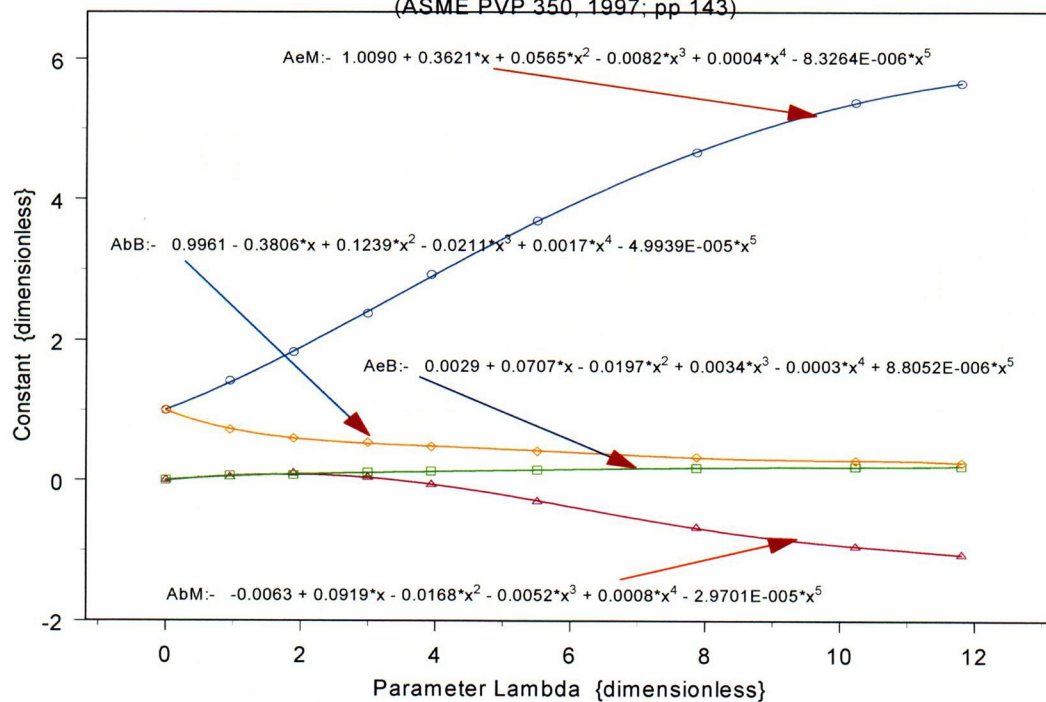


Figure 28: Curve fit equations for the “extension and “bending” components in Reference 10. Tables 1c and 1d for membrane loading and Tables 1g and 1h for bending loading of Reference 10 were used.

PWSCC Crack Growth Rate

To evaluate the potential for crack growth due to PWSCC, the crack growth rate equation from EPRI-MRP 55 [10] was used. The crack growth rate as a function of the stress intensity factor with a correction for temperature effects is given as [11]:

$$\frac{da}{dt} = \exp\left[-\frac{Q_g}{R} \left(\frac{1}{T} - \frac{1}{T_{ref}}\right)\right] \alpha (K - K_{th})^\beta$$

Where:

da/dt = crack growth rate at temperature T {m/s}

Q_g = thermal activation energy for crack growth {31.0 kcal/mole}

R = universal gas constant {1.103x 10³ kcal/mole-°R}

T = absolute operating temperature at crack tip {°R}

T_{ref} = absolute reference temperature for data normalization {1076.67 °R}

α = crack growth amplitude {2.67x10⁻¹²}

K = crack tip SIF {Mpa√m}

K_{th} = threshold SIF for crack growth {MPa√m}

β = exponent {1.16}

Analysis

The surface flaws were modeled such that the upper flaw tip was at the analysis location. This flaw geometry would permit the evaluation of the growth toward the J-weld, which is of interest in this application. The analysis in which potential for PWSCC flaw growth was predicted; the graph for surface flaw growth in the direction of the J-weld was plotted. For the through-wall flaw, the center of the flaw was located at the analysis elevation. When the propensity for PWSCC flaw growth was predicted, growth towards the J-weld was plotted. For each plant, twenty one (21) separate analyses was performed to ensure all possible nozzle geometry, flaw geometry and flaw orientation were addressed.

In the analysis performed, the SIF was calculated both in English and SI units. The crack growth was first computed in the SI units and then converted to English units. For surface flaws, the initial flaw used was the shallowest detected flaw from the EPRI mockup tests [4] (0.035 inch deep for ID initiated flaws and 0.0665 inch deep for OD initiated flaws). The flaw lengths were based on an aspect ratio of ten (10) as discussed earlier. For through-wall axial flaw, the flaw length used was 0.5 inch. The stress intensity based on the applicable stress intensity was computed and then compared to the threshold SIF. If the SIF was less than the threshold SIF, then no flaw growth would occur. The analysis was performed using a Mathcad [12] worksheet. The SIF and crack growth equations were solved in a recursive manner for time increments of about one month. Therefore, if growth were to occur ($K > K_{th}$), the crack dimensions could be increased by the amount of growth and the SIF would be recalculated. The Mathcad worksheets utilized in the evaluation for ANO-2 are presented in Appendix II and those for WSES-3 in Appendix III.

4.0 Discussion and Results

The goal of the inspection program designed for the reactor vessel head penetrations is to ensure that the structural integrity is not challenged during the upcoming operating cycle following the refueling outage when the inspections are performed. Safety analyses performed by the MRP have demonstrated that axial flaws in the nozzle tube material do not pose a challenge to the structural integrity of the nozzle. Axial flaws, if not inspected on a periodic basis can produce a primary boundary leak that can cause damage to the reactor vessel head (carbon steel) and create a conducive environment for initiating and propagating. OD circumferential flaws. These conditions do challenge the pressure boundary and hence critical importance is paid to proper periodic inspection and to the disposition of flaws that may be discovered. Therefore, proper analyses are essential to ascertain the nature of axial flaw growth such that appropriate determination can be accomplished.

The analyses performed in this report were designed to capture the behavior of postulated flaws that might exist in the un-inspected zone. The growth region for the postulated flaws was to the intersection of the J-weld with the tube OD. The flaw growth in the tube in the region of the fillet weld is not considered to challenge the J-weld. Field experience for flaws in the nozzle has demonstrated that propagation is confined to the nozzle base material. Therefore, considering the flaw propagation in the nozzle region adjacent to the fillet weld region is not expected to unduly challenge the J-weld.

In all cases the estimated flaw growth time was limited to the flaw reaching the J-weld to nozzle OD intersection. Hence the J-weld would not be unduly challenged. The design review of the reactor vessel head construction, the detailed residual stress analyses, the selection of representative nozzle locations, selection of representative fracture mechanics models, and the application of suitable crack growth law has provided the bases for arriving at a comprehensive and prudent decision.

The axial flaw geometry was selected for evaluation because this flaw has the potential for propagation into the pressure boundary weld (the J-groove weld) because the circumferentially oriented flaws will not propagate towards the pressure boundary weld. The hoop stress distribution at the downhill location and at an azimuth ninety degrees were chosen for evaluation because these locations have the closest proximity to the pressure boundary J-groove weld.

The uphill location is farther removed from the J-groove weld; hence the hoop stress is expected to be lower. The axial distribution of the hoop stress magnitude for both the ID and OD surfaces show that at axial location below the evaluated elevation, the stresses drop off significantly; hence potential for PWSCC flaw growth would be significantly lower. If flaws had been postulated flaws in the un-inspected zone on the uphill side, their results would be bounded by the analysis presented herein. Hence no additional analyses are required.

The fracture mechanics evaluation considered the flaw face to be subjected to the operating reactor coolant system (RCS) pressure. This is accomplished by

arithmetically adding the RCS pressure to the uniform stress coefficient in the surface flaw analysis and added to the membrane stress for the through-wall flaw analysis. In this manner, the stress imposed on the flaw is accurately and conservatively modeled.

The PWSCC flaw growth used the equations from Reference 8. The operating temperature for the flaw tip was taken to be 604 °F. Thus, the potential for flaw growth is maximized. The seventy fifth percentile curve from Reference 8 was used for calculating PWSCC flaw growth.

The model for evaluation was developed as a coupled stress intensity factor and flaw growth model. The calculations were performed in a recursive manner. The time step for each PWSCC growth block was seventy hours. At the end of the block, the incremental crack growth was doubled and added to the flaw length and a new flaw size was obtained. Therefore, the flaw is expected to grow in both directions. Using the new flaw length the SIF was computed and the growth for the subsequent block was calculated. This recursive method accounts for concomitant increase of the stress intensity factor as the flaw advances. A small time-step (block) ensures better approximation of the process. The detailed Mathcad calculation worksheets for ANO-2 are presented in Appendix II and that for WSES-3 in Appendix III.

The results of the evaluation are presented in Table IV for ANO-2 and Table V for WSES-3. In these tables the initial SIF at the flaw tip locations evaluated and the corresponding result is provided. When the analysis showed a potential for flaw growth, a figure number is provided, which shows the flaw growth and SIF behavior. For the ID surface flaws, the behavior of the two flaw tips were independent as mentioned earlier. For the OD surface flaw, SIF could only be computed at the deepest flaw tip and the flaw aspect ratio was used to obtain the surface growth behavior. For the through-wall axial crack cases, the SIF was evaluated at both the ID and OD flaw tips. The flaw growth was computed by using an average of the SIF at these locations.

Table IV: ANO-2 Evaluation Results

Nozzle Identification		Surface Flaw Origin ID or OD	Initial Stress Intensity Factor (ksi√in)		Result/Figure Number
Location on RV Head	Azimuth on Nozzle		Deepest Point	Surface Point	
"0" Degree	Downhill	ID	10.32	5.79	PWSCC Growth; Figure 29
"8.8" Degree	Downhill	ID	9.39	5.34	PWSCC Growth; Figure 30
"28.8" Degree	Downhill	ID	7.07	3.92	No Potential for PWSCC Growth
"49.6" Degree	Downhill	ID	2.06	0.99	No Potential for PWSCC Growth
"8.8" Degree	90 Degree	ID	7.99	4.51	No Potential for PWSCC Growth
"28.8" Degree	90 Degree	ID	3.20	1.89	No Potential for PWSCC Growth
"49.6" Degree	90 Degree	ID	3.06	1.87	No Potential for PWSCC Growth
"0" Degree	Downhill	OD	8.32	NA	PWSCC Growth; Figure 31
"8.8" Degree	Downhill	OD	8.36	NA	PWSCC Growth; Figure 32
"28.8" Degree	Downhill	OD	11.14	NA	PWSCC Growth; Figure 33
"49.6" Degree	Downhill	OD	17.14	NA	PWSCC Growth; figure 34
"8.8" Degree	90 Degree	OD	3.30	NA	No Potential for PWSCC Growth
"28.8" Degree	90 Degree	OD	<0.0	NA	No Potential for PWSCC Growth
"49.6" Degree	90 Degree	OD	<0.0	NA	No Potential for PWSCC Growth
Nozzle Identification		Flaw Type Through-Wall	Initial Stress Intensity Factor (ksi√in)		Result/Figure Number
Location on RV Head	Azimuth on Nozzle		ID Surface	OD surface	
"0" Degree	Downhill	Axial	31.94	18.22	PWSCC Growth; Figure 35
"8.8" Degree	Downhill	Axial	29.81	18.11	PWSCC Growth; figure 36
"28.8" Degree	Downhill	Axial	22.95	21.92	PWSCC Growth; Figure 37
"49.6" Degree	Downhill	Axial	9.37	31.01	PWSCC Growth; Figure 38
"8.8" Degree	90 Degree	Axial	23.98	8.11	PWSCC Growth; Figure 39
"28.8" Degree	90 Degree	Axial	9.82	0.64	No Potential for PWSCC Growth
"49.6" Degree	90 Degree	Axial	9.49	<0	No Potential for PWSCC Growth

TableV: WSES-3 Evaluation Results

Nozzle Identification		Surface Flaw Origin ID or OD	Initial Stress Intensity Factor (ksi√in)		Result/Figure Number
Location on RV Head	Azimuth on Nozzle		Deepest Point	Surface Point	
"0" degree	Downhill	ID	9.04	5.03	PWSCC Growth, Figure 40
"7.8" Degree	Downhill	ID	8.19	4.68	PWSCC Growth, Figure 41
"29.1" Degree	Downhill	ID	4.58	2.58	No Potential for PWSCC Growth
"49.7" Degree	Downhill	ID	1.58	0.84	No Potential for PWSCC Growth
"7.8" degree	90 Degree	ID	5.67	3.22	No Potential for PWSCC Growth
"29.1" degree	90 Degree	ID	0.82	0.54	No Potential for PWSCC Growth
"49.7" Degree	90 Degree	ID	2.12	1.32	No Potential for PWSCC Growth
"0" Degree	Downhill	OD	4.14	NA	No Potential for PWSCC Growth
"7.8" Degree	Downhill	OD	4.34	NA	No Potential for PWSCC Growth
"29.1" Degree	Downhill	OD	2.63	NA	No Potential for PWSCC Growth
"49.7" Degree	Downhill	OD	4.89	NA	No Potential for PWSCC Growth
"7.8" Degree	90 Degree	OD	0.40	NA	No Potential for PWSCC Growth
"29.1" Degree	90 Degree	OD	<0.0	NA	No Potential for PWSCC Growth
"49.7" Degree	90 Degree	OD	<0.0	NA	No Potential for PWSCC Growth
Nozzle Identification		Flaw Type Through-Wall	Initial Stress Intensity Factor (ksi√in)		Result/Figure Number
Location on RV Head	Azimuth on Nozzle		ID Surface	OD surface	
"0" degree	Downhill	Axial	26.74	10.16	PWSCC Growth; Figure 42
"7.8" Degree	Downhill	Axial	25.37	10.55	PWSCC Growth; Figure 43
"29.1" Degree	Downhill	Axial	6.43	14.03	PWSCC Growth; Figure 44
"49.7" Degree	Downhill	Axial	5.57	9.36	No Potential for PWSCC Growth
"7.8" degree	90 Degree	Axial	16.68	2.69	PWSCC Growth; Figure 45
"29.1" degree	90 Degree	Axial	2.10	<0	No Potential for PWSCC Growth
"49.7" Degree	90 Degree	Axial	6.00	<0	No Potential for PWSCC Growth

The results presented for ANO-2 and WSES-3 demonstrate that flaw growth is possible for some penetration locations at the location evaluated. The time needed for the flaw to grow to the J-weld interface is obtained by subtracting the un-inspectable length height from the nozzle projection below the J-weld, (Appendix I;

Attachment 4). The growth distance was estimated from the inspection lower limit to the J-weld intersection for a particular nozzle location. The available length for flaw growth for the nozzles considered in this analysis are presented in Table VI. Since the stresses at locations below the current flaw location are at significantly lower magnitude of stress (including compressive), it is not plausible that PWSCC flaw growth could occur at elevations below the evaluated position. Therefore, the region that cannot be inspected is not expected to negatively impact the structural and leak integrity of the primary pressure boundary at the reactor vessel head penetrations.

Table VI Available Nozzle Length for (PWSCC) Flaw Growth

Nozzle Location	Freespan Nozzle Length {inch}	Un-Inspected Length above Nozzle Bottom {inch}	Length available for Flaw Growth {inch}
ANO-2			
"0" degree; downhill	2.48	1.764	0.716
"8.8" degree; downhill	2.48	1.764	0.716
"28.8" degree; downhill	2.48	1.764	0.716
"49.6" degree; downhill	2.48	1.764	0.716
"8.8" degree; ninety degrees	2.83	1.764	1.066
WSES-3			
"0" degree; downhill	2.88	1.544	1.336
"7.8" degree; downhill	2.88	1.544	1.336
"29.1" degree; downhill	2.88	1.544	1.336
"49.7" degree; downhill	2.88	1.544	1.336
"7.8" degree; ninety degrees	3.185	1.544	1.641

For those analysis cases where PWSCC growth was observed, the behavior of crack growth as a function of operating time are presented in Figures 29 through 45. In these figures the behavior of SIF is also presented. Figures 29 through 39 provide the information for ANO-2 CEDM nozzles and Figures 40 to 45 for WSES-3 CEDM nozzles.

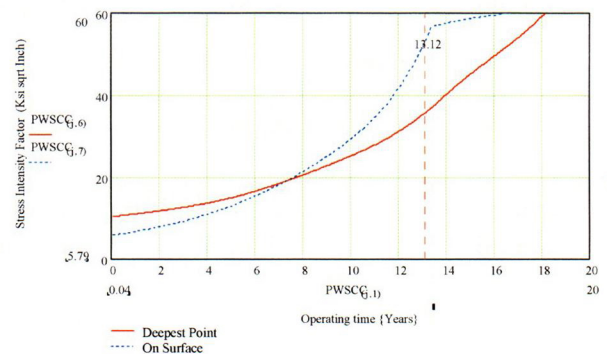
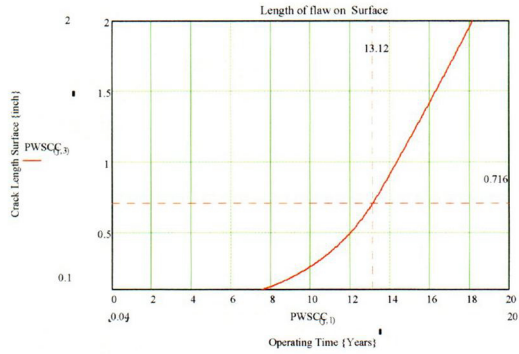


Figure 29: ANO-2; Plots for an ID surface crack growth and SIF versus operating time for the 0° nozzle at the 0° azimuth (downhill position). The assumed flaw reaches the J-weld interface in 13.12 operating years. (source: Appendix II, Attachment 1)

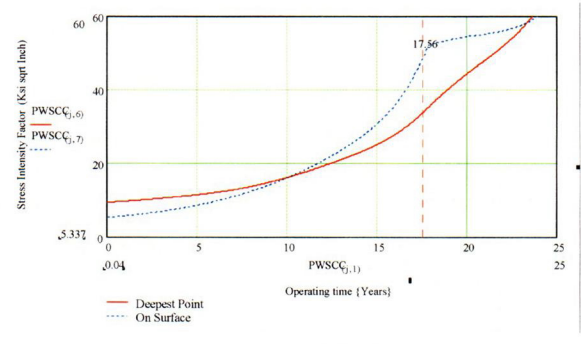
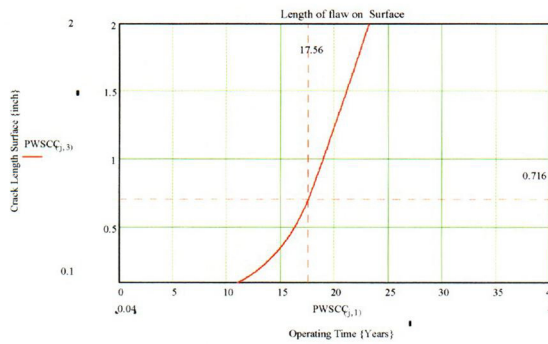


Figure 30: ANO-2; Plots for an ID surface crack growth and SIF versus operating time for the 8.8° nozzle at the 0° azimuth (downhill position). The assumed flaw reaches the J-weld interface in 17.56 operating years. (source: Appendix II, Attachment 4)

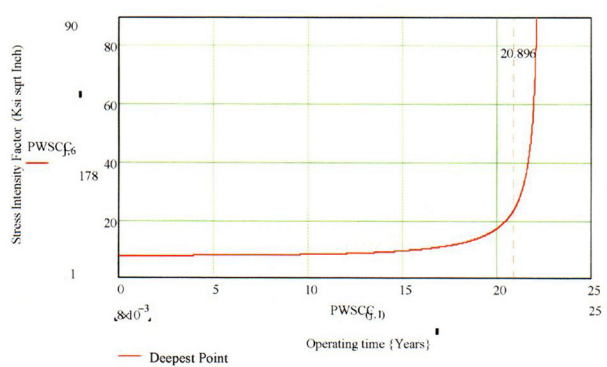
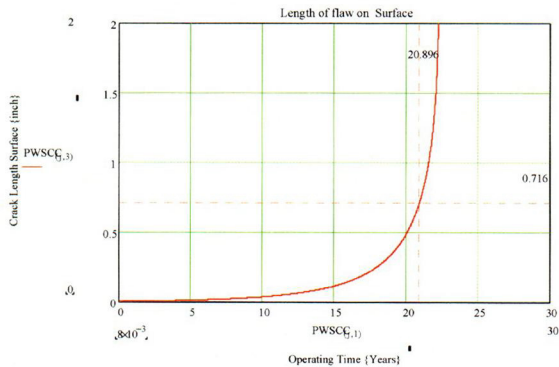


Figure 31: ANO-2; Plots for an OD surface crack growth and SIF versus operating time for the 0° nozzle at the 0° azimuth (downhill position). The assumed flaw reaches the J-weld interface in 20.90 operating years. (source: Appendix II, Attachment 8)

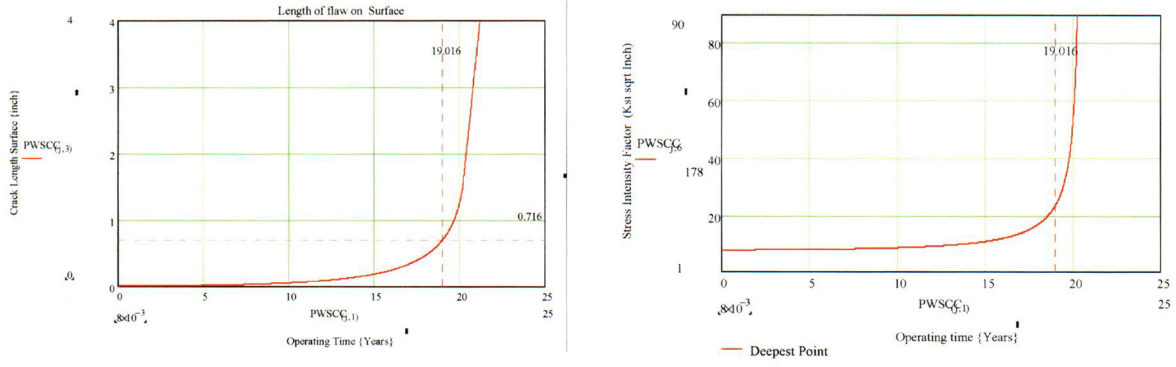


Figure 32: ANO-2; Plots for an OD surface crack growth and SIF versus operating time for the 8.8° nozzle at the 0° azimuth (downhill position). The assumed flaw reaches the J-weld interface in 19.02 operating years. (source: Appendix II, Attachment 9)

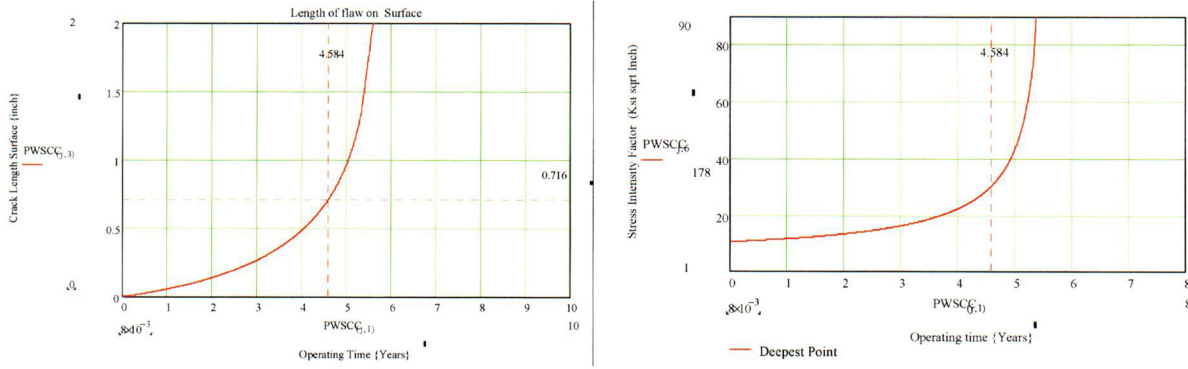


Figure 33: ANO-2; Plots for an OD surface crack growth and SIF versus operating time for the 28.8° nozzle at the 0° azimuth (downhill position). The assumed flaw reaches the J-weld interface in 4.58 operating years. (source: Appendix II, Attachment 10)

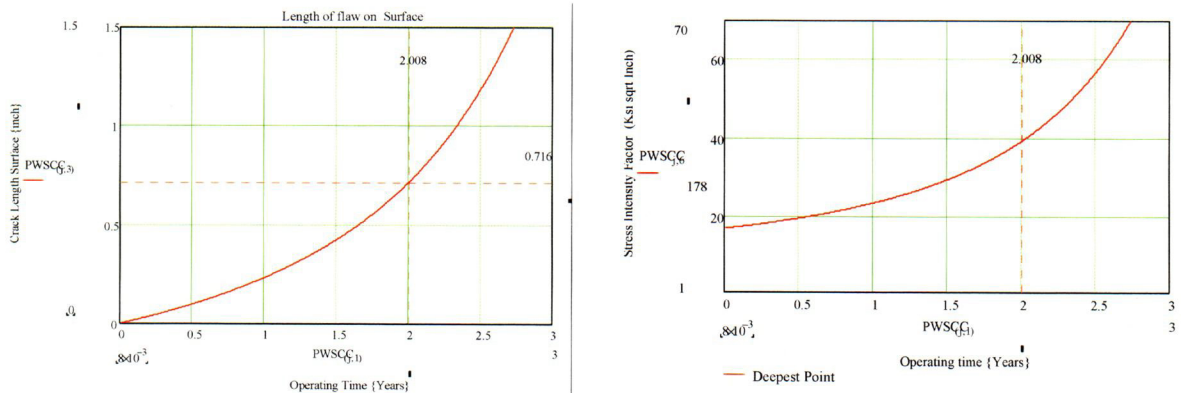


Figure 34: ANO-2; Plots for an OD surface crack growth and SIF versus operating time for the 49.6° degree nozzle at the 0° degree azimuth (downhill position). The assumed flaw reaches the J-weld interface in 2.01 operating years. (source: Appendix II, Attachment 11)

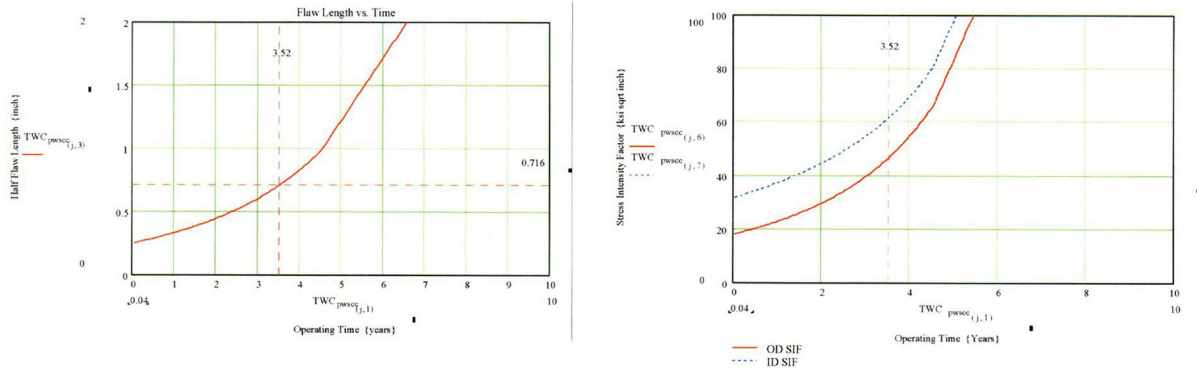


Figure 35: ANO-2; Plots for a through-wall axial crack growth and SIF versus operating time for the 0° nozzle at the 0° azimuth (downhill position). The assumed flaw reaches the J-weld interface in 3.52 operating years. (source: Appendix II, Attachment 15)

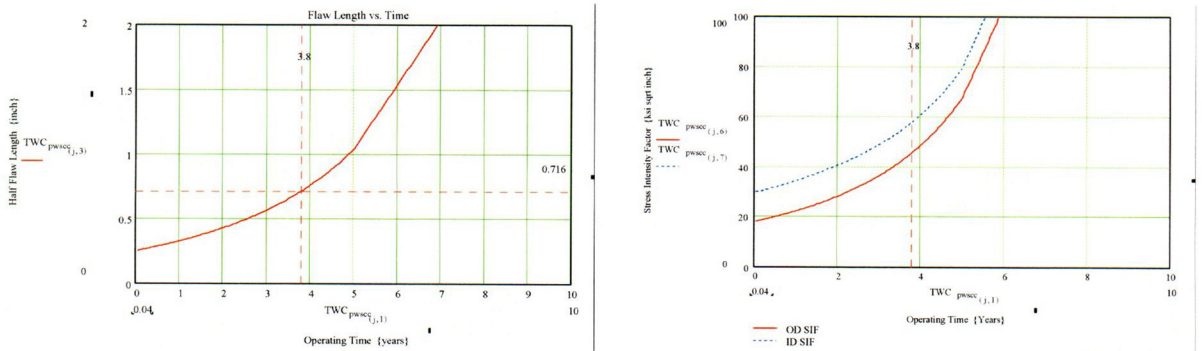


Figure 36: ANO-2; Plots for a through-wall axial crack growth and SIF versus operating time for the 8.8° nozzle at the 0° azimuth (downhill position). The assumed flaw reaches the J-weld interface in 3.80 operating years. (source: Appendix II, Attachment 16)

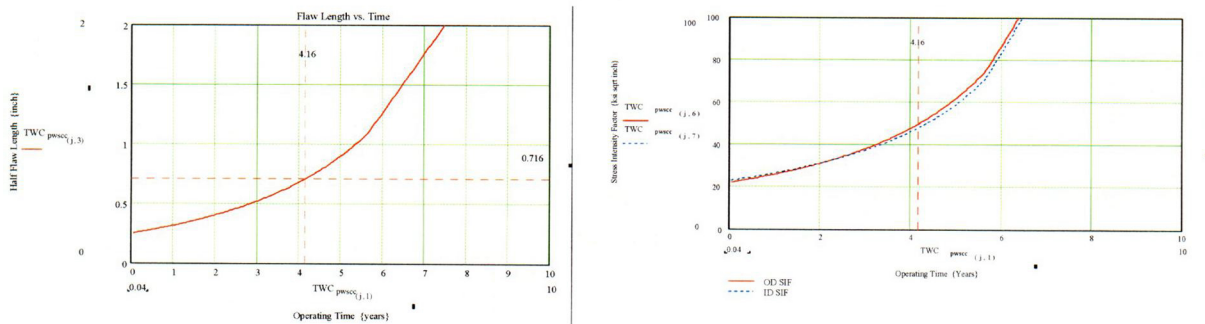


Figure 37: ANO-2; Plots for a through-wall axial crack growth and SIF versus operating time for the 28.8° nozzle at the 0° azimuth (downhill position). The assumed flaw reaches the J-weld interface in 4.16 operating years. (source: Appendix II, Attachment 17)

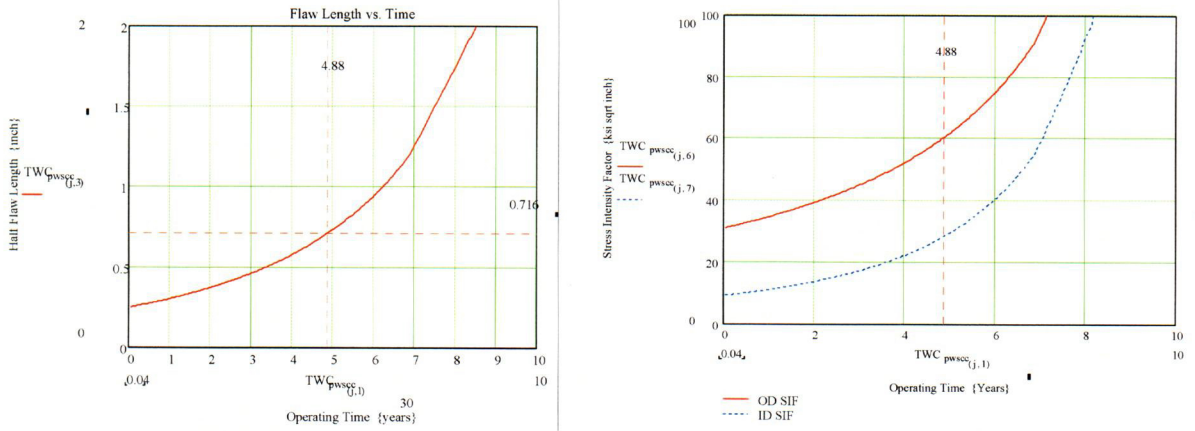


Figure 38: ANO-2; Plots for a through-wall axial crack growth and SIF versus operating time for the 49.6° nozzle at the 0° azimuth (downhill position). The assumed flaw reaches the J-weld interface in 4.88 operating years. (source: Appendix II, Attachment 18)

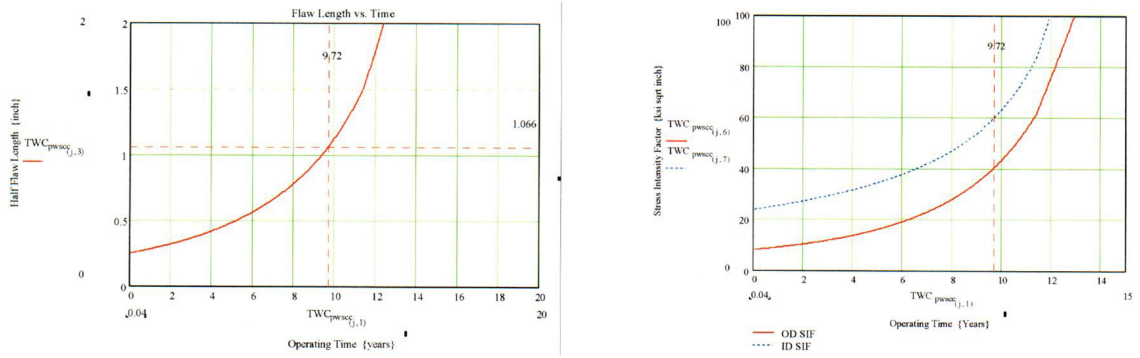


Figure 39: ANO-2; Plots for a through-wall axial crack growth and SIF versus operating time for the 8.8° nozzle at the 90° azimuth. The assumed flaw reaches the J-weld interface in 9.72 operating years. (source: Appendix II, Attachment 19)

The graphs for the SIF for surface flaws (ID initiated) show that the surface SIF is higher than the SIF at the deepest penetration; hence, it follows that the flaw growth would tend to be higher on the surface than in the through-thickness direction. This behavior is observed in flaws that have been found in-service where the crack profile has a “canoe” shape rather than a semi-elliptical profile. The information obtained from the graphical results, such as time to reach J-weld intersection and the final SIF at that time, are provided in Table VII for ANO-2.

Table VII: ANO-2 Results for PWSCC Growth Cases

Nozzle Identification		Surface Flaw Origin ID or OD	Final Stress Intensity Factor {ksi√in}		Time to Reach J-Weld Intersection {Operating Years}
Location on RV Head	Azimuth on Nozzle		Deepest Point	Surface Point	
"0" Degree	Downhill	ID	36.08	54.61	13.12
"8.8" Degree	Downhill	ID	34.62	49.75	17.56
"0" Degree	Downhill	OD	26.32	NA	20.90
"8.8" degree	Downhill	OD	23.71	NA	19.02
"28.8" Degree	Downhill	OD	30.76	NA	4.58
"49.6" Degree	Downhill	OD	40.15	NA	2.01

Nozzle Identification		Flaw Type Through-Wall	Final Stress Intensity Factor (ksi√in)		Time to Reach J-Weld Intersection {Operating Years}
Location on RV Head	Azimuth on Nozzle		ID Surface	OD surface	
"0" Degree	Downhill	Axial	61.54	46.66	3.52
"8.8" Degree	Downhill	Axial	57.77	45.99	3.8
"28.8" Degree	Downhill	Axial	47.88	50.17	4.16
"49.6" Degree	Downhill	Axial	28.93	60.52	4.88
"8.8" Degree	90 Degree	Axial	60.52	40.86	9.72

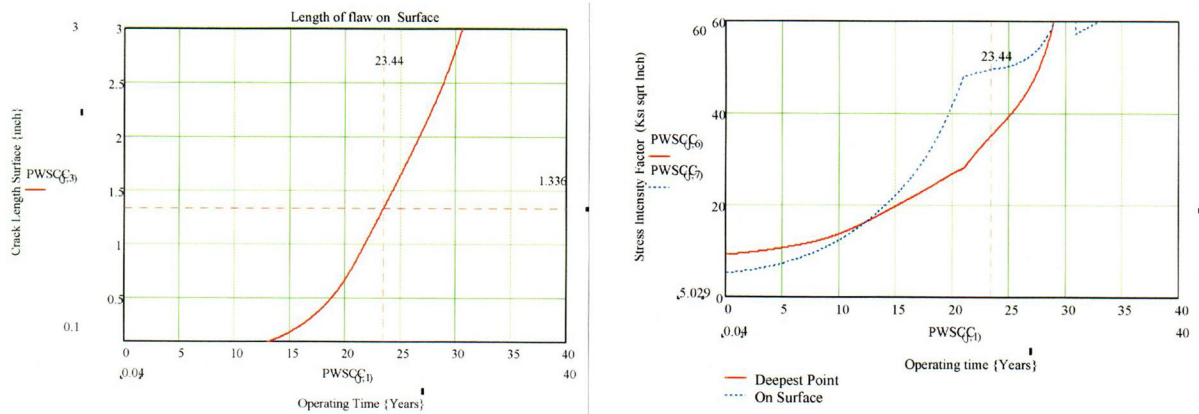


Figure 40: WSES-3; Plots for an ID surface axial crack growth and SIF versus operating time for the 0° nozzle at the 0° azimuth (downhill position). The assumed flaw reaches the J-weld interface in 23.44 operating years. (source: Appendix III, Attachment 1)

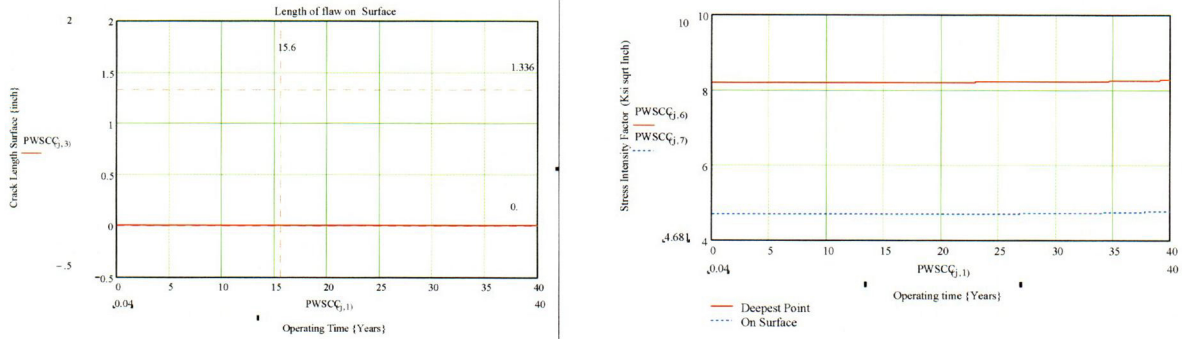


Figure 41: WSES-3; Plots for an ID surface axial crack growth and SIF versus operating time for the 7.8° nozzle at the 0° azimuth (downhill position). The assumed flaw **does not** reach the J-weld interface in 40 operating years, because the SIF was barely above the threshold value (source: Appendix III, Attachment 2)

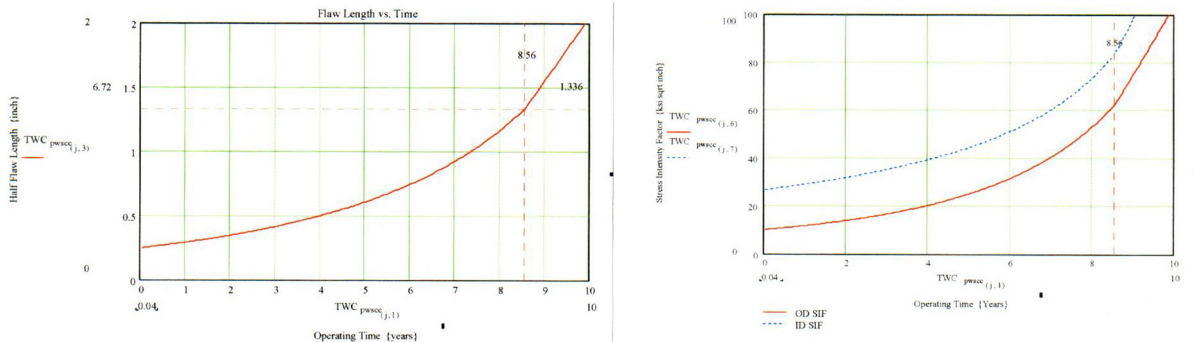


Figure 42: WSES-3; Plots for a through-wall axial crack growth and SIF versus operating time for the 0° nozzle at the 0° azimuth (downhill position). The assumed flaw reaches the J-weld interface in 8.56 operating years. (source: Appendix III, Attachment 15)

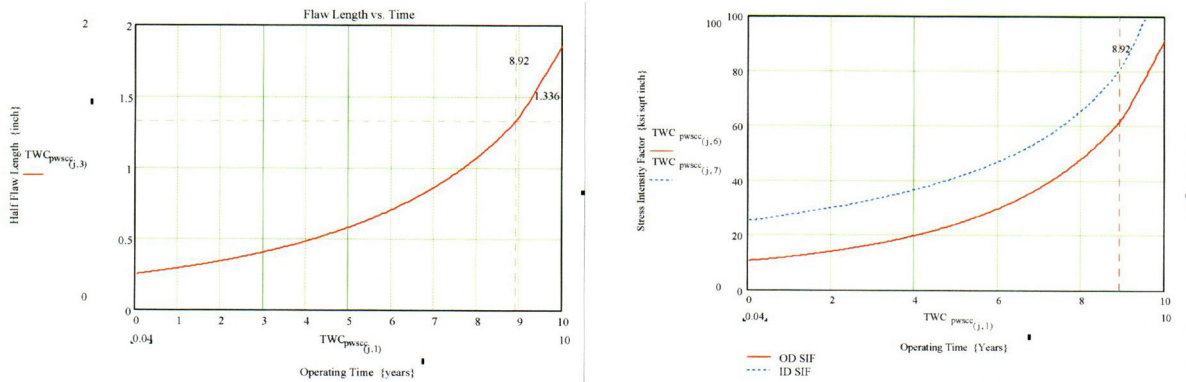


Figure 43: WSES-3; Plots for a through-wall axial crack growth and SIF versus operating time for the 7.8° nozzle at the 0° azimuth (downhill position). The assumed flaw reaches the J-weld interface in 8.92 operating years. (source: Appendix III, Attachment 16)

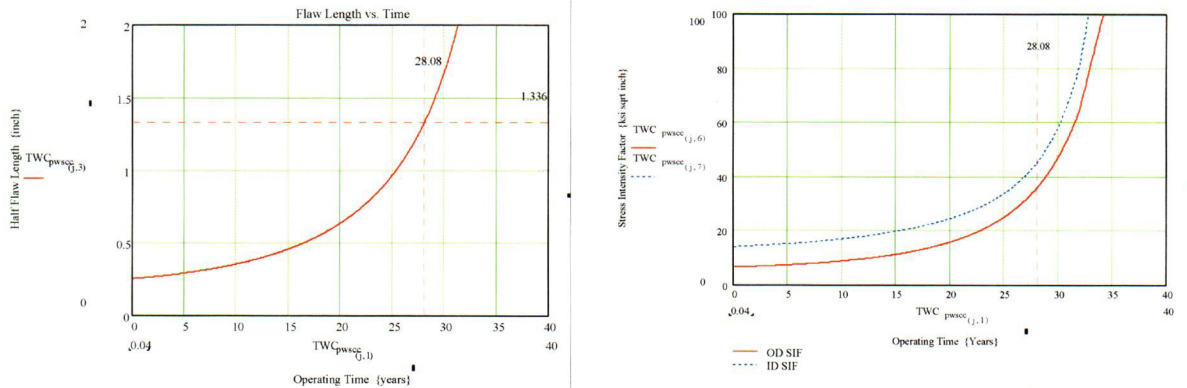


Figure 44: WSES-3; Plots for a through-wall axial crack growth and SIF versus operating time for the 29.1° nozzle at the 0° azimuth (downhill position). The assumed flaw reaches the J-weld interface in 28.08 operating years. (source: Appendix III, Attachment 17)

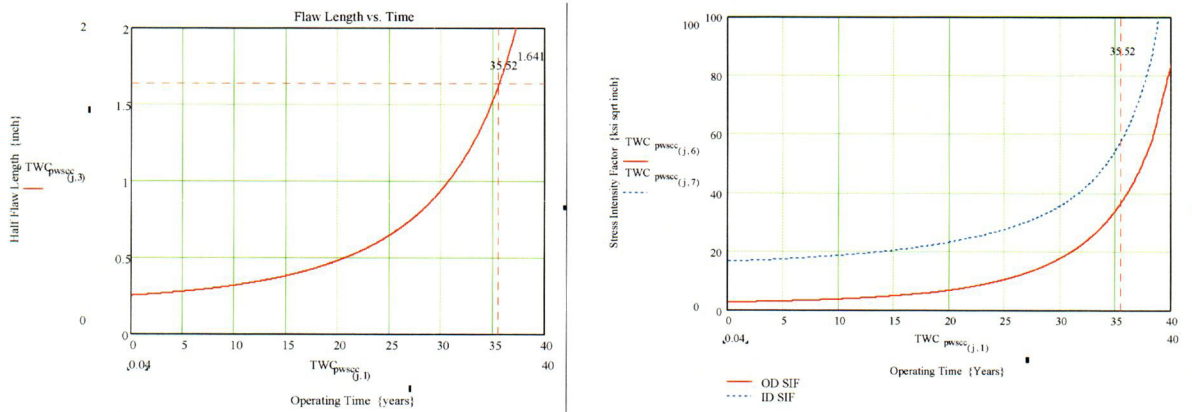


Figure 45: WSES-3; Plots for a through-wall axial crack growth and SIF versus operating time for the 7.8° nozzle at the 90° azimuth. The assumed flaw reaches the J-weld interface in 35.52 operating years. (source: Appendix III, Attachment 19)

As was observed in the graphs for ANO-2, the WSES-3 graphs show similar trends. The SIF for surface flaws (ID initiated) show that the surface SIF is higher than the SIF at the deepest penetration. The information obtained from the graphical results, such as time to reach J-weld intersection and the final SIF at that time, are provided in Table VIII for WSES-3.

Table VIII: WSES-3 Results for PWSCC Growth Cases

Nozzle Identification		Surface Flaw Origin ID or OD	Final Stress Intensity Factor {ksi√in}		Time to Reach J-Weld Intersection {Operating Years}
Location on RV Head	Azimuth on Nozzle		Deepest Point	Surface Point	
"0" degree	Downhill	ID	35.00	49.39	23.44
"7.8" Degree	Downhill	ID	8.26	4.77	>40
Nozzle Identification		Flaw Type Through-Wall	Final Stress Intensity Factor (ksi√in)		Time to Reach J-Weld Intersection (Operating Years)
Location on RV Head	Azimuth on Nozzle		ID Surface	OD surface	
"0" degree	Downhill	Axial	84.05	62.72	8.56
"7.8" Degree	Downhill	Axial	80.68	67.65	8.92
"29.1" Degree	Downhill	Axial	46.46	36.58	28.08
"7.8" degree	90 Degree	Axial	58.68	36.43	35.56

5.0 Conclusions

The evaluation performed and presented in the preceding sections support the following conclusions:

- 1) The shortest PWSCC growth time for ANO-2 is a part through-wall OD axial flaw on the 49.6 degree nozzle at the downhill location. The growth time to reach the J-weld interface was calculated to be 2.01 years. This time is in excess of one operating cycle of eighteen (18) months.
- 2) The shortest PWSCC growth time for WSES-3, is for a through-wall axial flaw for the central CEDM location ("0" degree). The growth time to reach the J-weld interface was calculated to be 8.56 years. This time is in excess of five operating cycles of eighteen (18) months duration.
- 3) The conservatisms used in the analysis (pressure applied to flaw faces and high aspect ratio) provide assurance that an undetected flaw at the lowest elevation for inspection will not reach the J-weld interface within one operating cycle. Therefore adequate opportunities exist to detect the postulated flaw before it reaches the J-weld.

- 4) The regions below the lowest inspection elevation experience lower stresses and, hence, significantly lower potential for flaw growth by PWSCC. Therefore at these lower locations PWSCC flaw growth is not expected.
- 5) The analysis presented herein demonstrates that there will be no negative impact on the level of quality and safety by excluding the un-inspectable region, (1.764 inches for ANO-2 and 1.544 inches for WSE-3), at the bottom of the CEDM nozzle. Therefore, the proposed inspection extent provides an acceptable level of quality and safety.

6.0 References

- 1) NRC Order; Issued by letter EA-03-009 addressed to "Holders of Licenses for Operating Pressurized Water Reactors"; dated February 11, 2003.
- 2) Drawing Number M-2001-C2-23, ANO Design Engineering Drawing files & 1564-506 WSES-3 Design Engineering Drawing files.
- 3) a: E-mail from R. V. Swain (Entergy) to J. G. Weicks (Entergy); Dated 5/15/2003.
b: E-mail from R. V. Swain to J. G. Weicks; Dated 5/12/2003.
- 4) EPRI NDE Demonstration Report; "MRP Inspection Demonstration Program – Wesdyne Qualification": Transmitted by e-mail from B. Rassler (EPRI) to K. C. Panther (Entergy); Dated 3/27/2003.
- 5) a: DEI Calculation titled " ANO Unit 2 CEDM and ICI Stress Analysis- Using Monotonic Stress Strain curves"; Calculation Number C-7736-00-5; dated 2/5/2002.
b: DEI Calculation titled " Waterford 3 CEDM and ICI Stress Analysis- Using Monotonic Stress Strain curves"; Calculation Number C-7736-00-4; dated 2/4/2002.
- 6) Axxum 6; Data Analysis Products Division, Mathsoft Inc., Seattle, WA; February 1999.
- 7) "Stress Intensity Factor Influence Coefficients for Internal and External Surface Cracks in Cylindrical Vessels"; I. S. Raju and J. C. Newman, Jr.; ASME PVP Volume 58 "Aspects of Fracture Mechanics in Pressure Vessels and Piping"; 1982.

- 8) a: "Ductile Fracture Handbook – Volume 3, Chapter 8, section 1.5"; Electric Power Research institute; NP-6301-D-V3; June 1989
b: "Ductile Fracture Handbook – Volume 3, Chapter 8, section 1.9"; Electric Power Research institute; NP-6301-D-V3; June 1989NASGro
- 9) "NASA- NASGRO 3.0 "A Software for Analyzing Aging Aircraft"; S. R. Mettu et al.; Scientific and Technical Information; NASA; Report Number STI-19990028759; 1999.
- 10) "New Stress Intensity factor and Crack Opening Area Solutions for Through Wall Cracks in Pipes and cylinders": Christine C. France, et al.; ASME PVP Volume 350 "Fatigue and Fracture"; 1997.
- 11) "Materials reliability Program (MRP) Crack Growth Rates for Evaluating Primary Water Stress Corrosion cracking (PWSCC) of Thick Wall Alloy 600 Material": MRP-55 Revision 1; Electric Power Research Institute; May 2002.
- 12) Mathcad – 11; Data Analysis Products Division; Mathsoft Inc.; Seattle WA; November 2002.

ENCLOSURE 4

**APPENDIX I
ENGINEERING REPORT M-EP-2003-002**

Appendix I

Attachment Number	Attachment Content
1	Data Input Concurrence from ANO
2	Data Input Concurrence from WSES-3
3	NDE Dead Zone Information
4	Determination & Verification of CEDM Freespan for ANO-2 and WSES-3

**Design Input Sheet for Fracture Mechanics Evaluation of CEDM nozzles below the Attachment J-weld
{ANO Unit 2 and WSES Unit 3}**

Item	Source	Input Used	Concurrence
Length from bottom of nozzle to top of thread relief counterbore (includes 1 inch thread length plus 1/4 inch thread relief counterbore)	Drawing M-2001-C2-23 revision 4 (CE drawing E-234-760-2) ANO-2 E-74170-112-01 WSES-3	1.25 inches	Site Design Engineering: ANO: <u>Jamie GoBell</u> <i>Jamie GoBell 5/8/03</i> WSES3: _____
Maximum Chamfer Dimension along the axis of the nozzle, including 1/32" tolerance	Same Drawing as above	0.094 inches	Site Design Engineering: ANO: <u>Jamie GoBell</u> <i>Jamie GoBell 5/8/03</i> WSES3: _____
NDE Dead Zone	Ronnie Swain's Notes of 4/23/03 attached to e-mail of 4/23/03	0.300	Site Quality Programs/NDE ANO: _____ WSES3: _____
Residual Stress Distribution	DEI calculations : C-7736-00-5 ANO-2 C-7736-00-4 WSES-3	Nodal stresses below J-weld	DEI Calculations were performed for Westinghouse under contract to Westinghouse for ANO-2 and WSES3 RVHP evaluations. Westinghouse (OEM) provided design input. Westinghouse and DEI have Appendix "B" qualified QA program and these calculations were performed under the applicable program. This provides reasonable assurance that the results are applicable.
PWSCC Crack Growth rate	EPRI-MRP 55 revision 1.	Seventy-fifth Percentile Curve	EPRI report based on information provided by all utilities and the analyses for the report was performed under EPRI QA program. The report was reviewed by Utility peer group (MRP) for correctness, completeness and applicability. The information is reasonable for use for ANO-2 and WSES-3 application.
Nozzle Dimensions (ID and OD)	Drawing M-2001-C2-23 revision 4 (CE drawing E-234-760-2) ANO-2 E-74170-112-01 WSES-3	OD = 4.05"; ID = 2.719" OD = 4.05"; ID = 2.719"	Site Design Engineering: ANO: <u>Jamie GoBell</u> <i>Jamie GoBell 5/8/03</i> WSES3: _____

SEE ATT. 3
FOR DEAD
ZONE INPUTS
RSL 6/9/03

1: Concurrence is only required for items that have a signature block. The Residual Stress results and PWSCC crack growth rate report have been provided under approved QA programs and there is reasonable assurance of the result's accuracy. Hence for these two items specific concurrence is not required.

Engineering Report:
M-EP-2003-002 Rev. 00
Appendix I: Attachment 1

**Design Input Sheet for Fracture Mechanics Evaluation of CEDM nozzles below the Attachment J-weld
{ANO Unit 2 and WSES Unit 3}**

Item	Source	Input Used	Concurrence
Thread length	E-234-760-2 ANO-2 E-74170-112-01 WSES-3	1.25 inches	Site Design Engineering: ANO: _____ WSES3: <u>Nana Ray</u>
Chamfer Dimension	Same Drawing as above	0.094	Site Design Engineering: ANO: _____ WSES3: <u>Nana Ray</u>
NDE Dead Zone	Ronnie Swain's Notes of 4/23/03 attached to e-mail of 4/23/03	0.300	Site Quality Programs/NDE ANO: _____ WSES3: _____
Residual Stress Distribution	DEI calculations : C-7736-00-5 ANO-2 C-7736-00-4 WSES-3	Nodal stresses below J-weld	DEI Calculations were performed for Westinghouse under contract to Westinghouse for ANO-2 and WSES3 RVHP evaluations. Westinghouse (OEM) provided design input. Westinghouse and DEI have Appendix "B" qualified QA program and these calculations were performed under the applicable program. This provides reasonable assurance that the results are applicable.
PWSCC Crack Growth rate	EPRI-MRP 55 revision 1.	Seventy-fifth Percentile Curve	EPRI report based on information provided by all utilities and the analyses for the report was performed under EPRI QA program. The report was reviewed by Utility peer group (MRP) for correctness, completeness and applicability. The information is reasonable for use for ANO-2 and WSES-3 application.
Nozzle Dimensions (ID and OD)	E-234-760-2 ANO-2 E-74170-112-01 WSES-3	OD = 4.05"; ID = 2.719" OD = 4.05"; ID = 2.719" 2.728" NR	Site Design Engineering: ANO: _____ WSES3: <u>Nana Ray</u>

SEE ATT. 3
FOR DEAS ZONE
INPUT. RST
6/9/03

1: Concurrence is only required for items that have a signature block. The Residual Stress results and PWSCC crack growth rate report have been provided under approved QA programs and there is reasonable assurance of the result's accuracy. Hence for these two items specific concurrence is not required.

WSES-3 Design Input Concurrence Sheet

Engineering Report: M-EP-2003-002 Rev. 00
Appendix I: Attachment 2

NDE Dead Zone Design Input

June 6, 2003

Design Input to Engineering Report M-EP-2003-002:

At the request of Entergy, Westinghouse reviewed UT data for 10 penetrations taken from the 2R15 ANO-2 reactor head inspection. This inspection was performed with a 7010 ultrasonic end-effector, using 0.250" diameter, 24mm PCS Time-of-Flight-Diffraction ultrasonic transducers. The penetrations were chosen by their location on the head, in order to provide a representative sample of the entire head. The analysis was performed in order to determine the ultrasonic dead band located immediately above the threaded region of the CEDM nozzles. This review determined the dead band to be 0.200".



Ronald V. Swain
UT Level III
Waterford 3 SES

ANO-2 & WSES-3 CEDM Freespan Measurement

To support the crack growth rate evaluation for the portion of the CEDM nozzle that extends below the J-groove weld on the ANO-2 and W-3 heads, the length of this portion of the nozzle is required. Because this length varies with the nozzle location, an Excel spreadsheet was developed to calculate the various parameters of the nozzle J-groove weld configuration.

To describe the geometry, the following nomenclature is used: The location of the nozzle relative to the curvature of the head is identified by the angle in degrees between the vertical centerline of the head, and a line created by the radius of curvature of the bottom surface of the cladding where it intersects with the centerline of the nozzle. The nozzle locations included in the crack growth rate evaluation are identified as the following:

ANO-2		Waterford-3	
Nozzle location	Penetration No.	Nozzle location	Penetration No.
0°	1	0°	1
8.8°	2, 3, 4, 5	7.8°	2, 3
28.8°	30, 31, 32, 33, 34, 35, 36, 37	29.1°	36, 37, 38, 39, 40, 41, 42, 43
49.6°	70, 71, 72, 73, 74, 75, 76, 77, 78, 79, 80, 81	49.7°	88, 89, 90, 91

The point location around the OD of the nozzle is identified by the azimuth angle with the zero degree azimuth location being the point furthest from the vertical centerline of the head, which is also the lowest point that the J-groove weld attaches to the nozzle (the "low-hillside"). The length of the portion of the nozzle that extends down below the J-groove weld is calculated at the zero degree azimuth for each of the nozzle locations evaluated.

The length, "L", of the portion of the nozzle that extends down below the J-groove weld is defined as the vertical distance from the point where the surface of the cladding would intersect with the outside surface of the nozzle at the zero degree azimuth location down to the bottom of the nozzle (see attached sketch).

Using ANO drawings M-2001-C2-23, M-2001-C2-26, M-2001-C2-32, M-2001-C2-55, and M-2001-C2-107, and Waterford drawings 1564-506, 1564-1036, and 1564-4086, the length "L" was calculated as shown in the following table:

ANO-2		Waterford-3	
Nozzle location	L (inches)	Nozzle location	L (inches)
0°	2.50	0°	2.88
8.8°	2.49	7.8°	2.88
28.8°	2.48	29.1°	2.86
49.6°	2.48	49.7°	2.92

Verified by:

ANO-2	
<i>Jamie GoBell</i>	6/4/03
Jamie GoBell	Date

Waterford-3	
<i>Nara Ray</i>	6/4/03
Nara Ray	Date

